Ústav merania SAV, Bratislava

Mgr. Michal Teplan

Audio-visual stimulation and relaxation, linear and nonlinear EEG measures

Dizertačná práca

Vedný odbor: 39-52-9 bionika a biomechanika

Školiteľ: Doc. RNDr. Viktor Witkovský, CSc.

Školiteľ konzultant: RNDr. Anna Krakovská, CSc.

Bratislava, marec 2006

Acknowledgements

I would like to express my grateful acknowledgement to the supervisors of this thesis RNDr. Anna Krakovská, CSc. and Doc. RNDr. Viktor Witkovský, CSc. for their substantial advises and concerns during the whole research period. Further to Ing. Pavol Krakovský for his kind donation of EEG recording unit and to Mgr. Svorad Štolc for his consulting and contributions especially in software implementations.

This work was supported by Slovak Grant Agency for Science (grant nos. 2/1136/21 and 2/4026/04).

Abstract

Two different problems reflecting brain functioning are addressed: Impact of audio-visual stimulation (AVS) on human EEG and EEG characteristics of human relaxation. Within subtle physiological changes, number of linear and nonlinear measures is examined for their sensitivity. Standard, modified and newly designed EEG measures are employed.

- In order to identify direct, transient, as well as long-term changes in human cortex under influence of repetitive impact of AVS various linear and nonlinear measures were estimated. In the course of 2 months, 25 repetitions of a 20 min AVS program with stimulation frequencies in the range 2-18 Hz were applied to 6 healthy volunteers. EEG data were recorded from 6 head locations during relaxed wakefulness prior, during and after AVS. Entrainment as a direct reaction to AVS was well developed in majority of cases, being strongest in backward regions and spreading also to other cortex locations. Transient effects displayed significant power decreases of beta bands, and increase of theta-1 and alpha-1 coherence in central cortex regions. For long-term effects evolution of examined measures during the whole experiment period was analyzed with respect to the significance of their linear regression. Following changes were observed: increased power in lower frequency bands (4-10Hz) in frontal and central cortex locations, increased spectral decay over the whole cortex, decreased correlation dimension in some locations, and increased frontal inter-hemispheric alpha-1 coherence in contrast to decrease of linear correlation and mutual information. Our results show that regular training with AVS does induce changes in the cortex functioning, such as those commonly reported to be features specific to relaxation or altered states of consciousness. It seems that AVS training could be more effective in inducing long-continuint changes of EEG than regular 20 minute listening to relaxation music.

- Psychophysiological characteristics of psychosomatic relaxation are addressed. Experiment consisted of 88 relaxation sessions of 8 subjects. 6-channel EEG data of 3-minute duration were examined. Firstly EEG characteristics of rest were revealed in a form of linear regression trends. On the contrary to general expectations, during resting conditions - 3-minute session in darkened room in lying position with eyes closed - both alpha-1 and relative alpha-1 powers were decreasing. Decrease of total power over the whole cortex implied gradual diminishing of overall brain activity during the resting process. Then EEG features derived from linear regression model were selected according their ability to discern between more and less successful relaxation. Recordings were categorized into 2 categories formed according to subjective assessments of participants. Quite a few features pointed to lower contribution of the slowest waves (delta-1 range) in some cortex areas as a distinctive characteristic of more successful relaxation. Finally, EEG feature selection for practical recognition of two relaxation classes is presented. Discriminant analysis was employed in a form of Fisher classifier and artificial neural networks. Under restriction to ten feature dimensions, promising results of feature selection yielded total classification error 12 - 16 %.

With permission up to 25 dimension, error of 3 - 4 % was achieved for training set cardinality 0.9. Newly explored relaxation features fill the lack of EEG relaxation characteristics in the literature. The promising results of this exploratory study might progress into EEG descriptors of resting states and in combination with some other non EEG indicators they may contribute to discrimination of relaxation levels. Potential applications involve clinical, pharmacological, self-regulative areas and actual problems with stress management.

Contents

1

Introduction

In the area of psychophysiology two different problems reflecting brain functioning are attacked. These are brain response to audio-visual stimulation and brain characteristics during relaxation. The common aspect of both problems is monitoring of brain activity through electroencephalogram recordings from the scalp.

We provide more detailed introduction to the investigated problems in the individual parts of the thesis; however, here we would like to present basic background for studied problems. Modern medicine applies variety of imaging techniques of the human body. The group of electro-biological measurements comprises variety of methods. From them, electroencephalography is a medical imaging technique that reads scalp electrical activity generated by brain structures. During more than 100 years of its history, encephalography has undergone massive development. Firstly, brain waves were explored and gradually their dependence on physiological conditions was revealed. Waves were classified into different groups according to their wavelength. Nowadays EEG atlases are provided, filled with different brain-waive patterns and respective diagnoses. EEG belongs to established clinical diagnosis tools. However further understanding of brain functioning is still very actual for widening horizons of both theoretical and practical knowledge.

Audio-visual stimulation (AVS) is a simple method for external influence of the brain. Cortex activity might be manipulated to certain extent by brain wave entrainment mechanisms. AVS is rather popular and also experimentally tested for improvements in various clinical conditions. Photic driving response was proven to be useful for investigation of neurological disorders, such as Alzheimer disease, schizophrenia, or depressions.

However, some findings concerning the rhythmic brain activity as a reaction to AVS seem to be inconsistent. The main purpose of the first part of this study was to investigate the effects of AVS on the EEG on the immediate, short-term, and long-term basis. Up to now, most of the EEG research on AVS has focused on direct and short-term effects of AVS (during and shortly after the stimulation). To our knowledge, this is the first study dealing with EEG features under repetitive stimulation sessions during a longer time period.

Reasons for the second part of the study are related to actual problems of stress that is acknowledged to belong to one of the major problems of modern society. While calling for stress reduction, need for stress-monitoring tools might be growing. Analyses of resting status of patients could be related to sleep deprivation or stress reduction problems. Developed method could also be beneficial in development and testing of efficiency of pharmacological substances related to hypnotic and sedative drugs, and for assistance in biofeedback during self-regulative trainings.

There are a few physiological variables, which might be sensitive to level of physical and mental rest. However in the literature we had found no clear characterization of EEG features of relaxation. In order to explore EEG dynamics and basic features during relaxation, our aim was to find the strongest changes in EEG measures during general rest and then to discern beneficial relaxation from unsuccessful relaxation by another EEG features. And finally we present an implementation for recognition of two relaxation categories by means of feature selection and discriminant analysis with Fisher classifier and artificial neural networks.

Moreover, we have utilized both linear and nonlinear approaches for analysis of EEG characteristics. In contrast to the linear description (as e.g., frequency analysis), it is natural to expect that the neuronal dynamics may behave in a non-linear manner. The growing need for a better understanding of brain dynamics and the recent emergence of a physics of non-linear systems have stimulated the development of more advanced data analysis techniques, often referred to as non-linear methods. Traditional signal-processing procedures (as for example Fourier analysis) reflect information about one-dimensional time series. On the other hand, the dynamical view suggests that a single time series may be seen as a manifestation of more-dimensional dynamics of the whole system. Under certain conditions, it is possible to reconstruct behaviour of a dynamical system from a single variable like the single-channel EEG. Then, the reconstructed dynamics is analyzed with non-linear methods. Although the applicability of these techniques to real systems has been questioned repeatedly (Paluš et al., 1999), it is generally accepted that some non-linear measures might be useful if used with care. Complexity measures related to the concept of entropy rates estimation were reported by Rosipal (2001) to be useful for determining depth of anaesthesia. Results by Kobayashi et al. (2000) showed successful discrimination of sleep stages by measure of correlation dimension. AVS examined by Jin et al. (2002) had decreasing effects on EEG complexity, shown by the first positive Lyapunov exponent as one of non-linear measures of complexity. These and similar findings indicate that non-linear measures may be as good or even better in discrimination of brain states, compared to the existing, mainly spectrally based techniques. For comparison of an efficiency of linear and non-linear approaches, we used both of them for EEG data analyses in this thesis.

This work is organized in the following way. In the second chapter history, brain waves, and applications of EEG are introduced. Then EEG measuring techniques are described. After that linear and nonlinear methods for EEG analysis are addressed in the fourth chapter. In the following Part A AVS experiment along with results are addressed. Results are provided for direct, transient, and long-term AVS effects. Part A is concluded by discussion. Part B starts with chapter 6 and it deals with EEG characteristics of relaxation. After methods are described, results are provided for measures' trends reflecting general rest, EEG features capable to distinguish between two relaxation categories, and for feature selection with discriminant analysis of two relaxation classes. Discussion finalizes part B. Then follows sumarization of results and contribution for praxis. The work is concluded by appendixes containing additional illustrations.

1.1 Goals of the thesis

Goal of this thesis is to investigate two psycho-physiological problems:

- Effects of audio-visual stimulation (AVS) on human cortex activity.

- Effects of psychosomatic relaxation.

In the context of the two tasks performance of untraditional EEG measures has to be compared to traditional ones.

Specifically, main tasks of this thesis are listed bellow:

- Revelation of unique EEG characteristics during brain AVS training:

- Impact of AVS directly during stimulation in different frequency bands, and long-term evolution of direct impact.

- Transient effects of AVS (a few minutes after AVS influence) and their time progress.

- Long-term effects of AVS from the perspective of the whole AVS training.

- Investigation of efficiency of linear and nonlinear measures for EEG analysis in the context of AVS.

- Design of modified and new EEG measures.

- Testing the effects of popular AVS device on the subjective states of participants.

- EEG characteristics during human psychosomatic relaxation:

- Regression trends of EEG measures during sensori-motorical rest.

- Selection of EEG features discriminating two relaxation categories based on subjective assessments of participants.

- Classification of the relaxation level: Feature selection with discriminant analysis in a form of Fisher classifier and artificial neural networks.

- Development of complex Octave/Matlab software implementation for EEG processing and analysis.

2

EEG: History, brain waves, applications

Modern medicine applies variety of imaging techniques of the human body. The group of electro-biological measurements comprises items as electrocardiography (ECG, heart), electromyography (EMG, muscular contractions), electroencephalography (EEG, brain), magnetoencephalography (MEG, brain), electrogastrography (EGG, stomach), electrooptigraphy (EOG, eye dipole field). Imaging techniques based on different physical principles include computer tomography (CT), functional magnetic resonance imaging (fMRI), positron emission tomography (PET), and single photon emission computed tomography (SPECT).

Electroencephalography is a medical imaging technique that reads scalp electrical activity generated by brain structures. The electroencephalogram (EEG) is defined as electrical activity of an alternating type recorded from the scalp surface after being picked up by metal electrodes and conductive media (Niedermeyer and da Silva, 1993).

The EEG measured directly from the cortical surface is called electrocortiogram while when using depth probes it is called electrogram. In this chapter we will refer only to EEG measured from the head surface. Thus electroencephalographic reading is a completely non-invasive procedure that can be applied repeatedly to patients, normal adults, and children with virtually no risk or limitation.

When brain cells (neurons) are activated, local current flows are produced. EEG measures mostly the currents that flow during synaptic excitations of the dendrites of many pyramidal neurons in the cerebral cortex. Differences of electrical potentials are caused by summed postsynaptic graded potentials from pyramidal cells that create electrical dipoles between soma (body of neuron) and apical dendrites (neural branches). Brain electrical current consists mostly of Na^+, K^+, Ca^{++}, and Cl^- ions that are pumped through channels in neuron membranes in the direction governed by membrane potential (Atwood and MacKay, 1989a).

The detailed microscopic picture is more sophisticated, including different types of synapses and involving variety of neurotransmitters (Malmivuo and Plonsey, 1995). Only large populations of active neurons can generate electrical activity recordable on the head surface. Between electrode and neuronal layers current penetrates through skin, skull and several other layers. Weak electrical signals detected by the scalp electrodes are massively amplified, and then displayed on paper or stored to computer memory (Tyner and Knott, 1989). Due to capability to reflect both the normal and abnormal electrical activity of the brain, EEG has been found to be a very powerful tool in the field of neurology and clinical neurophysiology.

The human brain electric activity starts around the 17-23 week of prenatal development. It is assumed that at birth the full number of neural cells is already developed, roughly 10^{11} neurons (Nunez, 1995). This makes an average density of 10^4 neurons per mm^3. Neurons are mutually connected into neural nets through synapses. Adults have about 500 trillion (5.10^{14}) synapses. The number of synapses per one neuron with age increases, however the number of neurons with age decreases, thus the total number of synapses decreases with age too. From the anatomical point of view, the brain can be divided into three sections: cerebrum, cerebellum, and brain stem. The cerebrum consists of left and right hemisphere with highly convoluted surface layer called cerebral cortex. The cortex is a dominant part of the central nervous system. The cerebrum comprises centres for movement initiation, conscious awareness of sensation, complex analysis, and expression of emotions and behaviour. The cerebellum coordinates voluntary movements of muscles and balance maintaining. The brain stem controls respiration, heart regulation, biorhythms, neurohormone and hormone secretion, etc.(Fundamentals of Biomedical Engineering. Electroencephalogram, 2002). The highest influence to EEG comes from electric activity of cerebral cortex due to its surface location.

2.1 History

During more than 100 years of its history, encephalography has undergone massive development. The existence of electrical currents in the brain was discovered in 1875 by an English physician R. Caton. Caton observed the EEG from exposed brains of rabbits and monkeys. In 1924 H. Berger, a German neurologist, used his ordinary radio equipment to amplify the brain's electrical activity measured on the human scalp. He announced that weak electric currents generated in the brain can be recorded without opening the skull, and depicted graphically on a strip of paper. The activity that he observed changed according to the functional status of the brain, such as in sleep, anaesthesia, lack of oxygen and in certain neural diseases, such as in epilepsy. Berger laid the foundations for many of the present applications of electroencephalography. He as the first used the word electroencephalogram for describing brain electric potentials in humans. He was right with his suggestion, that brain activity changes in a consistent and recognizable way when the general status of the subject changes, as from relaxation to alertness (Bronzino, 1995). Later in 1934 Adrian and Matthews published the paper verifying concept of "human brain waves" and identified regular oscillations around 10 to 12 Hz which they termed "alpha rhythm" (Bronzino, 1995).

2.2 Brain waves classification

For obtaining basic brain patterns of individuals, subjects are instructed to close their eyes and relax. Brain patterns form wave shapes that are commonly sinusoidal. Usually, they are measured from peak to peak and normally range from 0.5 to 100 μV in amplitude, which is about 100 times lower than ECG signals. By means of Fourier transform power spectrum from the raw EEG signal is derived. In power spectrum occurence of sine waves with different frequencies is visible. Although the spectrum is continuous, ranging from 0 Hz up to one half of sampling frequency, the brain state of the individual may make certain frequencies more dominant. Brain waves have been categorized into four basic groups (Fig. 2.1):

- beta (>13 Hz),
- alpha (8-13 Hz),
- theta (4-8 Hz),
- delta (0.5-4 Hz).

The best-known and most extensively studied rhythm of the human brain is the normal alpha rhythm. Alpha can be usually observed better in the posterior and occipital regions with typical amplitude about 50 μV (peak-peak). According to our experiences alpha was also significant between posterior and central regions in comparison to other regions. Alpha activity is induced by closing the eyes and by relaxation, and abolished by eye opening or alerting by any mechanism (thinking, calculating). Most of persons are remarkably sensitive to the phenomenon of "eye closing", i.e. when they close their eyes their wave

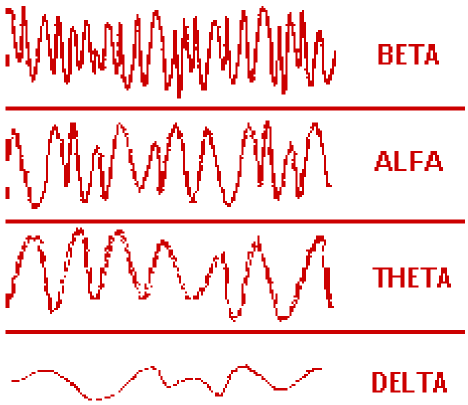

Figure 2.1: Brain wave samples with dominant frequencies belonging to beta, alpha, theta, and delta band.

pattern significantly changes from beta into alpha waves. The precise origin of the alpha rhythm is still not known. Alpha waves are usually attributed to summated dendrite potentials. Evoked potentials (e.g. generated in brain stem) often consist of fibre potentials (axonal) and synaptic components (Bickford, 1987).

EEG is sensitive to a continuum of states ranging from stress state, alertness to resting state, hypnosis, and sleep. During normal state of wakefulness with open eyes beta waves are dominant. In relaxation or drowsiness alpha activity rises and if sleep appears power of lower frequency bands increase. Sleep is generally divided into two broad types: nonrapid eye movement sleep (NREM) and REM sleep. NREM and REM occur in alternating cycles. NREM is further divided into stage I, stage II, stage III, stage IV. The last two stages correspond to deeper sleep, where slow delta waves show higher proportions. With slower dominant frequencies responsiveness to stimuli decreases.

Various regions of the brain do not emit the same brain wave frequency simultaneously. An EEG signal between electrodes placed on the scalp consists of many waves with different characteristics. A large amount of data received from even one single EEG recording presents a difficulty for interpretation.

Individual's brain wave patterns are unique. In some cases, it is possible to distinguish persons only according to their typical brain-wave activity. For example, subjects who regard themselves as rational types or as holistic/intuitive types may demonstrate certain higher activity in their frontal left and frontal right hemisphere respectively.

2.3 Applications

The greatest advantage of EEG is speed. Complex patterns of neural activity can be recorded occurring within fractions of a second after a stimulus has been administered. EEG provides less spatial resolution compared to fMRI and PET. Thus for better allocation within the brain, EEG images are often combined with MRI scans. EEG can determine the relative strengths and positions of electrical activity in different brain regions.

According to R. Bickford (Bickford, 1987) research and clinical applications of the EEG in humans and animals are used to:

(1) monitor alertness, coma and brain death;
(2) locate areas of damage following head injury, stroke, tumour, etc.;
(3) test afferent pathways (by evoked potentials);
(4) monitor cognitive engagement (alpha rhythm);
(5) produce biofeedback situations, alpha, etc.;
(6) control anaesthesia depth ("servo anaesthesia");
(7) investigate epilepsy and locate seizure origin;
(8) test epilepsy drug effects;
(9) assist in experimental cortical excision of epileptic focus;
(10) monitor human and animal brain development;
(11) test drugs for convulsive effects;
(12) investigate sleep disorder and physiology.

Symmetry of alpha activity within hemispheres can be monitored. In cases of restricted lesions such as tumour, hemorhage, and trombosis, it is usual for the cortex to generate lower frequencies. EEG signal distortion can be manifested by reduction in amplitude; decrease of dominant frequencies beyond the normal limit; production of spikes or special patterns. Epileptic conditions produce stimulation of the cortex and the appearance of high-voltage waves (up to 1000 μV) referred to as "spikes" or "spike and wave" (Bickford, 1987). EEG patterns have been shown to be modified by a wide range of variables, including biochemical, metabolic, circulatory, hormonal, neuroelectric, and behavioural factors (Bronzino, 1995). By tracking changes of electric activity during such drug abuse-related phenomena as euphoria and craving, brain areas and patterns of activity that mark these phenomena can be determined.

As the EEG procedure is non-invasive and painless, it is being widely used to study the brain organization of cognitive processes such as perception, memory, attention, language, and emotion in normal adults and children. For this purpose, the most useful application of EEG recording is the ERP (event related potential) technique.

Evoked potentials

Evoked potentials or event-related potentials (ERPs) are significant voltage fluctuations resulting from evoked neural activity. Evoked potential is initiated by an external or internal stimulus (Bickford, 1987). ERPs are suitable methodology for studying the aspects of cognitive processes of both normal and abnormal nature (neurological or psychiatric disorders (Picton et al., 2000)).

Mental operations, such as those involved in perception, selective attention, language processing, and memory, are proceed over time ranges in the order of tens of milliseconds. Whereas PET and MRI can localize regions of activation during a given mental task, ERPs can help in defining the time course of these activations (Facts on ERP, 1995).

Amplitudes of ERP components are often much smaller than spontaneous EEG components, so they are not to be recognized from raw EEG trace. They are extracted from set of single recordings by digital averaging of epochs (recording periods) of EEG time-locked to repeated occurrences of sensory, cognitive, or motor events (Gevins and Rmond, 1987). The spontaneous background EEG fluctuations, which are random relatively to time point when the stimuli occurred, are averaged out, leaving the event-related brain potentials. These electrical signals reflect only that activity which is consistently associated with the stimulus processing in a time-locked way. The ERP thus reflects, with high temporal resolution, the patterns of neuronal activity evoked by a stimulus.

Quantitative electroencephalography

Technological advances increased ability of encephalography to read brain activity data from the entire head simultaneously. Quantitative EEG (QEEG) applies multi channel measurements that can better determine spatial structures and localize areas with brain activity or abnormality. The results are often used for topological brain mapping represented with colour maps in 2D and 3D to enhance visualization.

Brain computer interface

Brain computer interface (BCI) is a communication system that recognizes user's command only from his or her brainwaves and reacts according to them. For this purpose PC or/and subject is trained. Simple task can consist of desired motion of an arrow displayed on the screen only through subject's imaginary of the motion of his or her left or right hand. As the consequence of imaging process, certain characteristics of the brainwaves are raised and can be used for user's command recognition, e.g. motor mu waves (brain waves of alpha range frequency associated with physical movements or intention to move) or certain ERPs.

EEG Biofeedback

The basic mechanism of the feedback is to correct the course of a process, intervening in a previous point of its development or cycle. Originally the knowledge about the operation of the Autonomic Nervous System (ANS) was that it commands a group of unconscious, involuntary and autoregulated biological functions. In the 1960s, the experimental psychologist Miller manifested (Miller, 1971) that some biological functions under the control of ANS could be manipulated and placed under conscious control through instrumental learning. He expected that if there was an indicator revealing the state of some of those functions, it would be possible to condition it, in the same way as it would be possible to condition the functions of the Somatic Nervous System. Biofeedback is a technique to learn voluntary control of physiologic functions of which the subject is usually not aware, with the purpose of recovering, maintaining or improving health and/or performance.

The classical modalities of biofeedback are the electrodermal (skin resistance), thermal, the electromyographic, electroencephalografic (neurofeedback), heart biofeedback, and respiratory biofeedback.

Neurofeedback is a brain biofeedback with online EEG monitoring serving as input information for a subject who is trained. It is suggested that this learning procedure may help a subject to modify his or her brainwave activity. One of the methods involved in neurofeedback training is the so-called frequency following response: Changes in the functioning of the brain in desired way, e.g. increases in alpha activity, generates appropriate visual, audio, or tactile response so that the practitioner can be aware of the right direction of the training.

Biofeedback was reported as promising approach with possible broad application field. Treatment of ADHD, epilepsy, addictions, as well as sleep and learning disorders have been found as most promising applications of EEG biofeedback (Lubar, 1989; Sterman, 1996; Tansey, 1985). Biofeedback in general was either experimentally or routinely applied to: Manifestations of stress, fatigue and syndrome of chronic fatigue, anxious states, phobias, syndrome of panic, obsessive-compulsive disturbance, depression, learning disabilities, especially those related to attention deficit with or without hyperactivity (ADD/ADHD), alcoholism and drug addiction, migraine and tension headaches, chronic back pain, in the nape and shoulders, etc., essential arterial hypertension, heart arrhythmia, muscle problems like sprain, bruxism, repetitive strain injuries, etc., rehabilitation in sequels of stroke (spastic or flaccid), cerebral concussion, cerebral palsy, asthma and allergic diseases, Raynaud's disease, insomnia, fecal and urinary incontinence, self-healing in general. Further to normal (non pathological) conditions as: relaxation, stress reduction, pain management, sleep improvement, enhancement of memory, intuition, creativity, IQ improvement, accelerated learning, peak performance (e.g. for sport), accessing anomalous states of consciousness. Enhancement of the ability to access and maintain different states of physiological arousal (mind states) might alter subjects' mental performance, normalize behavior, and stabilize mood. EEG biofeedback may be also used as a training technique for Brain Computer Interface (see 3.3.3).

Critchley and co. systematically addressed the question of brain activity in relation to a subject's intention to relax, both with and without the aid of biofeedback (Critchley et al., 2001). They used PET to investigate cerebral activity relating to the cognitively driven modulation of sympathetic activity. Their subjects were trained to perform a biofeedback relaxation exercise that reflected electrodermal activity and were subsequently scanned performing repetitions of four tasks: biofeedback relaxation, relaxation without biofeedback and two corresponding control conditions in which the subjects were instructed not to relax. They observed activity relating to the voluntary intent to relax in the left anterior cingulate, globus pallidus and parietal cortex. Activation of the anterior cingulate and cerebellar vermis was specifically associated with the influence of biofeedback on intentional relaxation. Right medial temporal lobe activity, adjacent to the amygdala was related to the recorded rate of sympathetic relaxation across all tasks. According to the authors these functional neuroanatomical findings suggest differential regional contributions to the control of bodily states of sympathetic arousal.

3

EEG measurement

Generally, encephalographic measurements employ a system consisting of

- electrodes with conductive media,
- amplifiers with filters,
- A/D converter,
- recording device.

Electrodes read the signal from the head surface; amplifiers bring the micro volt signals into the range where they can be digitalized accurately, converter changes signals from analog to digital form, and personal computer (or other relevant device) stores and displays obtained data. A set of the equipment is shown in Fig. 3.1.

Scalp recordings of neuronal activity in the brain, identified as the EEG, allow measurement of potential changes over time in basic electric circuit conducting between signal (active) electrode and reference electrode (Kondraske, 1986). Extra third electrode, called ground electrode, is needed for getting differential voltage by subtracting the same voltages showing at active and reference point. Minimal configuration for mono-channel EEG measurement consists of one active electrode, one (or two specially linked together) reference and one ground electrode. The multi-channel configurations for QEEG may comprise up to 128 or 256 active electrodes.

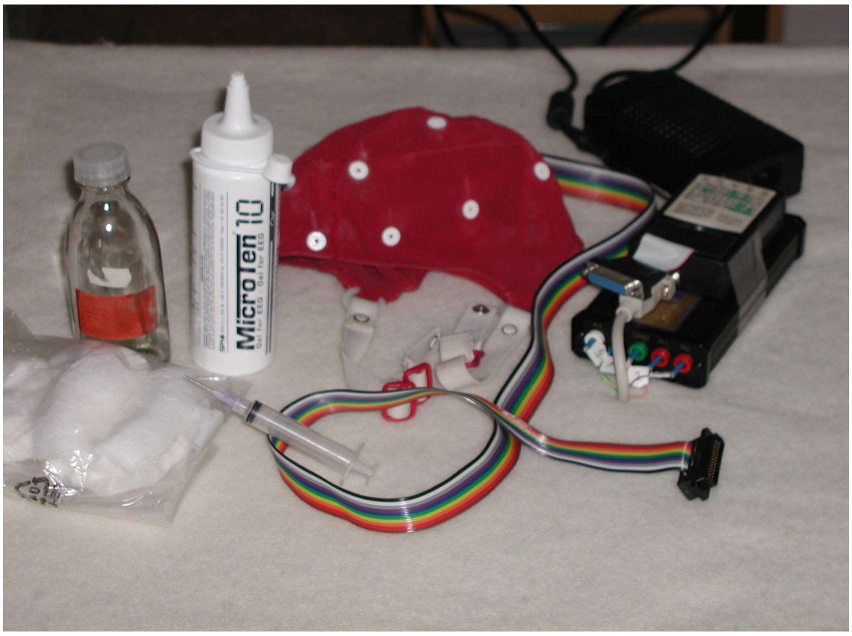

Figure 3.1: Equipment for EEG recording: amplifier unit, electrode cap, conductive jelly, injection, and aid for disinfection.

3.1 Recording electrodes

The EEG recording electrodes and their proper function are critical for acquiring appropriately high quality data for interpretation. Many types of electrodes exist, often with different characteristics. Basically there are following types of electrodes:

- disposable (gel-less, and pre-gelled types)
- reusable disc electrodes (gold, silver, stainless steel or tin)
- headbands and electrode caps
- saline-based electrodes
- needle electrodes

For multi-channel montages, electrode caps are preferred, with number of electrodes installed on its surface (Fig. 3.2). Commonly used scalp electrodes consist of Ag-AgCl disks, 1 to 3 mm in diameter, with long flexible leads that can be plugged into an amplifier (Bronzino, 1995). AgCl electrodes can accurately record also very slow changes in potential (Picton et al., 2000). Needle electrodes are used for long recordings and are invasively inserted under the scalp.

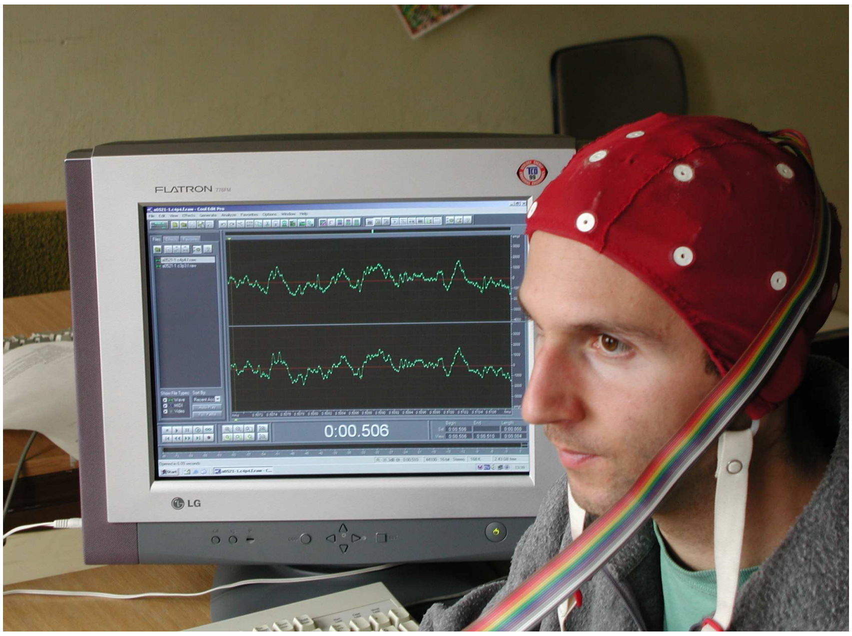

Figure 3.2: Electro cap with electrodes implanted according 10-20 electrode placement system.

Skin preparation differs, generally cleaning of the skin surface from oil and brushing from dried parts is recommended. With disposable and disc electrodes, abrasive paste is used for slight skin abrasion. With cap systems, abutting needle at the end of injection is used for skin scraping, which can cause irritation, pain and infection. Especially when person's EEG is measured repeatedly and cap is mounted for the same electrode points, there is a threat of certain pain and bleeding. That is why the right hygiene and safety protocol should be kept.

Using the silver-silver chloride electrodes, the space between the electrode and skin should be filled with conductive paste also helping to stick. With the cap systems, there is a small hole for injection of conductive jelly. Conductive paste and conductive jelly serve as media to ensure lowering of contact impedance at electrode-skin interface.

In 1958, International Federation in Electroencephalography and Clinical Neurophysiology adopted standardization for electrode placement called 10-20 electrode placement system (Jasper, 1958). This system standardized physical placement and designations of electrodes on the scalp. The head is divided into proportional distances from prominent skull landmarks (nasion, preauricular points, inion) to provide adequate coverage of all regions of the brain. Label 10-20 designates proportional distance in percents between ears and nose where points for electrodes are chosen. Electrode placements are labeled according adjacent brain areas: F (frontal), C (central), T (temporal), P (posterior), and O (occipital). The letters are accompanied by odd numbers at the left side of the head and with even numbers on the right side (Fig. 3.3). Left and right side is considered by convention from point of view of a subject.

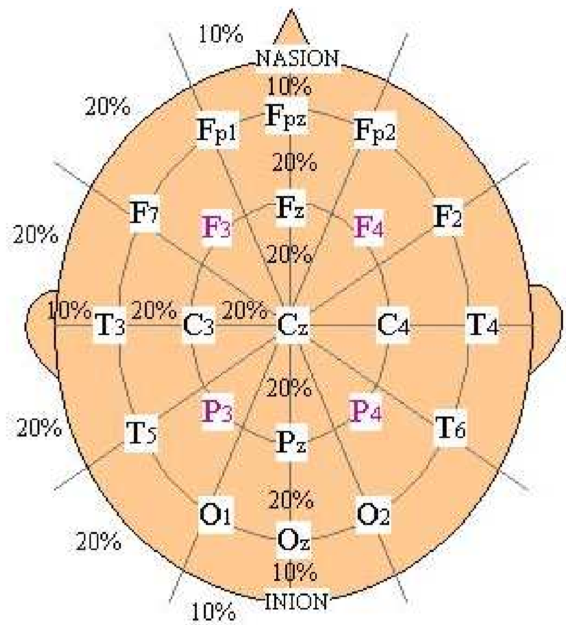

Figure 3.3: Point labels for 10-20 electrode placement system.

As it is known from tomography different brain areas may be related to different functions of the brain. Each scalp electrode is located near certain brain centres, e.g. F7 is located near centres for rational activities, Fz near intentional and motivational centres, F8 close to sources of emotional impulses. Cortex around C3, C4, and Cz locations deals with sensory and motor functions. Locations near P3, P4, and Pz contribute to activity of perception and differentiation. Near T3 and T4 emotional processors are located, while at T5, T6 certain memory functions stand. Primary visual areas can be found bellow points O1 and O2. However the scalp electrodes may not reflect the particular areas of cortex, as the exact location of the active sources is still open problem due to limitations caused by the non-homogeneous properties of the skull, different orientation of the cortex sources, coherences between the sources, etc (Nunez, 1995).

High impedance can lead to distortions that can be difficult to separate from actual signal. It may allow inducing outside electric frequencies on the wires used or on the body. Impedance monitors are built in some commercially available EEG devices. In order to prevent signal distortions impedances at each electrode contact with the scalp should all be bellow 5 $K\Omega$, and balanced within 1 $K\Omega$ of each other. Similar standard is required for clinical use of the EEG and for publication in most reputable journals. Practically, impedance of the whole circuit comprising two electrodes is measured, but built in impedance checks usually display results already divided by two. Control of all impedances is desirable also after finishing every single measurement.

Several different recording reference electrode placements are mentioned in the literature. Physical references can be chosen as vertex (Cz), linked-ears, linked-mastoids, ipsilateral-ear, contralateral-ear, C7 reference, bipolar references, and tip of the nose. Reference-free techniques are represented by common average reference, weighted average reference, and source derivation. Each technique has its own set of advantages and disadvantages. The choice of reference may produce topological distortion if relatively electrically neutral area is not employed. Linking reference electrodes from two earlobes or mastoids reduces the likelihood of artificially inflating activity in one hemisphere. Nevertheless, the use of this method may drift away "effective" reference from the midline plane if the electrical resistance at each electrode differs (Kaiser, 1994). Cz reference is advantageous when it is located in the middle of active electrodes, however for close points it makes poor resolution. Reference-free techniques do not suffer from problems associated with an actual physical reference. Nevertheless referencing to linked ears and vertex (Cz) are predominant.

With modern instrumentation, the choice of a ground electrode plays no significant role in the measurement (Effects of Electrode Placement, 2004). Forehead (Fpz) or ear location is preferred (Collura, 1998), but sometimes wrist or leg is also used. The combination of all active electrodes with reference and ground electrode compose channels. An overall electrode configuration is called montage.

3.2 Amplifiers and filters

The signals need to be amplified to make them compatible with devices such as displays, recorders, or A/D converters. Amplifiers adequate to measure these signals have to satisfy very specific requirements. The basic requirements that a biopotential amplifier has to satisfy are (Nagel, 1995):

- The physiological process to be monitored should not be influenced in any way by the amplifier.
- The measured signal should not be distorted.

- The amplifier should provide the best possible separation of signal and interferences.
- The amplifier has to offer protection of the patient from any hazard of electric shock.
- The amplifier itself has to be protected against damages that might result from high input voltages as they occur during the application of defibrillators or electrosurgical instrumentation.

The input signal to the amplifier consists of five components:

The desired biopotential, undesired biopotentials, a power line interference signal of 50/60 Hz and its harmonics, interference signals generated by the tissue/electrode interface, and noise. Proper design of the amplifier provides rejection of a large portion of the signal interferences. The desired biopotential appears as the differential signal between the two input terminals of the differential amplifier (Nagel, 1995).

The amplifier gain is the ratio of the output signal to the input signal. In order to provide optimum signal quality and adequate voltage level for further signal processing, the amplifier has to provide a gain of 100-100,000 (Nagel, 1995) (the highest need not to be the best, combination of more parameters is involved, e.g. the range of the A/D converter, sampling rate, noise of the used elements) and needs to maintain the best possible signal-to-noise ratio. In order to decrease an impact of electrically noisy environment differential amplifiers must have high common-mode rejection ratios (at least 100 dB) and high input impedance (at least 100 $M\Omega$). The common-mode rejection ratio is the ratio of the gain of differential mode (wanted signal) over the gain of the common mode (original input signal between the inputs and ground).

Special electrically shielded rooms minimize the impact of urban electric background, in particular 50/60 Hz alternating current line noise. For usual medical purposes, shielded room is not necessary. For research purposes when maximal amount of information is desired, shielded room is recommended. Under such conditions amplifiers run on batteries and an optical cable leads to the PC standing outside from the shielded space. In addition to the optical cable, electrical/optical and optical/electrical converters are necessary. Usually information of interest lies bellow this line noise and we can use low-pass filters with cut-off bellow 50/60 Hz, or for keeping higher frequency bands a notch filter can be applied, that is able to reduce only a narrow band around 50/60 Hz (but distorts phases).

When computers are used as recording devices, channels of analog signal are repeatedly sampled at a fixed time interval (sampling interval), and each sample is converted into a digital representation by an analog- to-digital (A/D) converter. The A/D converter is interfaced to a computer system so that each sample can be saved in the computer's memory. The resolution of the converter is determined by the smallest amplitude that can be sampled. This is obtained by dividing the voltage range of the A/D converter by 2 raised to the power of the number of bits of the A/D converter (Bronzino, 1995). A/D converter usually uses minimally 12 bits (discerning 4,096 value levels). Ability to resolve 0.5 μV is recommended (Brunet, Young et al., 2000). Sufficient sampling rate is required, at least double of the highest frequency component of our interest.

Analog (hardware) filters have to be integrated in the amplification unit. A high-pass filter is needed for reducing low frequencies coming from bioelectric flowing potentials (breathing, etc.), that remain in the signal after subtracting voltages toward ground electrode. Its cut-off frequency usually lies in the range of 0.1-0.7 Hz. To ensure that the signal is band limited, a low-pass filter with a cut-off frequency equal to the highest frequency of our interest (Bronzino, 1995) is used (usually in the range from 40 Hz up to less than one half of the sampling rate). Analog low-pass filters prevent distortion of the signal by interference effects with sampling rate, called aliasing, which would occur if frequencies greater than one half of the sampling rate survive without diminishing.

Once data are stored, digital filtering can be used. The strength of the analog filters is limited thus for displaying and processing of the signals further decreasing of DC components is usually needed. It is possible to choose from linear (FIR, IIR) filtering or novel non-linear filtering methods. The choice should be done according to the objectives put on the signal processing. Predominantly finite impulse response (FIR) filters are used which do not distort wave phases. The data points width typically range on the order of 1000 and one of the window function (Blackman, Hanning, Hamming, or rectangular) should be chosen. Filters should be designed in a way to influence useful signal properties minimally.

Before performing the final measurements the whole EEG system should be tested. Inter-channel calibrations with known wave signal parameters should not display significant discrepancies. The output noise (referred to input) consists mainly from the noise caused by the analog amplifier circuitry and by A/D converter circuitry. Noise value should be consistent with manufacturer information, about 0.3-2 μV pp. (range from negative peak to positive peak) but this value depends on the way of noise estimation and on the system configuration (low-pass filter, sampling rate, choice of circuitry). The noise can be determined by connecting the inputs of the amplifier together, or abased them into a salty solution, or "short-circuiting" the inputs, and then measuring the output of the amplifier. The number of useful information bits can be counted as a power of two from the ratio of average EEG signal amplitude over the noise amplitude (e.g. 50μV/1μV results in over 5 bits).

One of the limitations of recordings is due to storage requirements. For example, 1 hour of eight channels 14-bit signal sampled with 500 Hz occupies 200 MB of the memory. Portable recording systems were developed for used during longer monitoring of a subject without limiting movement of a person. Some of the commercial EEG recording systems comes from following suppliers: Lexicor, Electrical geodesics, Biosemi, NeuroScan, Sigma Medizin, Contact Precision Instruments, Stellate, Thought Technology, Xltek.

Here follows the summarization of EEG measurement system components:

- Electrode cap with conductive jelly or Ag-AgCl disc electrodes with conductive paste.
- Amplifiers with overall amplification gain between 100-100,000, with input impedances at least 100 $M\Omega$, and common-mode rejection ratio at least 100 dB.
- Analog filters integrated in the unit with high pass filter with cut-off frequency in the range of 0.1-0.7 Hz and low pass filter with cut-off frequency less than one half of the sampling rate. In fact, frequencies above 50 Hz are rarely involved as they contribute negligibly to power spectrum of EEG.
- At least 12 bit A/D converter with accuracy lower than overall noise (0.3-2 μV pp.), and sampling frequency usually between 128 – 1024 Hz.
- Sufficiently quick PC for taking over data for recording and eventually for online analysis, with adequate volume of hard disc.
- Digital high pass FIR filter with similar cut-off frequency as analog high pass.

The general quality of recording equipment depends on the right combination of the mentioned parameters. Before further data processing, raw EEG signal should be checked for artefacts.

3.3 Artefacts

Scanning for signal distortions belongs to basic evaluation of the EEG traces. Artefacts are usually considered to be sequences with higher amplitude and different shape in comparison to signal sequences that doesn't suffer by any large contamination. The artefact in the recorded EEG may be either patient-related or technical. Patient-related artefacts are unwanted physiological signals that may significantly disturb the EEG. Technical artefacts, such as AC power line noise, can be decreased by decreasing electrode impedance and by shorter electrode wires. The most common EEG artefact sources can be classified in following way:

Patient related:

- any minor body movements
- EMG
- ECG (pulse, pace-maker)
- eye movements
- sweating

Technical: - 50/60 Hz

- impedance fluctuation
- cable movements
- broken wire contacts
- too much electrode paste/jelly or dried pieces
- low battery

Excluding the artefact segments from the EEG traces can be managed by the trained experts or automatically. For better discrimination of different physiological artefacts, additional electrodes for monitoring eye movement, ECG, and muscle activity may be important.

4

Methods for EEG analysis

In this chapter we introduce some of the linear and nonlinear measures we used for EEG signal analysis in chapter 5 and 6. At the beginning methods for analyzing single signals are noted and then methods for quantification of association between pairs of signals are described.

When using methods for biosignal analysis, attention should be kept on difficulties necessarily joint to real biological signals. To obtain characteristics of real physiological signal we face problems of contamination by noise, physiological and technical artefacts and nonstationarity. Stationarity of the EEG signal is a model that is rarely satisfied, especially when longer data segments are considered. For any computational method certain minimal number of data points is needed. If the signal were stationary, longer sequences could be taken with providing appropriate results. On the other hand if nonstationarity of the signal was more significant, loss of ability to extract important features from time series would be present.

Since many features of EEG signals can not be generated by linear models, it is generally argued that nonlinear measures are likely to give more information than conventional linear measures (Quiroga et al., 2002). A recently applied promising methodology of EEG signal processing is based on the theory of nonlinear dynamical systems, information theory, chaos theory and theory of stochastic processes.

4.1 Spectral measures

Well-established methodology to investigate the changes in EEG recordings is based on the transformation of the EEG signal into the frequency domain where inspection of the waveforms belonging to different frequency bands is usually applied.

Linear spectral methods are based on using a spectral transformation such as Fourier Transform. Discrete Fourier transform H_n (Press et al., 1988) from N consecutive sampled values h_k with sampling interval Δ is given by

$$H_n = \sum_{k=0}^{N-1} h_k e^{2\pi ikn/N} \tag{4.1}$$

where n denotes frequency component belonging to frequency

$$f_n = \frac{n}{N\Delta} \tag{4.2}$$

and n runs from 0 to N-1. Practically Fast Fourier transform procedure is applied. One can obtain power spectral density of the signal by taking the modulus-squared of the discrete Fourier transform:

$$P_{f_n} = |H_n|^2 \tag{4.3}$$

Total power spectrum is a sum of power components over the whole spectral interval; 0.5 - 45 Hz in our study. Frequency band power ratio and spectral edge frequency are derived from this transform.

Frequency band powers

Frequency spectrum was divided into 9 bands: delta-1 (0.5-2 Hz), delta-2 (2-4 Hz), theta-1
(4-6 Hz), theta-2 (6-8 Hz), alpha-1 (8-10 Hz), alpha-2 (10-12 Hz), beta-1 (12-16 Hz), beta-2 (16-30 Hz), and gamma (30-45 Hz) and corresponding powers were computed.

Frequency band power ratio

Each power component is an estimate of a power in the frequency interval with width $\frac{1}{N\Delta}$. Usually one is interested in contribution of certain broader frequency interval to total power spectra of the signal. This is quantified through frequency band power ratio of certain frequency band:

$$PR_{f_1,f_2} = \sum_{f_1}^{f_2} P_{f_n} \tag{4.4}$$

where f_n is counted according to 4.2.

Spectral edge frequency

Another measure derived from the estimates of power is spectral edge frequency. It points the frequency f_e, bellow which certain percentage of the total power lies. Under total power overall power between f_{min} and f_{max} is meant. For example for 95% portion f_e is given by

$$\sum_{f_{min}}^{f_e} P_{f_n} = 0.95 \sum_{f_{min}}^{f_{max}} P_{f_n} \tag{4.5}$$

4.2 Linear and nonlinear measures of complexity

For traditional EEG feature extraction signals are described in terms of frequency and amplitude. But already after a first inspection of EEG signals the observer can notice their "complexity". Some signals vary more than others. Some appear extremely random, while others seem to demonstrate certain repetitive pattern. Signal variability or system complexity has been correlated with physiological conditions. These features can be used for comparison across different patient populations, because they are invariant, insensitive to absolute measures such as amplitude and frequency.

The complexity in this context is generally understood to be regularity or predictability of EEG patterns. The periodic repetition of patterns in EEG provides an indication of contribution of deterministic nature of the system influencing the signal. Such systems are considered to have lower complexity compared to systems generating fully random signal which are understood to be highly complex (Rosipal, 2001). When the brain is in normal alert state EEG reflects firing of millions of postsynaptic potentials coming from cortex volume and firing asynchronously. The alert EEG pattern displays virtually no repetitive patterns, no deterministic origin, so it is difficult to detect underlying states of the brain. When the brain activity is diminished, the neuronal activity of the thalamus, that produces an oscillatory activity, synchronizes firing of neo-cortical neurons, coinciding with a decrease in the overall excitability of neo-cortical neurons. This leads to the EEG trace showing more regular behavior with dominant frequencies significantly shifted to lower frequency activities. Irregular, minimally predictable patterns in the EEG are associated with a system of high complexity while regular, more predictable traces of EEG are considered to be less complex. This suggests that measures reflecting changes in regularity and predictability of EEG patterns associated with the transition between different brain states may serve as valuable indicators for these brain changes. Nonlinear complexity measures detect the degree of variability in the EEG signal concentrating on the dynamics of the process.

Complexity measures related to the concept of entropy rates estimation were reported to be useful for determining depth of anaesthesia (Rosipal, 2001). The findings indicate that these measures may be as good or better indicators of depth of anaesthesia in comparison to the existing, mainly spectrally based techniques. Results from work of Kobayashi et al. (2000) showed successful discrimination of sleep stages by measure of correlation dimension. Recognition power of the mentioned methods is dependant on sufficiently expressive changes in EEG pattern. The question is whether these methods may display any useful changes in connection with less striking physiological changes, e.g. during sensorimotorical and mental rest.

Spectral entropy

Spectral entropy is a stochastic complexity measure based on spectral domain. Normalized distribution of power over frequency with respect to the total power spectrum will yield a probability density function (PDF). According to application of Shannon's channel entropy an estimate of the spectral entropy can be counted:

$$H = -\sum_{f} p_f \ln(p_f) \tag{4.6}$$

where p_f is PDF value at frequency f.

The entropy has been interpreted as a measure of uncertainty or system complexity. High uncertainty is due to a large number of processes (e.g. random noise) while low uncertainty is due to a small number of dominating processes (e.g. regular motions) (Rezek and Roberts, 1998). For example randomly distributed noise has high entropy values, while regular motion, such as sinusoids, gives low entropy values.

Histogram-based entropy

Histogram-based entropy estimators are related to Shannon entropy concept that determines the degree of uncertainty or the rate of information acquisition from the given time series. Histogram is constructed from time series values and estimate is calculated as

$$H_{hb} = -\sum_{i} n_i \ln(n_i) \tag{4.7}$$

where the summation runs through all bins and n_i is the histogram value of *i-th* bin. We used this formula for calculation of Shannon entropy and another estimation using further modifications (Moddemeijer, 1989) termed here histogram-based entropy. For the latter, EEG data normalized by their standard deviation were employed whereas for the former, data without normalization were used. The number of bins was set to be equal to the square root of the number of data points.

Correlation dimension

Theory of chaotic systems gave rise to the question whether it is possible to distinguish between fully random processes and processes with deterministic origin but showing high levels of irregularity. Problems with application of methods from chaotic systems are connected with nonstationarity of the EEG, relatively high noise component and other factors. Advantages of new nonlinear methods based on the theory of dynamical systems were shown on known dynamical systems (Lorenz, Henon system, etc.). In spite of the fact, that nonlinearity of majority of biological signals have not been proved (Paluš et al., 1999; Paluš, 1996), nonlinear measures may permit the extraction of characteristics of the EEG signal that quantitatively appeared to distinguish between different brain states.

Some methods of non-linear dynamics are based on Taken's embedding theorem for noiseless systems (Takens, 1981). Phase space reconstruction of the whole system from a single variable x_n can be obtained. According to the embedding theory, under some conditions, the state portrait, topologically equivalent to the original one, can be reconstructed from the signal. A set of delay coordinates is a convenient choice for the reconstruction. State of the system is defined by a point $X_n = (x_{n-m+1}, ..., x_n)$ with embedding dimension m. With assumption that the attractor of the system is a differentiable manifold of dimension D, the embedding with $m \geq 2D + 1$ saves a lot of important properties of the original attractor. In this context complexity of the system is often estimated by the correlation dimension (CD). Correlation dimension of an attractor may be estimated by Grassberger - Procaccia algorithm (Grassberger and Procaccia, 1983). CD may indicate chaos or identify low-dimensional determinism. The geometrical character of the attractor may provide an important information about the system. Correlation dimension is defined as

$$D_2 = \lim_{\epsilon \to 0} \frac{\ln \sum_{i=1}^{N(\epsilon)} p_i^2}{\ln \epsilon} = \lim_{\epsilon \to 0} \frac{\ln C_2(\epsilon)}{\ln \epsilon} \tag{4.8}$$

$C_2 = \sum_{i=1}^{N(\epsilon)} p_i^2$ is the probability that a hyper cube with a size ϵ contains two points of the attractor. It is approximately equal to the probability that the distance between two points of the attractor is less then ϵ. Attractor can be reconstructed by embedding technique. Series of embedded vectors are constructed which elements are m samples taken at intervals of τ samples, i.e. $\mathbf{x}_m(i) = (x_i, x_{i+\tau}, ..., x_{i+(m-1)\tau})$. Correlation sum C_2 may be estimated as

$$C_2(\epsilon) = \frac{2}{N(N-1)} \sum_{i}^{N} \sum_{j>i}^{N} \Theta(\epsilon - \|\mathbf{x}_m(i) - \mathbf{x}_m(j)\|) \tag{4.9}$$

In 4.9 N denotes number of data points, $\mathbf{x}_m(i)$ embedded vectors comprising subsequent data points of a time series, Θ denotes Heaviside function defined in the previous section, and $||.||$ represents usually maximum norm in a phase space of embedded vectors. The embedding dimension m determines the size of the segment which is used to form the embedding vectors and thus the length if the patterns that can be modeled. In order to find correlation dimension from 4.8 we have to plot $\ln C_2(\epsilon)$ as a function of $\ln \epsilon$ and follow the slope of the obtained curve. Expression

$$\nu(\epsilon) = \frac{d \ln C_2(\epsilon)}{d \ln \epsilon} \tag{4.10}$$

is called correlation exponent, and the limit of $\nu(\epsilon)$ for vanishing ϵ represents the correlation dimension.

Reliable estimation of the CD requires sufficient amount of data points. Compromise has to be made between the requirements for a sufficiently long EEG window and stationarity. For stacionarity EEG window of tens of seconds in duration can be regarded as quasi-stationary, depending on subject's behavioral state (da Silva, 1987).

4.3 Linear and nonlinear interdependency measures

In the study of electroencephalographic signals synchronization phenomena have been increasingly recognized as a key feature for establishing the communication between different regions of the brain (Gray et al., 1989). Synchrony is used to denote relations between items of information processed by different locations. Highly synchronized EEG means a high similarity in the wave shape occurring within a given point or period in time. The basic idea is that the similarity of the signal also means similarity in functioning. Interdependence can be evaluated by different measures possessing linear or nonlinear character. Arguments for using non-linear interdependencies based on chaotic toy models were described in (Quiroga et al., 2000). Quiroga et al. (2002) reasoned that in EEG analysis nonlinear synchronization measures might surpass traditional linear methods such as the cross correlation or the coherence function. Non-linear interdependencies (e.g., mutual information) have the ability of being sensitive to every kind of interaction, either linear or non-linear.

For investigation of the cooperation between hemispheres, we estimated linear correlation of paired signals from left and right hemispheres by linear correlation coefficient (Pearson's correlation) and with respect to restriction to certain frequency bands by coherence. As a nonlinear measure with broader scope for evaluating interdependency, mutual information was estimated.

Linear correlation coefficient

For evaluating association between two finite time series $X = \{X_i\}_{i=1}^N$ and $Y = \{Y_i\}_{i=1}^N$ linear correlation coefficient is most widely used:

$$r = \frac{\sum_i (X_i - \bar{X})(Y_i - \bar{Y})}{[\sum_i (X_i - \bar{X})^2 \sum_i (Y_i - \bar{Y})^2]^{1/2}} \tag{4.11}$$

where $\bar{X}$ and $\bar{Y}$ are means of time series X and Y respectively. The value of r lies between -1 and 1, inclusive. It takes on a value of 1, termed "complete positive correlation", when the data points lie on a perfect straight line with positive slope and a value of -1, termed "complete negative correlation" with the negative slope. A value of r near zero indicates that time series X and Y are uncorrelated.

Coherence

EEG coherence estimates the degree of synchrony between the activity of two brain regions, however, the exact relationship of coherence to cortical activity is not known (Reiterer, 2002). Coherence may be used for measuring of level of synchronization in the functioning of the hemispheres. Time series X and Y are divided into M consecutive time windows indexed by j. Then one has to compute spectral powers of chosen frequency band f (between f_{min} and f_{max}) in order to obtain new time series $P^X(f) = \{P_j^X(f)\}_{j=1}^M$ and $P^Y(f) = \{P_j^Y(f)\}_{j=1}^M$. Coherence between two series X and Y is defined as a square from linear correlation of cumulative power spectra:

$$K_{XY}(f) = \left[\frac{cov(P^X(f), P^Y(f))}{[var(P^X(f))var(P^Y(f))]^{1/2}}\right]^2 \tag{4.12}$$

where in the numerator stands covariance

$$cov(P^X(f), P^Y(f)) = 1/M \sum_j^M [P_j^X(f) - \bar{P}^X(f)][P_j^Y(f) - \bar{P}^Y(f)] \tag{4.13}$$

and in the denominator variances expresed as

$$var(P^X(f)) = 1/M \sum_j^M [P_j^X(f) - \bar{P}^X(f)]^2 \tag{4.14}$$

for P^X, where $\bar{P}^X(f)$ denotes mean of $P^X(f)$, and for P^Y alike. Value of coherence ranges from "0" to "1". Coherence "1" means that the corresponding frequency components of both signals are identical and only amplitude and constant phase delay may exist. Coherence "0" means that the corresponding frequency components of both signals are not correlated (Rappelsberger, 2000).

Mutual information

The concept of mutual information was firstly established in the field of communications theory (Shannon and Weaver, 1949). It have been adopted to EEG analysis (Callaway and Harris, 1974) for evaluating certain nonlinear "correlation" between two time series. Mutual information measures the amount of information shared between two time series (Gel'Fand and Yaglom, 1959). For series X and Y it can be counted as

$$MI(X,Y) = \sum_{X_m, Y_n} P_{XY}(X_m, Y_n) log_2 \left[\frac{P_{XY}(X_m, Y_n)}{P_X(X_m)P_Y(Y_n)}\right] \tag{4.15}$$

where $P_X(X_m)$ denotes value of the normalized histogram of the distribution of observed values X_m (all data values included in bin indexed by m) in the first time series X, the same for $P_Y(Y_n)$, and $P_{XY}(X_m, Y_n)$ is the joint distribution of both series (Abarbanel et al., 1996). For independent time series X and Y is MI(X,Y)=0 and otherwise it will take positive values with a maximum for identical signals.

4.4 Development of modified and new measures

After evaluating performance of a number of EEG measures, it was a natural task to use our experiences for improvement, modification and development of new measures that could be more effective or more "sensitive" to changes in EEG. Within this sense three measures follow, from which the last one is our original product.

Spectral edge

From analysis of power band results we considered the fact, that spectral edge at 95 percents of total power need not be the most optimal parameter for spectral edge regarding its ability to capture EEG changes in our experiment. 95% portion was used by Rosipal (2001) as suitable for monitoring physiology of anaesthesia. From analyzes of our long-term AVS EEG data we tried to estimate two other optimal values. Spectral edge is connected to relative band powers. According to significant trends of relative powers covering frequency intervals from delta-1 to alpha-1 and from delta-1 to alpha-2 ranges we chose 61 and 78 % respectively, as these were average values of power contributions in these merged bands. These values are estimates where spectral edge could provide steepest trends, i.e. higher sensitivities for long-term AVS effects.

Spectral decay

Examination of spectral properties may lead to indication wheather data are of deterministic or stochastic nature. Whereas in chaotic systems the power spectrum falls exponentially at high frequencies, in stochastic systems the power spectrum decays via a power law (Sigeti, 1995):

$$P(f) \sim 1/f^{\alpha} \tag{4.16}$$

with f being a frequency. Different types of noise are recognized according to their behavior in frequency spectrum. As an example, white noise with $\alpha = 0$ or random walk time series with power spectrum that decreases as $1/f^2$ can be mentioned. Parameter α is called spectral decay, fractal exponent, or power-law exponent.

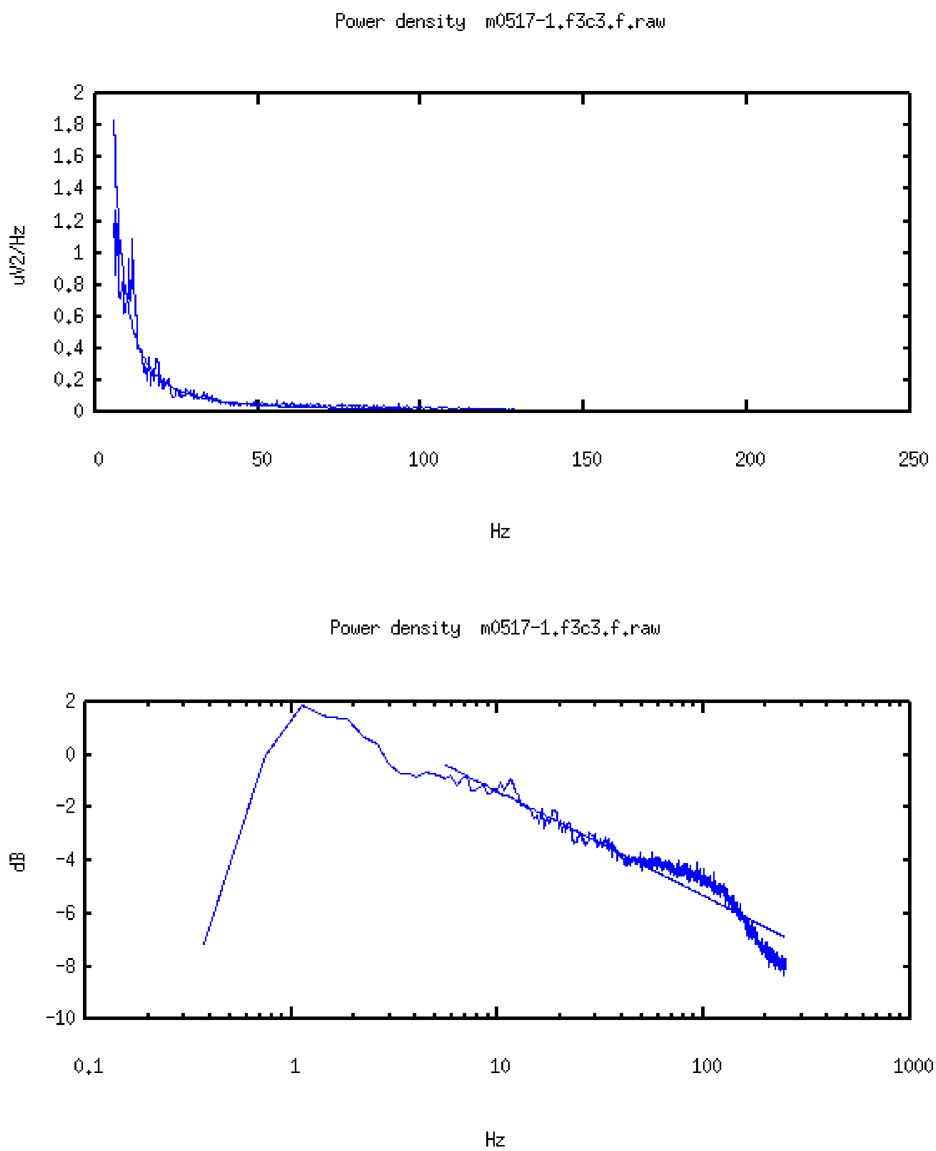

Figure 4.1: Example of EEG power fitted by power-law function. Upper picture: lin-lin view of EEG power, lower picture: log-log view where power fit becomes linear. From 3-minute EEG data from a single session.

Spectral decay is usually not employed in EEG studies. From Fig. 4.1 it can be seen that EEG spectrum may by interpolated by power-law function: On the upper graph a sample of spectral power density in double linear scale is presented, while on the lower graph the same situation in double logarithmic scale is shown. Parameter α is taken as value of spectral decay measure. α is computed as a slope of linear fit of the power spectrum density in the double logarithmic scale.

For our purposes spectral decay may be regarded as one of linear (meant spectrally based) measures of complexity. Lower values of spectral decay reflect higher appearance of higher frequencies. Such signals are considered to be less regular or more complex. Frequency interval 5-250 Hz was taken for determination of α.

Relative length

EEG signal comprises different frequency components oscillating with different amplitudes. The length of the EEG curve reflects appearance of different frequency components to the whole spectrum, reaching higher values in a case when higher frequencies are more contributed.

This was an inspiration for development of a measure that reflects related facts and possesses no other free parameter that should be optimized (e.g. as for spectral edge frequency).

Instead of length of EEG curve it is sufficient to count absolute values of increments in signal amplitude. Thus we define relative length as a sum of amplitude changes between 2 successive data points normed by overall signal standard deviation and by length of time window (no. of data points):

$$RL = \frac{\sum_{i=1}^{N-1} |X_{i+1} - X_i|}{(N-1)SD(X)} \tag{4.17}$$

It should be invariant to signal length, so EEG interval of different length may be compared.

Correction due to different sampling frequency (sr) can be easily made with multiplication by sr_{orig}/sr_{new}, with sr_{new} being a new and sr_{orig} an original frequency. Different reaction to sampling frequency change is expected only if undersampled with loss of important frequency ranges, or when signal to noise ratio is too small. Assuming that EEG signal is well pre-processed, with average value near zero, it is also invariant to multiplication of EEG signal by a constant. With division by overall signal standard deviation relative length is not sensitive to absolute powers but rather to relative powers (4.1).

Relative length is a newly proposed measure evaluating certain kind of complexity of EEG signals. Higher relative length points to higher signal complexity due to increased contribution of higher frequencies. Similarity of relative length measure with tension of the curve used in image processing can be mentioned. Tension is characterized by the first derivatives, in discrete situation it is proportional to $\sum_i |X_i - X_{i-1}|^2$.

Calculation of fractal dimension by Higuchi algorithm (Accardo et al., 1997) is also based on summation of differences of two succesive data points. We compared performance of Higuchi measure with measure of relative length on extensive sleep EEG data. Considerable correlation coefficient (0.83) was found. However, in comparison to all other measures, the advantage of the measure proposed here is much shorter computation time due to its simple formula.

4.5 Subjective assessment

Volunteer's subjective perception of the training process was monitored to set objective changes into the frame of the subjects' experience. Before each day procedure subjects evaluated their general well-being by answering a question "How do you currently feel?". After 3-min relaxation prior to AVS session subjects evaluated their general release accomplished during the relaxation (appendix A, Fig. 8.2). The task was formulated as "Assess a level of your relief accomplished during the prestimulation period.". Both measures were rated on 7-point bipolar scale. Although subjects might interpret these questions slightly differently, relative movements on the scale are supposed to indicate changes of subjects' states. At the beginning and at the end of the whole experiment participants rated their skills regarding ability to relax and expressed their attitude towards effectiveness of AVS machines (appendix A, Fig. 8.1 and 8.3). Specifically, whether they think AVS training may improve person's relaxation abilities.

4.6 Statistical methods

Statistical methods used in Part A (Audiovisual stimulation of the brain):

Evolution of examined measures was tested for obtaining trends in direct AVS effects (section 5.2), trends in transient effects (section 5.3), and for long-term AVS effects (section 5.4). Evolutions of test group averages during the course of the AVS training were calculated for each followed measure. For these 25-data-point time series linear regression model $Y = a + bX + e$ was derived, where X is the explanatory variable, Y is the dependent variable, slope of the line is b, a is the intercept, and e is residual - a random variable with zero mean. Its significance was tested by an ANOVA F-test (Anděl, 1985). The significance criterion was $p \leq 0.05$ (testing for H_0: $b = 0$ against H_1: $b \neq 0$). For consistency at a personal level, we have added another criterion for considering any trend as significant: Maximally one of the subjects could have opposite trend compared to significant group-average trend. For significant trends distribution of residuals from regression model was checked by Shapiro-Wilk test for normality.

For long-term AVS effects, between-group comparison was implemented again by linear regression F-test, here testing for slopes, $H_0 : b^{AVS} = b^{control}$ against $H_1 : b^{AVS} \neq b^{control}$, with treshold p $\leq$ 0.05. Trend of control group was considered as significant again only when curve of average measure had significantly different slope from the flat one plus both subjects from control group had their trends in the same direction (increase or decrease).

For exploring of the transient AVS effects (section 5.3) data recorded after AVS were compared to those recorded before AVS. Differences in individual measures during post stimulation period in respect to prestimulation period were examined by Wilcoxon matched-paired test (Anděl, 1985). In each group there were 25 values obtained as inter-person averages with the respect to the number of the session. For significant change at personal level Wilcoxon test appeared to be too strong critetion, thus we used as a treshold for significancy the following weaker criterion: Majority of increases or decreases from 25 pairs of values had to correlate with the group direction (increase or decrease).

Statistical methods used in Part B (EEG characteristics during relaxation):

More criteria were used to determine the strongest trends during 3-minute periods (section 6.2). One of them was again F-test of linear regression. The new one, residual relative change, is introduced in section 6.1.

Then we needed to distinguish two relaxation classes by appropriate EEG features (section 6.3). Parametric and nonparametric tests were utilized. The first of them was two-sample student's t-test, testing for equality of means with assumption of unequal variances (heteroscedastic t-test) (Anděl, 1985). By t-test we determined whether two sample means are equal, within requirements of normally distributed data. As only part of our data held this condition, for the rest of data we used nonparametric Kruskall-Wallis test for data violating normality (Anděl, 1985). It is able to distinguish any data on the basis of rank order, but for normally distributed data t-test is more suitable as it is stronger than Kruskall-Wallis test.

Finally, our goal was to classify EEG features into two groups formed according to subjective assessment of relaxation (section 6.4). Fisher discriminant analysis was employed as one of the methods within feature selection procedures. Further description can be found in section 6.1.

5

Audio-visual stimulation of the brain (Part A)

Throughout history, several studies were interested in the effect of external stimulation on the cortical EEG, predominantly in photic driving response (response to visual stimulation) (Adrian and Matthews, 1934; Walter and Walter, 1949; Townsend et al., 1975; Pigeau and Frame, 1992). Interest in using visual and auditory rhythmic stimulation as a means of inducing relaxation and hypnosis was raised in the middle of the last century (Morse, 1993). More recently devices using light and sound at specified frequencies were used to "drive" the EEG towards certain frequencies. In the last decades audio-visual stimulation has been reported as an effective method for relieving dental anxiety (Morse, 1993), to induce hypnagogic states (Dieter and Weinstein, 1995) helping to relieve tension and migraine headaches (Solomon, 1985; Anderson, 1989), and for therapeutic effect on premenstrual syndrome (Anderson et al., 1997). AVS was reported to improve behavioral and cognitive functions of learning disabled boys (Carter and Russell, 1993), may alleviate the cognitive dysfunctions in connection with closed head injury (Montgomery et al., 1994), and damages from aneurysms and strokes (Russell, 1997). Photic driving response was proven to be useful for investigation of neurological disorders, such as Alzheimer disease, schizophrenia, and depression.

AVS is a simple method to influence the brain from sensory channels. AVS primarily activates brain centers for sound and visual processing. From all sensory channels the visual channel is predominantly used by humans. Primary visual cortex serves as sensory area for visual input. It is situated mostly on the medial wall of the hemispheres at the occipital pole (area V1, Fig. 5.1), covering both sides of the calcarine sulcus. Visual analysis proceeds along many paths in parallel. It is treated in the visual association cortex located around the occipital poles (area V1 and V2). Form analysis continues in several other zones (including V3) and the highest level of cortical form discrimination, e.g. responding to complex generic forms such as faces, is located in the inferior temporal lobe (Atwood and MacKay, 1989b). Thus brain activity connected with visual processing can be measured from the adjacent scalp locations O1,O2, and T3,T5,T4,T6 (Fig. 5.4).

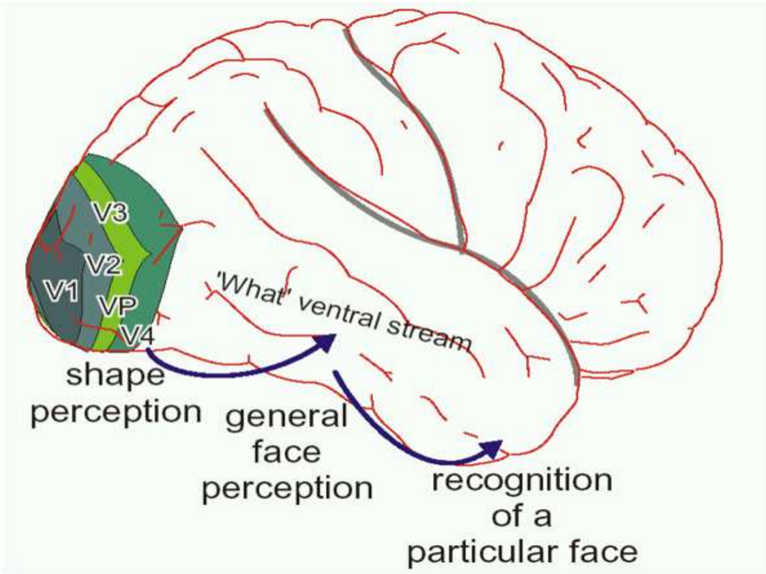

Figure 5.1: Localization and areas of the Primary (V1) and Secondary visual cortex.

Regions of auditory cortex located in the superior temporal lobe, are responsible for recognition of sound patterns, allowing interpretation of environmental sounds and of speech. From the inferior colliculus auditory signals run to the medial geniculate nucleus (part of thalamus). Tonotopic organization of the colliculus is retained there. Further one part of the medial geniculate nucleus, laminated ventral division, projects to the primary auditory cortex while other division projects to surrounding association areas. The primary auditory cortex is a small area deep within the lateral sulcus. It is divided into a series of isofrequency strips. The auditory association cortex is located behind the primary cortex and it functions as processor of complex sounds with combination sensitive neurons (Atwood and MacKay, 1989b).

Brain electrical activity resulting from sensory stimulation is referred to as an evoked potential (EP) or event-related potential (ERP). ERP are usually modeled as signals superimposed, without interaction, on background of ongoing EEG. A rapid change in a sensory stimulus evokes a transient evoked potential. If this stimulus occurs repetitively at a rate high enough to prevent the EPR from returning to a baseline state, the elicited response is called a steady-state evoked potential (SSEP)(Regan, 1989). A distinctive feature of the visual steady-state evoked potential (SSVEP) is that it comprises sinusoidal components at stimulus frequency and its harmonics. The latency of the response with the SSVEP, elicited by an unstructed flicker (low spatial frequency) in the range 7 to 15 Hz is approximately 200 to 275 milliseconds. In this case the signal comprises a frequency spectrum with several peaks, while stimulus in the form of an alternating checkerboard (high spatial frequency) consists of only one frequency maximum.

The mechanism organizing the rhythmicity of spontaneous EEG activity is still not clear. There are assumptions, that the cortex is able to synchronize its own neuronal activity because of its intracortical wiring connections through inhibitory interneurons (Weiss, 1994). On the other hand subcortical generators or pacemakers, like the thalamus or ascending reticular activating system (Birbaumer and Schmidt, 1999), may interplay with cortical "pacemakers" and together bring rhythmicity into existence.

In the situation with SSEP one may observe under certain conditions, in addition to mechanisms mentioned above, adaptation of the brain waves to external stimuli. The simplest expectation may be that EEG components caused by repetitive stimulation would be superimposed to a spontaneous EEG pattern. But typical ERP amplitude is about 2 μV, while typical amplitude of spontaneous ongoing EEG is about 25 μV (in alpha regime). One may assume that there isn't present just a simple additional effect but that mechanisms governing neuronal activity are sensitive enough to be entrained by repetitive low amplitude ERPs. Under "entrainment" of the brain waves this kind of resonant effect is understood. As the ensembles of neurons are able to synchronize their activity without external stimulus, small repetitive input may after a certain adaptation period synchronize their firing thresholds.

At least two parallel and complementary visual processing pathways exist, the so called P and M systems beginning with P and M retinal ganglion cells. Each of them is efficient for different scope of contrast and changes in luminescence. Low-frequency SSVEP are more likely to provide information about general mechanism directing both, driven and spontaneous rhythmic activity. The topography of the low-frequency SSVEP is generally characterized by amplitude maximum in occipitoparietal region. The phase topography of many subjects has shown one or more sharp 180 degree phase discontinuities between neighbouring measurement points. Several models have proposed explanation for these effects. Nunez brought attention to the possibility of travelling and standing waves mediated by rapidly conducting long corticocortico fibers. This model suggests that a sinusoidal drive may permit standing or travelling waves, depending on the specific features of cortical neuroanatomy and damping. Structured sinusoidal visual stimulus, with its more restricted projection to the striate cortex, is more likely to yield travelling waves. In contrast, an unstructed sinusoidal stimulus, with its more extensive cortical projections is more likely to allow interference and thus standing waves (Nunez, 1995).

Salansky et al. (1998) studied entrainment due to visual stimulation in the range of 1-20 Hz with frequency increment 0.4 Hz. They found resonance activation only for 20% of stimulation frequency values. Several studies have suggested that photic driving response has a more diffuse character on cortical EEG, not only in the occipital regions. In visual stimulation experiments conducted by Rosenfeld one group of subjects did not produce a photic driving response within the alpha band while low-baseline alpha participants showed transient AVS effects (Rosenfeld et al., 1997). Timmermann found that the overall effects of AVS in the alpha range on the cortical EEG did not have a significant effect on the corresponding alpha activity of the cortex (Timmermann et al., 1999). Preservation of alpha rhythm shortly after photic driving was reported by Sakamoto et al. (1993).

AVS examined by Jin et al. had decreasing effects on EEG complexity, shown by the first positive Lyapunov exponent as a nonlinear measure of complexity (Jin et al., 2002). Brauchli and co. used rhythmic audio-visual stimulation programs with different intensity of stimuli. They investigated how varying sensory input can affect mood, autonomic arousal, and electrocortical activity. Contribution of the alpha band decreased similarly during all their stimulation programs. Programs affected mood and autonomic variables differently, but not electrocortical variables. They interpreted the higher activation of the right hemisphere during all programs as an indication that audio-visual stimulation does induce changes in the brain, such as are commonly found in altered states of consciousness (Brauchli et al., 1995).

AVS may serve as a useful tool for possible clinical applications of neurofeedback therapy, serving as an adjunct method for priming desired cortical frequencies. Basically there are two ways how to try to attain brain pattern with desired features (e.g. increase of certain frequency band). One way is passive training with AVS. The second way is to observe ongoing EEG pattern and their characteristics and behaving according to them, called EEG biofeedback. One of the questions still remaining is whether AVS, EEG biofeedback training alone, or a combination of both AVS and EEG biofeedback is more effective to entrain EEG rhythms.

5.1 Materials

Subjects

Six right-handed healthy subjects (2 females and 4 males) volunteered for the audio-visual stimulation (AVS) training. Participants ranged in age from 24 to 39 years, with a mean of 25.5 years, s.d. 5.1 yrs., and 2 subjects (1 female and 1 male, aged 24 and 39 years) created the control group. They did not have any known neurological deficit and were not taking any drugs known to affect the EEG. The participants gave their written informed consent prior to their inclusion in the experiment.

Audio-visual stimulation

Overall training of each subject from the test group consisted of 25 AVS program sessions, each of 20-minute length. Each person attended only one session per working day. Due to weekends or other exceptional events, separation between stimulations could be prolonged to several days. During the session subject was lying in a darkened, electrically shielded room. AVS was provided by commercially available Voyager XL light and sound synthesizer. The device consisted of headphones and glasses with red light-emitting diodes connected to a portable unit providing various programs for AVS stimulation. We chose a program described as suitable for AVS beginners to make acquaintance with different "mind states" according to their frequency profile performed. This AVS program stimulated the brain at following frequencies (Fig. 5.2): 17 Hz during the first 3 minutes, then fast decrease to 10 Hz and slower decrease to 8 Hz during min. 4-8, again fast decrease to 5 Hz during min. 8-9, slower decrease to 4 Hz during min. 9-10, steady 4 Hz during next 3 minutes followed by decrease to 2 Hz during min. 13, steady 2 Hz during min. 14-17, and then stepwise return through 5,9 to 15 Hz at min. 17-20. Sound beats of a particular frequency were produced from 3 sine-wave pulses with close frequencies around 280 Hz. Visual stimulation was provided by rectangular red light pulses with a number of switches determining the stimulation frequency. This series was chosen to introduce a sequence of beta, alpha, theta, and delta frequency ranges to participants.

EEG recording

As we were interested in the changes in resting EEG, data from 3-minute period were recorded prior to each AVS training. Subjects were instructed to keep their eyes closed

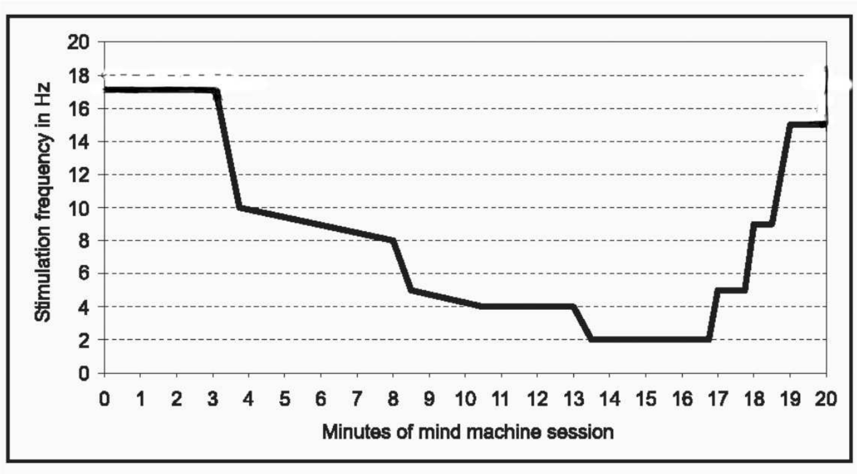

Figure 5.2: Scheme of frequency characteristics of stimulation procedure during one AVS session.

and relax both physically and mentally. After initial EEG recording, headphones and glasses were placed over the electrode cap and the participants were instructed to stay released and to follow the AVS (Fig. 5.3). Participants themselves adjusted brightness and loudness at the beginning of each AVS session to avoid their discomfort from too intense stimulation but yet to maintain stimulation to be effective enough. Subjects were provided with AVS for 20 min, with simultaneous EEG recording. After the stimulation, a post-session EEG during relaxed wakefulness with closed eyes was recorded for another 3 min. In the control group, volunteers took part in the same measurement procedure but instead of AVS they listened to relaxation music. The lying position during the EEG measurements was comfortable enough to avoid unwanted activities and to diminish the occurrence of some artifacts caused by feeble motion. On the other hand, the subjects sometimes fell asleep as the room was designed to be darkened and noiseless.

Unipolar EEG montage comprised eight channels with electrodes placed on F3, F4, C3, C4, P3, P4, O1, O2 locations according the International 10-20 system. The reference electrode was located at Cz and the ground electrode at Fpz point (Fig. 5.4).

A standard cap system (Electro Cap Inc.) with Ag-AgCl electrodes was employed. In order to prevent signal distortions, impedances at each electrode contact with the scalp were kept below 5 $K\Omega$, and balanced within 1 $K\Omega$ of each other.

Our EEG recording unit processed the following parameters: Number of channels: 8, amplifying gain: 402, sampling frequency: 500 Hz, A/D converter resolution: 16 bits, input resolution: 0.46 μV, noise: max 4.1 μV pp.(0.07 to 234 Hz), low pass filter: 234 Hz (-3dB),

Figure 5.3: Subject during audio-visual stimulation session.

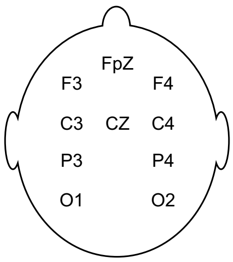

Figure 5.4: EEG montage used in this study: Active electrodes are placed at F3, F4, C3, C4, P3, P4, O1, O2 and reference and ground electrodes at Cz and Fpz points, respectively.

high pass filter: 0.07 Hz (-3dB). A digital high pass FIR filter with cut-off at 0.75 Hz, with the width of 3000 data points, and with a Blackman window was utilized.

From the 8-channel signal between active electrodes and reference electrode six difference signals F3C3, F4C4, C3P3, C4P4, P3O1, and P4O2 were derived by off-line transformation in order to avoid undesirable effects of common reference electrode.

The total of 3200 electroencephalograms were analyzed first by online visual control of the ongoing EEG in 8 channels and later by off-line analysis. Sequences contaminated by either subject-related or technical artefact and obvious sleep occurrences were excluded by eye inspection and according to the subject's assessment. For the purpose of this study, about 1200 3-minute electroencephalograms recorded prior to AVS trainings were employed. As the raw EEG was digitalized at 500 Hz, each 3-minute series contained 90000 data samples. A digital high pass FIR filter with cut-off at 0.75 Hz and with width 3000 data points and Blackman window was utilized.

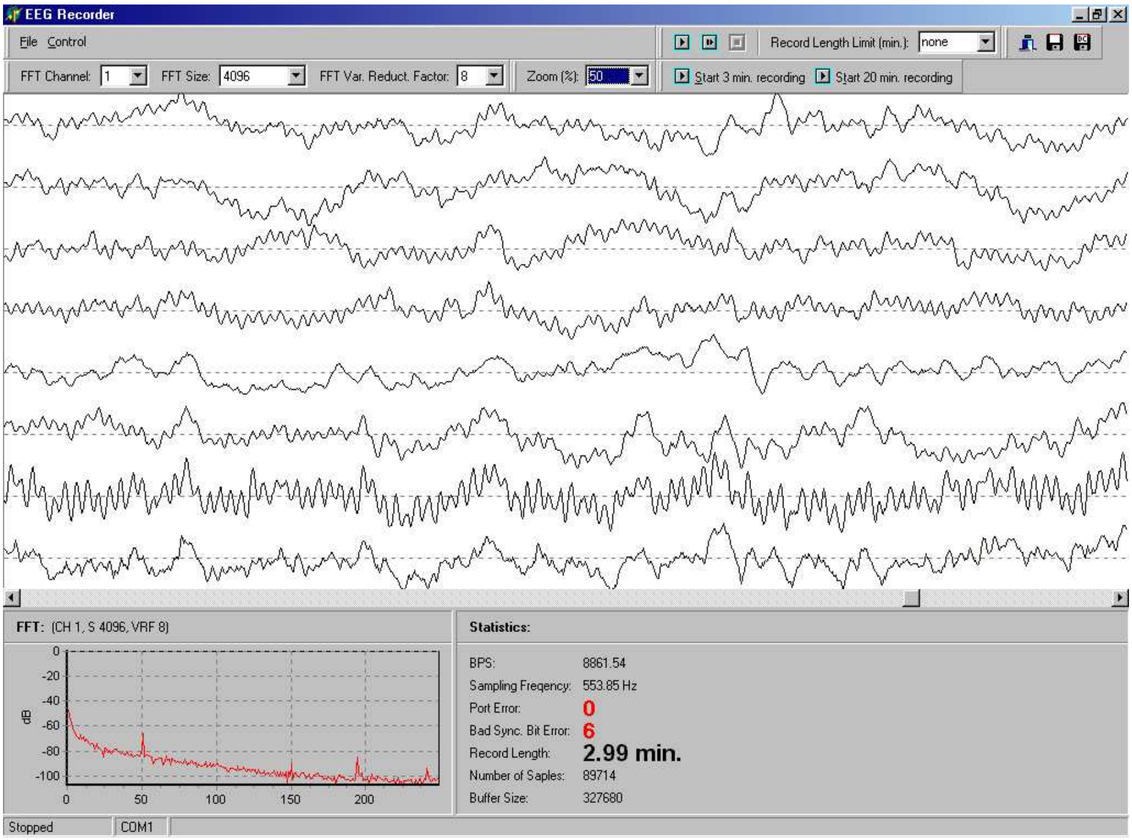

Figure 5.5: User interface for recording software enabling to display 8 channel EEG with online monitoring of power spectrum.

Measurement apparatus

For EEG recording we worked with two systems of amplifiers. The first system was manufactured by P. Krakovský and adapted according to our requests. The second device was commercially available NRS-2D (Lexicor medical technology, Inc.). Their technical parameters are sumarized in the table 5.1. Software for data recording was made by our colleague S. Štolc. This tool enabled us to observe 8 channel EEG with online monitoring of power spectrum (Fig. 5.5).

Table 5.1: Technical parameters of the amplifying units.

	Unit I	NRS-2D
No. of channels	8	2
Amplifying gain	402	8,000
Sampling frequency	500 Hz	128 Hz
A/D converter resolution	16 bits	12 bits
Noise [μV pp.]	max 4.1 (0.07 to 234 Hz)	max 2.5 average (0.5 to 32 Hz)
Low pass filter	234 Hz (-3dB)	32 Hz
High pass filter	0.07 Hz (-3dB)	0.5 Hz
Resolution	0.46 μV	
Input impedance		greater than 1 $G\Omega$
Notch filtering	-	60/50 Hz (Factory Definable)
Artifact rejection	-	automatic/adjustable

We chose the first unit for EEG amplifying and recording of the EEG data due to its higher number of channels and higher sampling rate. The second unit we used for electrode impedance checking and for preparational purposes.

5.2 AVS: Direct effects

Direct effects were mainly analyzed by relative powers in particular frequency bands. From the whole 20-minute stimulation period we used time windows with stable stimulation near 17, 4, and 2 Hz and a time window with unstable stimulation in alpha range. In order to observe only the first harmonics of stimulation response we used narrow frequency windows designated as "17 Hz" (17.3-17.43 Hz), "4 Hz" (3.81-3.94 Hz), and "2 Hz" (1.87-2.0 Hz). Broader frequency window 8-12 Hz was chosen for testing degree of entrainment within alpha range (marked as "10 Hz"), because stimulation in this range did not hold stable frequency.

Question of entrainment was researched through changes of situation compared to non-stimulation conditions. For the reference state we chose data prior to stimulation. From these 3 -minute resting intervals relative powers of the same narrow frequency bands were computed, resulting in reference values for each subject and session. Entrainment of brain waves was evaluated as a ratio of relative powers in narrow frequency bands comprising stimulation frequencies (17, 4, 2, and 10 Hz in separate time windows) to respective relative powers obtained from prestimulation sessions. Average reference relative powers through all persons and all cortex locations were 0.2 (SD=0.11) μV^2 for "17 Hz", 0.5 (0.36) μV^2 for "4 Hz", 1.5 (0.91) μV^2 for "2 Hz", and 34.9 (20.9) μV^2 for "10 Hz" ranges.

Brain-wave entrainment

Brain response to stimulation varied considerably. In Fig. 5.6 we present one of more apparent case of brain wave entrainment during stimulation procedure depicted in 5.2. Sensory input from AVS device comprised besides basic and also higher harmonic characteristics (schematic Fig. 5.2 consists only from basic frequencies). The reason is that visual input was rectangular due to sharp switches of LED diodes. Cortex reacted with angular output with several harmonic frequencies as well (Fig. 5.6). In this figure also occurence of preserved alpha waves is visible there (broad discontinuous stripe within 10-12 Hz).

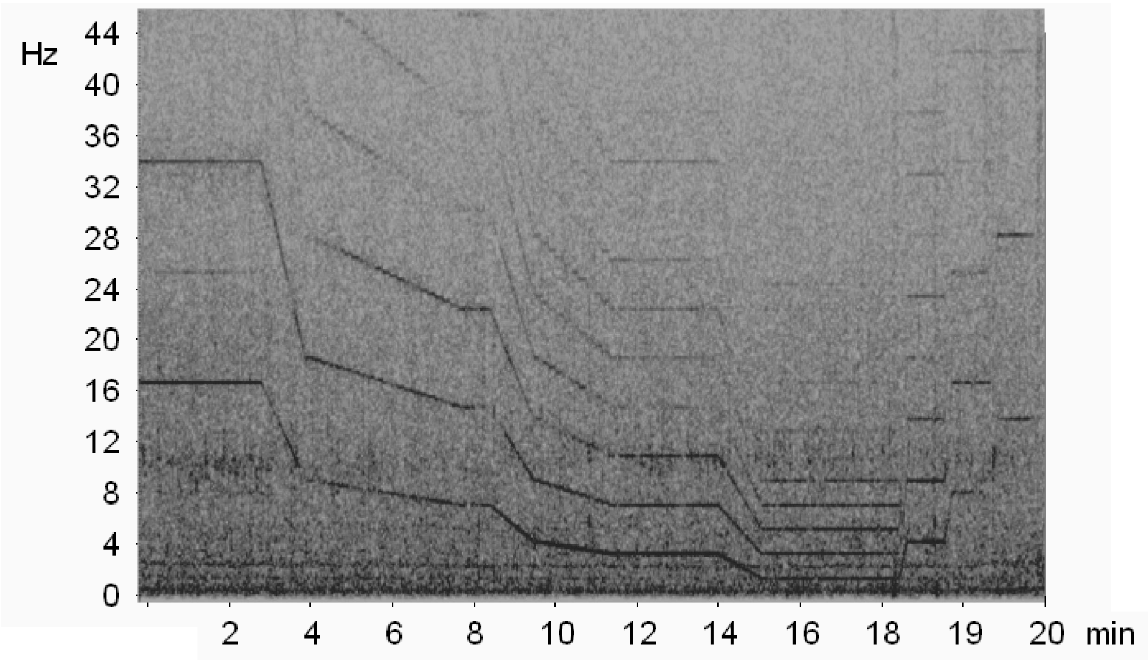

Figure 5.6: Sample of successful brain wave entrainment: Dominant frequencies (dark) versus time of a single EEG recording from occipital cortex region. Cortex was able to follow the course of stimulation. Multiple traces belong to higher harmonics due to angular input signal.

Direct reaction to AVS was well developed in majority of stimulation sessions. In Tab. 5.2 averaged entrainment values for all artefact-free data (across persons and sessions) are displayed. Relative powers in ”17 Hz”, ”4 Hz”, and ”2 Hz” increased in all cortex location. The highest increase was observed in occipital part as visual cortex is located there. It is apparent that from these regions the specific rhythm spread as far as to frontal areas of the cortex. Without focusing on mechanism of spreading (generally synaptic or volume conductance), its attenuation is notable in the table. In frontal region average reaction was attenuated from 4 to 7-times. The highest increase of average relative band power, 30 times, occured in the right occipital location during 17 Hz stimulation (Tab. 5.2). Single session maximum occured in left backward region during 17 Hz stimulation as well, reaching 217-times higher relative power compared to prestimulation period (Fig. 5.7).

Table 5.2: Comparison of relative band powers in narrow frequency bands. Ratio of powers from data during stimulation to powers from data prior to stimulation. Results for different head regions and for averages through all persons and their sessions. Standard deviations are provided in parentheses.

stimulation	ratio of relative band powers					
	F3C3	F4C4	C3P3	C4P4	P3O1	P4O2
17 Hz	4.7 (3.2)	4.1 (3.2)	12.3 (12.1)	12.6 (16.1)	27.3 (29.7)	30.1 (35.9)
4 Hz	3.3 (2.7)	3.1 (2.3)	17.6 (20.6)	13.7 (11.9)	24.4 (21.1)	26.4 (22.7)
2 Hz	2.0 (1.2)	1.8 (1.2)	5.8 (7.9)	4.5 (3.9)	8.8 (7.5)	8.8 (6.0)
10 Hz	0.9 (0.4)	1.0 (0.6)	0.8 (0.3)	0.7 (0.4)	0.8 (0.4)	0.9 (0.5)

Table 5.3: Ratio of total powers (0.5-45 Hz) during stimulation to total powers prior to stimulation for different stimulation frequencies. Averages through all persons and their sessions. Standard deviations are provided in parentheses.

stimulation	ratio of total powers					
	F3C3	F4C4	C3P3	C4P4	P3O1	P4O2
17 Hz	0.9 (0.5)	1.0 (1.0)	1.1 (0.9)	1.1 (0.8)	1.2 (0.8)	1.0 (0.4)
4 Hz	1.4 (1.9)	1.6 (2.6)	1.1 (1.0)	1.3 (1.4)	1.6 (1.0)	1.5 (0.9)
2 Hz	1.6 (2.2)	1.6 (1.5)	1.2 (1.2)	1.3 (1.1)	1.5 (1.2)	1.6 (1.2)
10 Hz	1.0 (1.0)	1.1 (1.0)	0.9 (0.6)	1.0 (1.0)	1.1 (0.6)	1.1 (0.7)

Interestingly, total power during stimulation increased in majority of average cases, with the highest increases of 1.6-times during 2 and 4 Hz stimulation in frontal and backward cortex locations (Tab. 5.3). It means that the whole cortex was excited by stimulation.

For closer inspection of single unaveraged cases we displayed boxplots to follow variability in AVS/rest ratio. In boxplots median, 25-th and 75-th percentiles, minimal, and maximal values are depicted. From boxplots in Figs. 5.7 - 5.9 we might see that variability of cortex reaction was considerable, with extreme values not always in occipital regions. For "4" and "2" Hz regimes maxima lie in central cortex region.

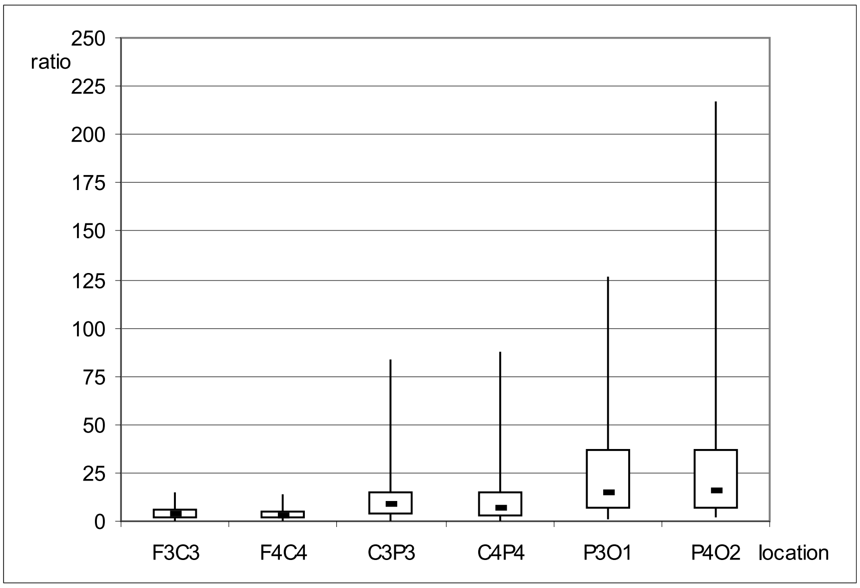

Figure 5.7: Boxplots for comparison of relative powers in 17 Hz narrow frequency band from data recorded during stimulation to data recorded prior to stimulation. Six different cortex regions are presented.

For quantification of a number of single sessions in which brain wave entrainment was attained accounted all cases where the AVS/rest ratio exceeded certain treshold value. In Tab. 5.4 there are displayed percentages of the cases when this ratio exceeded value of 1.5. It is apparent again, that the most successful entrainment is connected with EEG originating in occipital areas as the dipole sources directly reacting to visual stimulation are localized just there. Further apart from these sources the level of entrainment is diminishing. The number of sessions with at least 1.5-time increase of respective relative powers was registered from almost full number of cases (95-100%) in occipital regions to 46-85% in frontal regions.

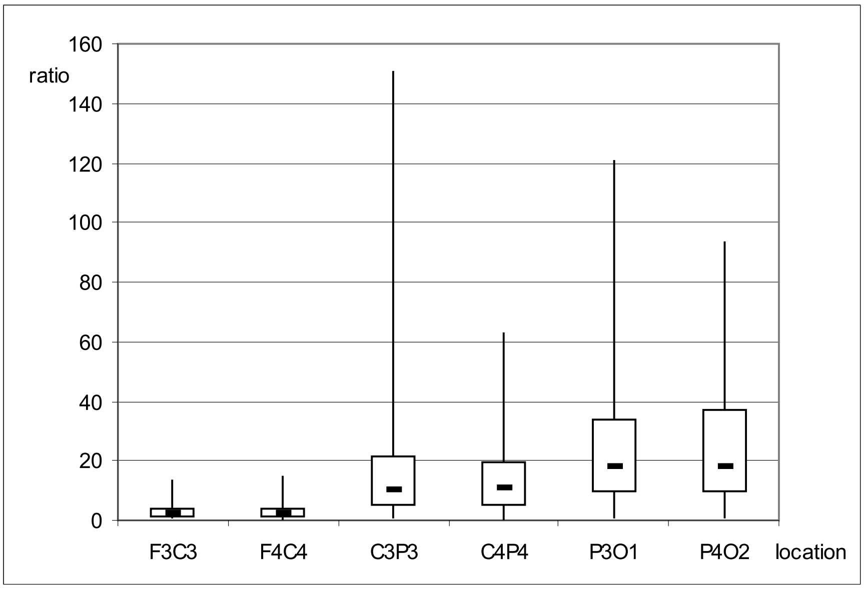

Figure 5.8: Boxplots for comparison of relative powers in 4 Hz narrow frequency band from data recorded during stimulation to data recorded prior to stimulation. Six different cortex regions are presented.

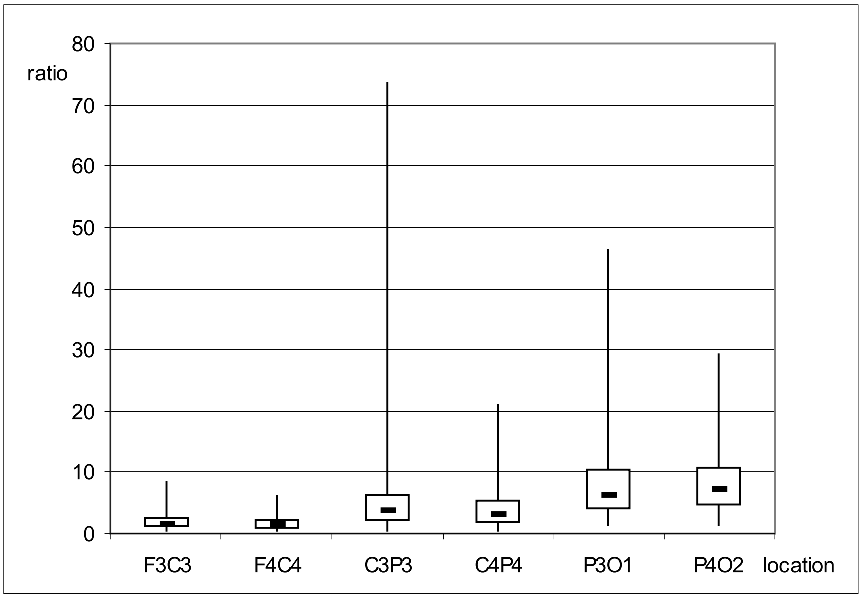

Figure 5.9: Boxplots for comparison of relative powers in 2 Hz narrow frequency band from data recorded during stimulation to data recorded prior to stimulation. Six different cortex regions are presented.

Table 5.4: Entrainment in different frequency bands: Percentage of sessions considered as successful entrainment. Criterion was a ratio of each session relative powers in narrow frequency bands from data during stimulation to data prior to stimulation.

band location	F3C3	F4C4	C3P3	C4P4	P3O1	P4O2
17 Hz	85.5	81.7	96.8	91.1	97.5	100
4 Hz	71.8	72.5	98.4	94.1	97.5	99.1
2 Hz	55.6	46.8	84.9	85.1	95.1	99.1

Also Lazarev et al. (2001) found that driving response varied with frequency and was demonstrable in majority of cases (70-100%) of children and adolescents; according to criterion peak amplitudes 20% larger than neighbouring frequencies. They observed the strongest response in alpha and theta range. In our case "17" and "4" Hz entrainments were stronger than "2" Hz entrainment. This is in agreement with general knowledge on SSVEP. SSVEP evoked by lower stimulation frequencies have longer time gaps to return to baseline state and thus interfering more with spontanous EEG activity.

As AVS consists from two components of stimulation, we also tested importance of audio stimulation and visual stimulation separately. Sources of auditory evoked potentials (EP) are located in temporal cortex and in auditory brainstem structures. We checked out an immediate reaction of audio stimulation on other than temporal locations. There was no apparent influence on FC, CP, neither PO areas within stimulating frequency range. While reaction to visual stimulation was apparent: Spreading of dominant peaks at stimulation frequency also to other head locations (FC, CP, and PO) was observed. This seems to be in accordance with literature (Zahradníková, 2004); we have found the notion on spreading of visual EP, but non on audio EP spreading.

Regarding subjective experiences, quite often participants reported different pleasant and colorful visions during certain stages of the stimulation session. Sometimes personal reminiscences surfaced. In one subject unbearable body feelings arose, so that he considered to withdraw from the experiment.

Trends in entrainment

For analyzing evolution of the entrainment for specific stimulation frequencies during the whole experiment period we examined trends of relative powers at group (inter-subjects averages) and subject's level. The most significant increases were observed during 4 Hz stimulation in central and occipital locations (Fig. 5.10). Response to "2" Hz increased in central cortex locations C3P3 and C4P4. Stimulation by alpha frequencies decreased in central and occipital right regions.

Table 5.5: Schematic depicting of rising (↗) and decreasing (↘) trends during AVS at specific frequencies.

band/ location	F3C3	F4C4	C3P3	C4P4	P3O1	P4O2
17 Hz	-	-	-	-	-	-
4 Hz	-	-	↗	↗	↗	-
2 Hz	-	-	↗	↗	-	-
10 Hz	-	-	-	↘	-	↘

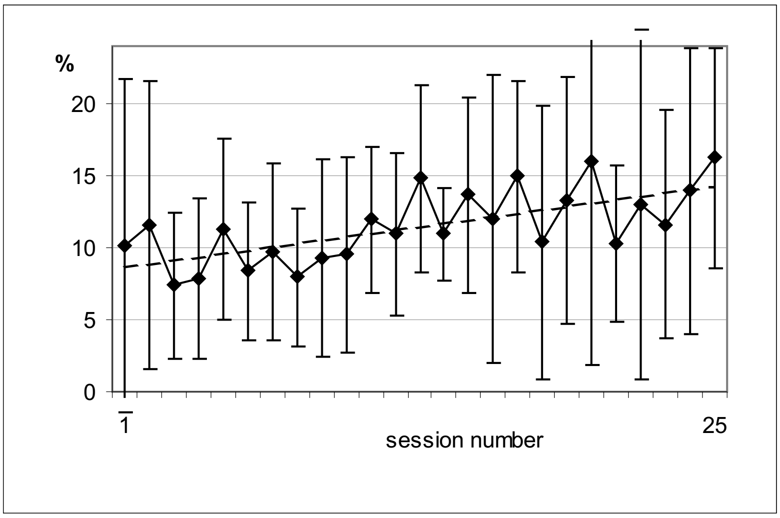

Figure 5.10: Evolution of relative power in narrow frequency band around 4 Hz (0.13 Hz width) in P3O1 location during 4 Hz stimulation (standard deviation depicted by bars).

5.3 AVS: Transient effects

For purpose of exploring transient effects of the stimulation, data recorded after AVS were compared to those recorded before AVS. In the following paragraphs we present transient effects and their evolution during the course of the experiment.

Transient effects

We examined differences in individual measures during post stimulation period in respect to prestimulation period. Wilcoxon matched-paired test was chosen to quantify differences between two groups (section 4.6). For significant change at personal level weaker critetion was applied (see section 4.6).

The strongest changes in spectral domain occurred in higher frequency bands 12 - 45 Hz across all cortex regions. Absolute power from this interval decreased after stimulation in comparison with period prior to stimulation.

Attenuation of beta-1 power in C3P3 ($p < 0.0005$), C4P4 ($p < 0.0005$), P3O1 ($p < 0.0005$), and in P4O2 ($p < 0.0005$) was observed compared to prestimulation period, beta-2 power in F3C3 ($p < 0.0005$), C3P3 ($p < 0.017$), C4P4 ($p < 0.038$), P3O1 ($p < 0.0005$), and in P4O2 ($p < 0.0005$); gamma in F3C3 ($p < 0.0005$), F4C4 ($p < 0.0005$).

Other spectral changes were found in spectral edge 95, a decrease in P4O2 ($p < 0.043$), and in spectral entropy, a decrease in P3O1 ($p < 0.0005$).

EEG complexity displayed a decrease with Shannon entropy in C3P3 ($p < 0.006$) and increase with correlation dimension in C4P4 location ($p < 0.03$).

Positive shifts were obtained for interdependencies evaluated synchronization between left and right hemisphere in both lower and higher frequency ranges. Overall interhemispheric cooperation slightly improved in wider frequency spectrum, inspite of the fact that both linear correlation and mutual information did not shift significantly.

The strongest increase was revealed for coherence in theta-1 band in central and parieto-occipital ($p < 0.0005, 0.012$) areas, alpha-1 coherence increase in central ($p < 0.0005$) and beta-2 coherence increase in frontal regions ($p < 0.039$).

Subjective measure evaluating general release accomplished during the second relaxation period indicated subjectively better relaxation performance compared to the first resting interval ($p < 0.002$).

For the whole collection of the results see appendix B, Fig. 8.4. Results from transient

AVS effects might be interpreted in the following way: Power attenuation in beta range may be understood through the fact that during post AVS resting session subjects were already lying for 25 minutes in darkened room with eyes closed. Their resting state differed from their normal conscious brain state more than that during resting session prior to AVS. Thus their conscious was altered from wake one connected with activity in beta domain. Similar results were obtained also from the control group. After half of an hour of resting participants felt significantly better, which was reflected in a rise of subjective evaluation of general release during the second relaxation period compared to the first relaxation period.

Trends in transient effects

From values of each individual measure obtained after AVS we subtracted values obtained prior to stimulation. Trends during the whole training process were tested by significance of nonzero slope in linear regression model (the same statistical test as used in evaluation of long-term AVS effects).

From spectral measures significant increase of absolute power in beta-1 (12-16 Hz) occured in F4C4 ($p < 0.003$) and decrease in C4P4 ($p < 0.01$) locations. Higher number of significant trends was found within relative band powers: Increase in theta-1 and theta-2 bands, increases in beta-1 and beta-2 in frontal channels (for the whole collection of the results see appendix B, Fig. 8.6 and 8.7).

Spectral entropy increased on the right side of the cortex (F4C4, C4P4, and P4O2 locations; $p < 0.027, 0.0028, 0.04$). Spectral decay increased in F4C4 area. From complexity characteristics we found that Shannon entropy significantly decreased in F4C4 region ($p < 0.046$), which was opposed by increase of correlation dimension in the same area ($p < 0.01$).

Connectivity between hemispheres in parieto-occipital region strengthen gradually, as both interdependency measures *linear correlation coefficient* and *mutual information* increased significantly ($p < 0.006, 0.036$). Increases were obtained for coherence in alpha-1 band in central regions ($p < 0.003$), and beta-1 coherence in central and parieto-occipital areas ($p < 0.0003, 0.005$).

Subtraction of the subjective measures that evaluated general release accomplished during the first and the second relaxation period showed no significant trend.

Summarisingly, mainly positive development of relative powers in 4-8 Hz and 12-30 Hz range, and in various coherences were found. These results may indicate that subjects, as the training progressed, were able to utilize sessions in some respect more effectively.

5.4 AVS: Long-term effects

Our aim was to uncover statistically significant trends in examined measures. Evolutions of test group averages during the whole course of the AVS training (i.e. two month) were calculated for each individual measure. Only EEG data of 3-minute duration prior to stimulation were taken. For these 25-data-point time series linear regression model $Y = a + bX + e$ was derived, and its significance was tested by an ANOVA F-test (section 4.6). Besides this, criterion for consistency at personal level was added (see section 4.6).

Spectral measures

In this section we present only absolute band powers, as there was higher number of significant trends from them than from relative power bands. In the appendix there are presented significant trends from both absolute and relative power bands. For the whole collection of the results see appendix B, Fig. 8.8 and 8.9.

We discovered significant trends in the contribution of lower frequencies and in the measure of right hemisphere activation. Significant increase of power in theta-1, theta-2, and alpha-1 band was observed in frontal and central regions. While theta-1 and theta-2 displayed significant increase in F3C3 (F(1,23) for all, $p < 0.04$ and $p < 0.0004$), C3P3 ($p < 0.002$ and $p < 0.008$), and C4P4 ($p < 0.024$ and $p < 0.0002$) locations, alpha-1 showed increase in all four areas F3C3 ($p < 10^{-5}$), F4C4 ($p < 2.10^{-5}$), C3P3 ($p < 0.0004$), C4P4 ($p < 5.10^{-5}$)(Fig. 5.12). Other significant trends were decrease of delta-1 power in C3P3 ($p = 0.046$), increase in alpha-2 in F3C3 ($p < 0.009$) and in C3P3 ($p < 0.04$), increase of beta-2 in C3P3 ($p < 0.007$) and C4P4 ($p < 0.0004$), increase of gamma in C4p4 ($p < 0.001$) and decrease in P3O1 ($p < 0.005$)(Fig. 5.12).

Other significant trends were decrease of delta-1 power (C3P3), increase of alpha-2 (F3C3, C3P3), increase of beta-2 (C3P3, C4P4), increase of gamma (C4p4), and decrease of gamma (P3O1), however these changes were not generally so extensive as changes in ranges mentioned above. A sample of spectral density shift in various frequency bands is presented in Fig. 5.11.

In spite of the fact that in parieto-occipital regions we did not detect rise of lower frequencies (apendix Fig. 8.9), the spectral edge 95 significantly decreased in P3O1 ($p < 0.0006$) and P4O2 ($p < 3.10^{-5}$) locations of the cortex (both approximately from 22.5 to 19 Hz) (Fig. 5.12). Spectral edge 61 increased in C3P3 ($p < 0.035$) and decreased in P4O2 ($p < 0.0024$). Spectral edge 78 increased in C3P3 ($p < 0.0011$).

The increase of lower frequency bands (4-10Hz) may correspond to findings on physio-

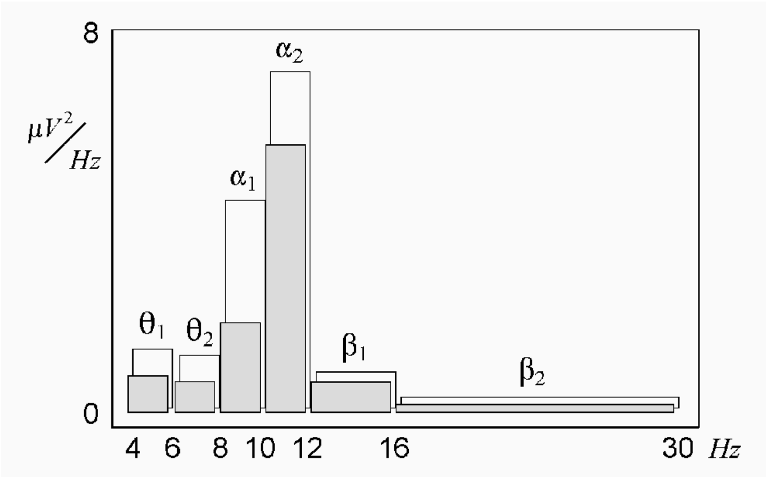

Figure 5.11: Spectral density of absolute power in C4P4 location after the whole experiment (white) compared to initial values (grey). 3-minute data prior to stimulation, group averages. The most expressive increase was observed in alpha-1 band.

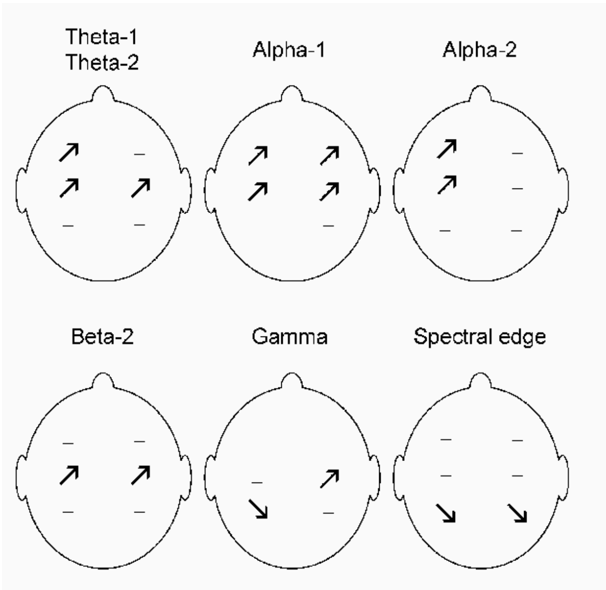

Figure 5.12: Illustration of significant trends in spectral measures across cortex regions. Complete spectral results are presented in appendix B (Fig. 8.8).

logical rest during meditation obtained by Aftanas and Golocheikine (2001), that reflects emotionally positive state and internalized attention. According to Basar et al. (2001) theta and alpha rhythms might reflect fundamentally different functional operations. A concept of 'selectively distributed theta system' was proposed by him, covering structures located in different brain areas able to produce theta activity spontaneously or as a reaction on external or internal stimulus. Theta might deal with integrative cognition and association functions and in frontal cortex also with response-controlling function: Increased theta power implies decreased reaction of the cortex to sensory stimulation (Basar et al., 2001). Increase of alpha rhythms might be functionally correlated to several types of cognitive, sensory and motor behavior (Schurmann and Basar, 2001).

In order to find out whether any long-term effect depending on relative alpha strength occurred, we divided participants into high and low-baseline alpha group according to initial values of their alpha band power ratio. In contrast to Rosenfeld et al. (1997), participants from the low-baseline alpha group didn't change their alpha band power ratio distinctly from participants from the high-baseline alpha group.

Total power (0.5-45 Hz) increased significantly in central region C4P4 ($p < 0.03$). Also in all other areas power increased (Fig. 5.13), which resembles findings of general increase of total power during sleep onset observed by Ogilvie et al. (1991). We detected left-right asymmetry of total power distribution in central cortex locations as well. Moreover, its dynamics during the whole course of the experiment displayed a shift from the left to the right hemisphere (Fig. 5.13). The phenomenon of enhancing the right hemisphere activation was reported to be state-effect linked to altered states of consciousness (Graham, 1977). The more detailed view on the frequency bands uncovered that the same power shift was apparent in central cortex regions in theta-2 and alpha-1 bands: During the training weeks the dominant activity of dipole sources in frequency interval 6-10 Hz moved from the left side to the right side of the cortex. In experiment without training done by Pereda et al. (1999) were found interhemispheric differences during waking in the alpha band: values from the right hemisphere were higher than those from the left one.

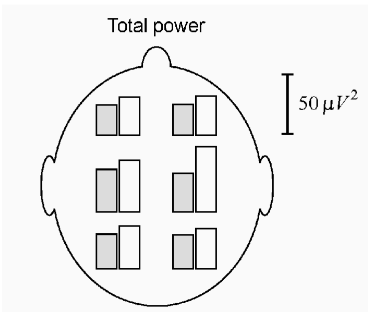

Figure 5.13: Progress of the total power during the whole training (from grey to white). 3-minute data prior to stimulation, group averages. The shift from the left to the right side activation during the course of the experiment in central region is apparent.

Linear and nonlinear complexity measures

Spectral entropy as a linear complexity measure significantly increased in C3P3 ($p < 0.005$) during the training period (Fig. 5.14).

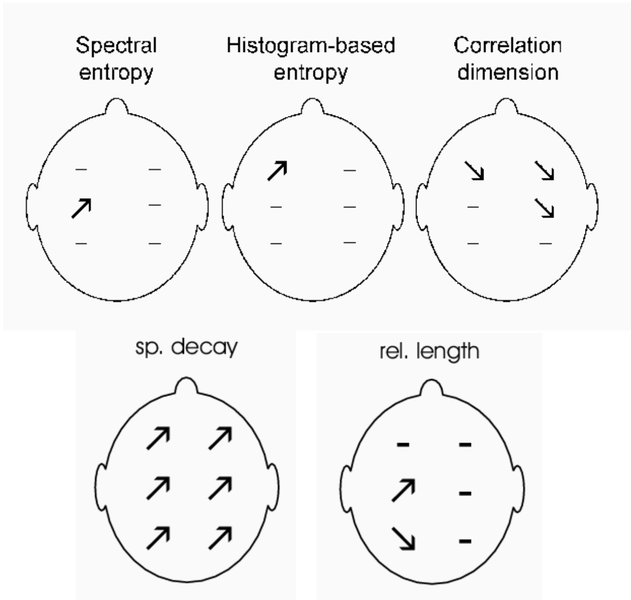

Figure 5.14: Illustration of significant trends in complexity measures across cortex regions. Complete complexity results are presented in appendix B (Fig. 8.9).

Spectral decay appeared to be one of the most successful measures for detecting long-term AVS changes. Strongly significant increases in all six cortex regions were obtained: F3C3 ($p < 5.10^{-6}$), F4C4 ($p < 4.10^{-5}$), C3P3 ($p < 7.10^{-8}$), C4P4 ($p < 4.10^{-8}$) (Fig. 5.15), P3O1 ($p < 3.10^{-7}$), and P4O2 ($p < 3.10^{-5}$). Relative length showed to be sensitive in some locations, as it increased in C3P3 ($p < 0.026$) and decreased in P3O1 ($p < 0.0024$) area.

Increase in both histogram-based entropy estimators was obtained in F3C3 location ($p < 0.048$) (Fig. 5.14). Topologically wider changes occurred also in the correlation dimension that decreased in all six locations, significantly in three of them: F3C3 ($p < 0.0007$), F4C4 ($p < 3.10^{-5}$) (Fig. 5.16), and C4P4 ($p < 0.0007$) (Fig. 5.14).

These decreasing trends correspond to some previous findings. Some authors reported decreasing values of CD with deepening of the level of sleep and the level of anaesthesia (Rosipal, 2001; Kobayashi et al., 2000). Aftanas and Golocheikine (2002) found a decrease in dimensional complexity estimate over midline frontal and central regions during medi-

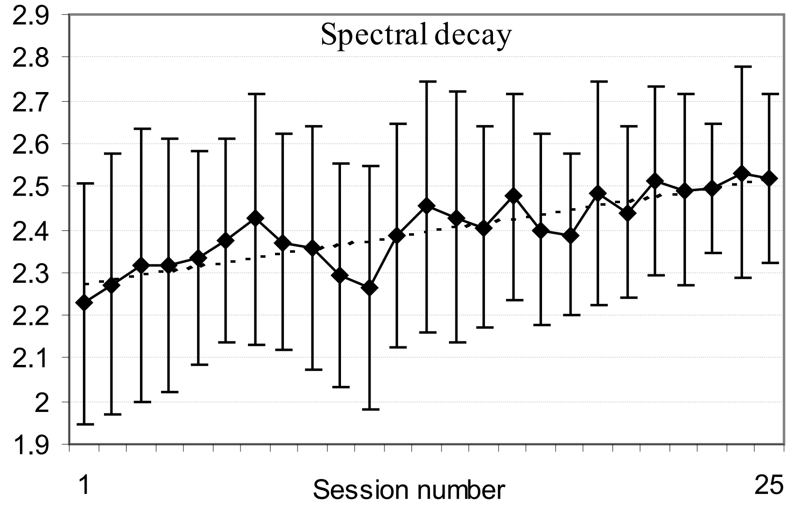

Figure 5.15: Evolution of spectral decay in C4P4 location (standard deviation depicted by bars).

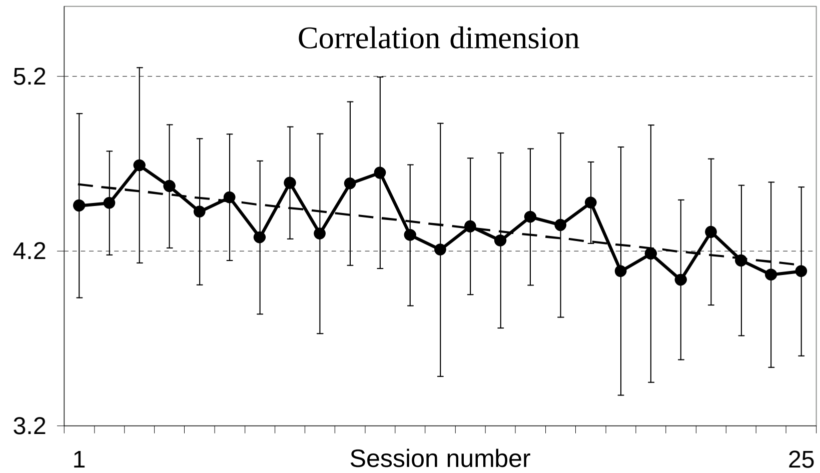

Figure 5.16: Evolution of correlation dimension estimates in F4C4 location (standard deviation depicted by bars).

tation. Elbert et al. (1994) found reduced CD in those areas in which networks became actively engaged.

In contrast, Jeong (2004) interprets reduced EEG complexity in connection with Alzheimer's disease as diminished information processing of the cortex due to the inactivation of previously active networks or a loss of dynamical brain responsivity to external stimuli.

Anyhow, claims of low-dimensional dynamics in brain behaviour have to be taken with very much scepticism. In spite of the fact that most estimates of low dimension from complex experimental data seem to be artefacts (most often artefacts due to small data set (Krakovska, 1995)), estimated CD is expected to provide a valuable relative, generic measure of the dynamical complexity of a signal. In this study, we tried to avoid problems with small data set size (we used 87,000 points) and with the effect of low pass filtering (our measuring device fully covered frequency band from 1 to 100 Hz). As a result, a significant indication of relatively low values of CD about 3-6 was found.

Theiler (1986) and other authors have shown that changes in some spectral properties of data, especially in correlations, may lead to spuriously low estimates of dimension. In accordance with these findings, we suppose that the observed decreasing trends in correlation dimension behaviour relates to the increase of power in alpha and theta bands.

Consequently, we treat CD not as an indicator of low-dimensional dynamics but only as a relative measure of changes in the course of the experiment.

We used a number of complexity measures of different origin. As it can be seen from Fig. 5.14 some of them seem to correlate to higher extend, e.g. correlation dimension and spectral decay. Their negative correlation may be supported by both theoretical and empirical arguments. It is also known that spectral decay should correlate with fractal dimension that was not used in this study. However, some other measures from Fig. 5.14, that were treated as complexity measures in this study, seem to point to different directions, probably due to their different origins and hence different properties regarding their reactions to EEG changes.

Interdependency measures

Interhemispheric interdependency measures namely *linear correlation coefficient*, *mutual information*, and *coherence* were evaluated between fronto-central (F3C3-F4C4), centro-parietal (C3P3-C4P4), and parieto-occipital (P3O1-P4O1) locations. Both linear correlation coefficient and mutual information significantly decreased in parieto-occipital parts ($p < 0.006$ and $p < 0.007$) (Fig. 5.17). Mutual information appeared to be almost two times more sensitive in relative change from initial values than linear correlation (28% vs. 16% decrease).

Principal match of both trends confirms that interhemispheric relationship was mostly of linear type. This is in agreement with findings of Pereda et al. (2001) and Breakspear and Terry (2002) stating that nonlinear interdependencies occur infrequently in normal human EEG.

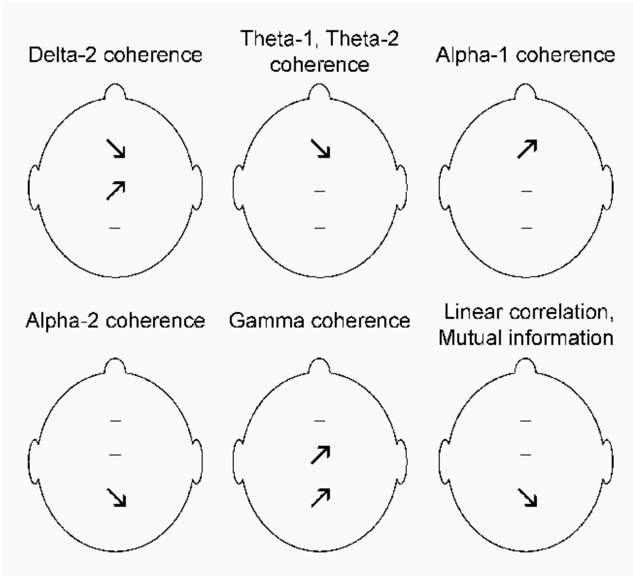

Figure 5.17: Illustration of significant trends in interdependency measures across cortex regions. Complete results for interdependencies are presented in appendix B (Fig. 8.9).

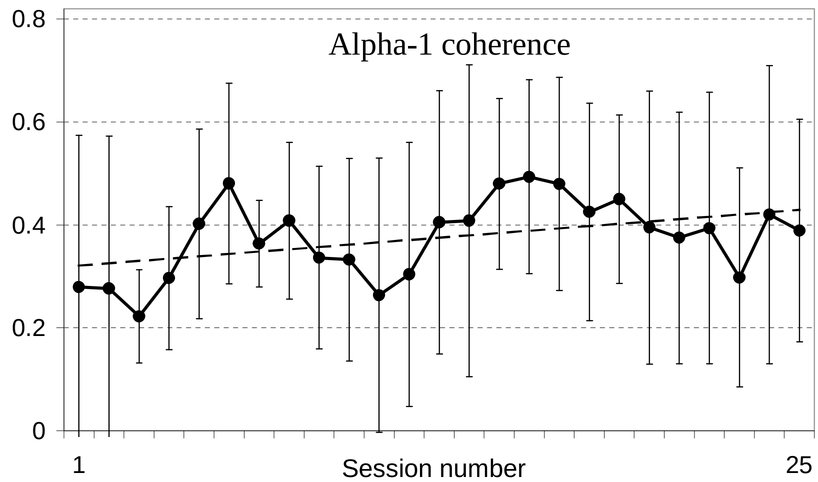

Figure 5.18: Evolution of frontal inter-hemispheric coherence in alpha-1 band (standard deviation depicted by bars).

Coherence analysis revealed significantly increased coherence in the alpha-1 band in frontal regions ($p < 0.027$) (Fig. 5.18), indicating improved frontal hemisphere cooperation in this specific frequency band. However, theta-1 and theta-2 coherences displayed opposite trends in this region ($p < 0.0003$ and $p < 0.036$) (Fig. 5.17). In other ranges delta-1 coherence increased in parieto-occipital area ($p < 0.049$), delta-2 coherence decreased in fronto-central ($p < 7.10^{-6}$) and increased in centro-parietal ($p < 0.014$) area, alpha-2 coherence decreased in parieto-occipital ($p < 0.01$), gamma coherence increased in centro-parietal ($p < 0.01$) and in parieto-occipital ($p < 0.024$) region.

The increase of alpha-1 coherence might be related to findings of Cantero et al. (1999) concerning significantly higher alpha coherence in frontal area compared to central and occipital locations during relaxation period.

Subjective assessment

At the beginning of our long-term training, only 2 out of 6 volunteers were optimistic about the possible impact of the AVS training on their relaxation abilities. One of them had neutral opinion, and three persons did not expect any progress of relaxation abilities for the future.

Perception of the training process showed the following results. General well-being before each day relaxation period (answering question "How do you currently feel?", appendix A, Fig. 8.2) displayed no significant trend. Subjective measure that evaluated general release accomplished during the relaxation interval ("Assess a level of your relief accomplished during the prestimulation period.") showed significantly increasing trend ($p < 0.037$) (Fig. 5.19) towards better performance. Both subjective measures were rated on 7-point bipolar scale. In spite of the fact that from the subjective results certain progress of relaxing effects is apparent, spontaneous relaxation abilities evaluated at the end of the whole experiment were perceived as unchanged.

Between-group comparison

Inspite of the fact that we did not employ fully acceptable control group, besides our test group we engaged in the same measurement procedure two other volunteers. Instead of AVS they listened to relaxation music. The significant results of the test group were compared with results obtained from this small control group. Between-group comparison was implemented by linear regression F-test (see section 4.6).

The control group did not display consistent agreement with the most of the significant trends from the test group. Significant trends in the same direction for the both groups were found only for power delta-1 in C3P3, power theta-1 in F3C3, power beta-2 in C4P4, power gamma in P3O1, spectral edge in P4O2, and spectral entropy in C3P3. On the other hand significant differences in trends between the groups tested by F-test were found for power gamma in C4P4 ($F(1,46)$ for all, $p = 0.015$, significant increase for AVS versus

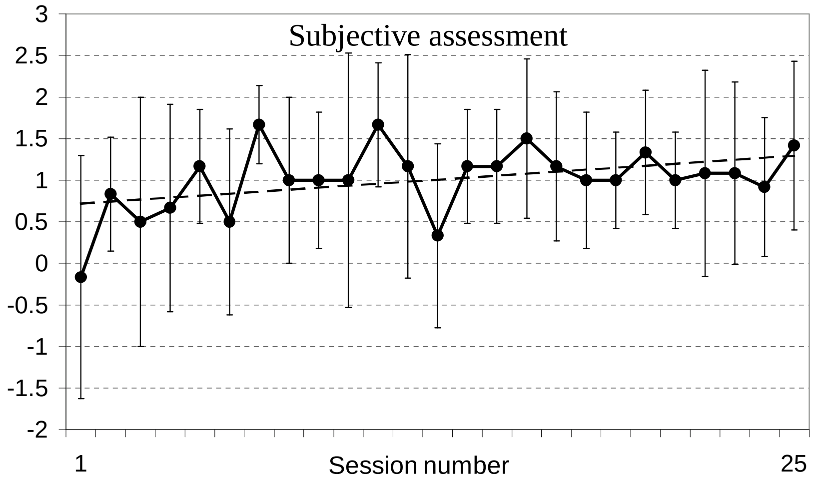

Figure 5.19: Evolution of subjective assessment of the relief accomplished during relaxation (standard deviation depicted by bars).

nonsignificant decrease for controls), histogram-based entropy in F3C3 ($p = 0.046$, significant increase/nonsignificant decrease), and for correlation dimension in F4C4 ($p = 0.014$, significant decrease/nonsignificant decrease). In all these cases only controls with the same direction (increase or decrease) of their trends were considered.

5.5 Discussion on AVS

In this section we discuss long-term effects of AVS. To our knowledge, our study represents the first attempt to systematically test the hypothesis that long-term use of varying audio-visual input can have extended effects on electro-cortical activity. Our results show that regular training with AVS does induce changes in the cortex functioning, similar to those commonly reported to be features specific to relaxation or altered states of consciousness.

In the literature, however, there is no clear definition of EEG descriptors of relaxation. One of the useful information sources appears to be the research on meditation, where various types of meditation can be considered as procedures with a relaxation effect (Banquet, 1973; Aftanas and Golocheikine, 2001; Travis, 2001). With increase of meditation condition, increase of depth of relaxation usually appears, confirmed by subjective and other physiological parameters, such as respiratory rate, skin conductance, plasma lactate.

Neurophysiological indicators for a state of sensorimotorical and mental rest are usually considered to be the increase of alpha and theta frequencies (Banquet, 1973; Brown, 1970) and inter-hemispheric synchronization, especially frontal alpha coherence (Travis, 2001). In our long-term AVS study, the power increase was not detected in alpha range (8-12 Hz), but more significantly in a rather shifted frequency range (4-10 Hz) merging the theta-1, theta-2 and alpha-1 range. The rise of coherence in alpha-1 band in frontal area was observed as well, although general synchronization did not occur, i.e. both linear correlation and mutual information in frontal region did not display any increase.

As a contribution to linear characteristics, we found significant trends in the behaviour of some non-linear measures. Long-term decrease in mutual information exactly followed decreasing evolution of linear correlation. Actually, mutual information appeared to be more sensitive than linear correlation.

However, trends of spectral entropy do not match changes in nonlinear complexity measures. This may be example of a case when nonlinear complexity measures might represent new possible indicators of dynamical changes of resting EEG, or these changes might be indexed better by a combination of linear and non-linear EEG variables.

Another relationship between non-linear and linear measures may be given by possible connection between the spectral features of data and dimensional estimates. It is possible that the decreasing trends of CD and increasing trend of theta and alpha band powers are reflections of the same spectral changes of EEG signals.

We can not exclude a possibility that certain contribution to increased relaxation effects could come from repetitive relaxation training itself, regardless the use of AVS. Subjects might adapt gradually to experimental conditions and develop a kind of conditioned response reflected in trends of studied measures.

In spite of the fact that we did not employ fully acceptable control group, we engaged in the same measurement procedure two other volunteers. Instead of AVS they listened to relaxation music. The significant results of the test group were compared with results obtained from this small control group. The control group did not display consistent agreement with most of the significant trends from the test group.

Thus it seems that AVS training could be more effective in inducing long-continuint changes of EEG than regular 20 minute listening to relaxation music. However, we must stress again that this fact was not supported by strong statistical evidence because our control and test group could not be properly compared.

Despite our findings about the measurable influence of AVS, we are very skeptical regarding the declarations found in various manuals of popular AVS machines claiming that after some training (minimally 30 repetitions) one may learn to distinguish among beta, alpha, theta and delta "states" and even to induce these states voluntarily when desired.

The present study was conducted to fill a gap in the knowledge of brain functioning during long-term AVS training. Gathered evidence in a form of trends of certain linear and nonlinear measures indicates that AVS training may serve as useful tool for evoking long-term changes in resting EEG and in the improvement of relaxation abilities.

However, further research is needed to support extensive clinical applications of AVS technology. For future studies we suggest investigation of long-term AVS with simultaneous recording of other relevant physiological parameters (e.g. ECG, electrodermal resistance, respiratory rate, or plasma lactate) for determination purposes, and post measurements after longer time-period from completion of long-term AVS experiment. As an implication for future studies we suggest testing of the AVS under proper control conditions (at least 10 vs. 10 subjects), with at least 30 stimulation repetitions, and with temporal electrode placement in addition to our montage, due to auditory cortex location.

6

EEG characteristics of relaxation (Part B)

In the second part of the thesis our experiences and measures from AVS experiment were applied to exploring EEG characteristics during psycho-physiological relaxation. The relaxation response is an integrated mind/body reaction, which has been found to have such benefits as increased mental and physical health and improved ability to deal with tension and stress. In the literature we had found no direct characterization of EEG features of relaxation. Analyses of resting status of patients may be useful for stress reduction also in connection with sleep deprivation. Another potential applications might be in development and testing of efficiency of pharmacological substances related to hypnotic and sedative drugs, concerning their impact on resting abilities.

Poor relaxation response is usually connected to problems of stress. Actually, stress is acknowledged as one of the major problems of modern society. While calling for stress reduction, need for monitoring tools for stress may grow. Knowledge about rest and relaxation status, as counterpart to stress level, might be used as indicator in neurofeedback application. Aim of such self-regulative training would be in voluntary attainment of higher quality of psycho-physiological rest.

Problems related to detection of resting states, physiological mechanisms of arousal and attention are currently studied for scientific, clinical and technical purposes. Our study may belong to broader topics from which one of the most actual area is reliable interaction between human subject and artificial system, e.g. of transportation nature where human factor is directly involved and undesirable change of operator's state may have severe consequences. Topic of sensori-motorical rest may be regarded as relevant for such research area, as it is supposed that under resting conditions changes of arousal and decrease of attention and reactivity usually occur.

It might be difficult to define relaxation properly. First of all, it is related to subjectivity and may vary across individuals. Implicitly, under the term *relaxation* it is usually meant certain positive and beneficial phenomenon. Periodical relaxation should have many other main and side effect on different psychical and physiological parameters of individuals (related e.g. to aging, digesting, general peace, psycho-somatic deceases). There exist no accepted references in a form of other physiological parameters. According to Travis (2001) five different categories of physiological variables might be sensitive to level of relaxation. Breath and heart rate index general metabolic level. Heart rate variability in the breath frequency (respiratory sinus arrhythmia or 'high frequency' heart rate variability) index differences in parasympathetic tone. Skin conductance levels reflect differences in sympathetic tone. Degree of sympathetic reactivity correlate with skin conductance responses to punctual stimuli during relaxation. On the other hand for characterization of stress level following parameters are reported as appropriate for use (Vavrinský, 2005): galvanic skin response, heart rate, blood pressure, and breath rate. (Foster, 1990) mentions physiological components of relaxation response to be decreased oxygen consumption, decreased respiratory rate, decreased heart rate, and increased alpha brain wave production.

By addition of selected EEG characteristics to set of established parameters additional information may be utilized for better observation of relaxation or stress status.

Researchers usually consider increased alpha production during mental and physical rest (Lindsley, 1952; Brown, 1970; Foster, 1990). According to Ossebaard relaxation itself is made up of several biological, psychological, and social components. The established observation that relaxed subjects show increased alpha wave activity may have inspired the idea that the presence of alpha activity equals relaxation. That is a reductionist circularity that denies the intricate nature of relaxation (Ossebaard (2000)).

Thus we set a goal to explore basic EEG characteristics during resting conditions. In this part of the thesis three consequent tasks were addressed:

1) Finding changes in EEG measures during sensori-motorical rest reflecting functioning of central nervous system. Characterization of the processes occurring during 3-minute resting conditions.

2) Selecting the most appropriate objective EEG features that are able to distinguish between more and less successful relaxation determined by subjective assessment.

3) EEG feature selection for practical recognition of two relaxation classes. Discriminant

analysis with Fisher classifier and artificial neural networks.

6.1 Materials and Methods

EEG recordings were used from AVS experiment and are described in the section 5.1. EEG montage, recording, amplifying, and filtering systems were the same as in the Part A of this thesis. Only data prior to AVS were counted. From each of 8 subjects we had 21-25 recorded sessions.

For task 1), from each participant we chose 11 recordings without artefacts (all 6 artefact-free difference signals). For task 2) and 3), out of 11, for each subject we chose 4 least and 4 most successful artefact-free relaxation sessions. Choice was done according to answers to the following task: "Assess a level of your relief accomplished during 3-minute resting period.". This subjective measure was rated on 7-point bipolar scale.

Three-minute EEG recordings were firstly filtered and remaining 174 sec. data were divided into 84 time windows for most of the measures and into 24 time windows for coherences. These values were obtained from optimization in order to achieve maximal number of time windows with minimal necessary frequency step in Fourier transform. In order to diminish variance of computed measures symmetrical moving average was applied using values from 5 preceeding to 5 successive data points.

40 different EEG measures explained in Part A were used. 29 single: total power, 9 absolute and 9 relative band powers, 3 spectral edges, spectral decay, 3 entropies, relative length, and 11 interdependencies: linear correlation coefficient, averaged mutual information, and coherences in 9 bands. Only correlation dimension was omitted due to its need for minimal number of data points - its evolution with smaller data windows could not be properly applied. Three portion parameters were used for spectral edge frequency. Besides established 95 also 50 and 80% were employed. These were chosen from search for optimal parameters in order to gain the steepest trends for spectral edge frequency during 3-minute resting data.

Sensitivity comparison

The important question is what to understand under measure of sensitivity in general. In our case it should be an ability to represent subtle psycho-physiological changes on time basis, or even to distinguish different subtle states.

We observed evolutions of various measures during 3-minute intervals, most of them could be interpolated by linear regression. For samples see Fig. 6.1. The criterion evaluating magnitude of trends may be p-value from testing wheather slope differing from flat one according to linear regression model (in the same way as it was used in section 5.4 and explained in section 4.6. Unfortunately, for majority of average trends this criterion was not suitable as their p-values were smaller than 10^{-10}.

Absolute changes (in respect to linear regression) are not suitable for different measures as they are expressed in different units, and thus not comparable. Relative changes (absolute changes divided by beginning value of their linear trend) do not reflect sensitivity well, as it is invariant only to multiplication by constant and not to addition (whereas p-values are invariant). However, when absolute change is divided by standard deviation of residuals in respect to linear regression, one obtains reasonable alternative to p-value:

$$\Delta^{res} = \frac{\Delta_{abs}}{std(res)} \tag{6.1}$$

It is not dependent on units, and invariant to multiplication and addition by constant. Thus not only absolute change is important but data variance around linear regression model is relevant as well.

For our purposes we used discriminating power defined in this way and termed it *residual relative change* (Δ^{res}). Dimensionless units are easy to interpret: for recognition of nonzero trend with naked eyes it is preferable for Δ^{res} to be above 1. Further above 1, more apparent

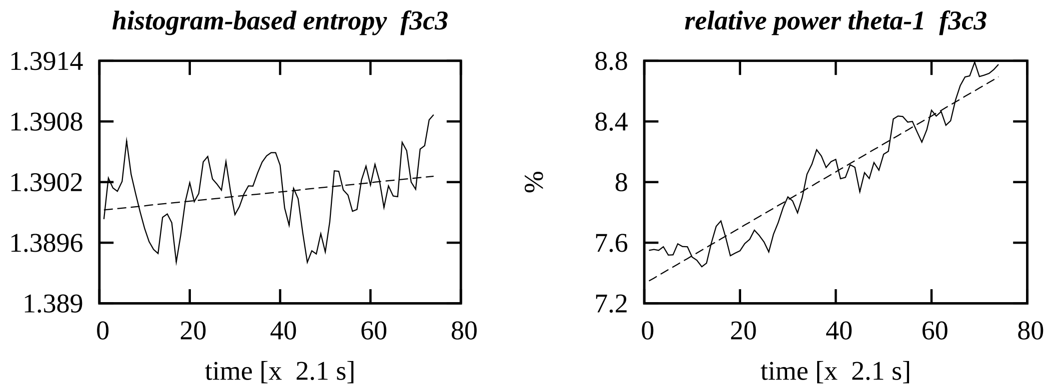

Figure 6.1: Samples of different trends during 3-minute evolution. Nonzero trends evaluated by residual relative changes and p-values (two upper values).

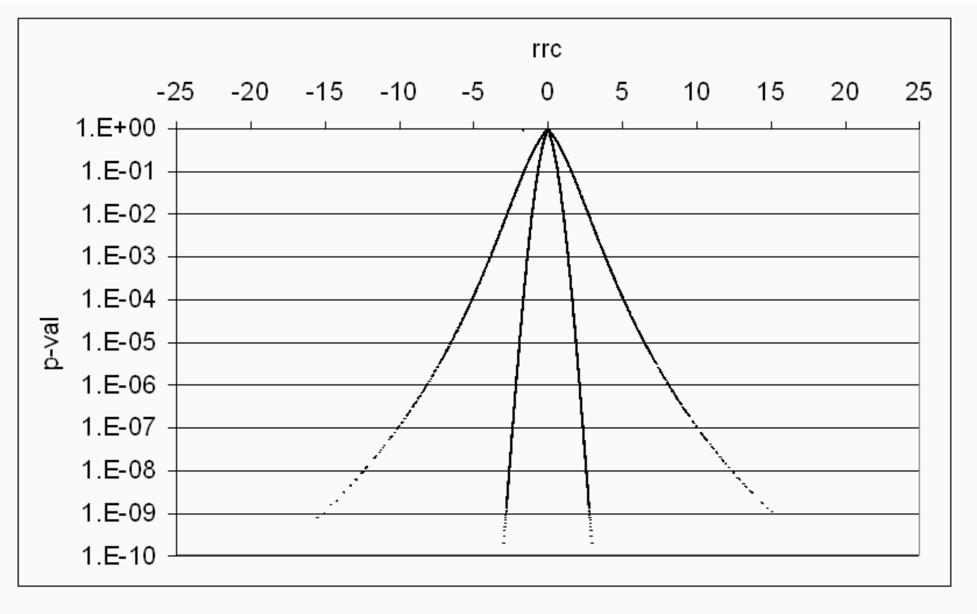

Figure 6.2: Relation of p-value of nonzero trend and residual relative change. All data from section 6.2 were used. Narrow 'hat' corresponds to measures with 74 points on abscissa axis (consisting from over 15000 points) and broad 'hat' corresponds to measures with 14 points on abscissa axis (consisting from over 2000 points).

the change is (Fig. 6.1). It is well related to subjective level of trend recognition from graph: two-times higher Δ^{res} matches approximately two-times higher subjective recognition ease. Or 2-times higher absolute change implies approximately two times higher Δ^{res} under assumption of similar standard deviation of residuals. P-values do not follow such linear scheme. Formula 6.1 has a similar form to that of t-statistics for slope estimate of linear regression, $t = \frac{\hat{b}}{std(\hat{b})}$, where $\hat{b}$ is estimate of slope usually counted from the least square minimization of residuals. Numerators of these two formulas differ only by constant. It can be shown, that between denominators there is a relation. In addition a few constants figure therein, namely number of data points and set of abscissa axis values. Thus p-values that result directly from this t-statistics and Δ^{res} are in unambiguous correspondence (see Fig. 6.2).

EEG features

Residual relative change is not the only type of feature suitable for discerning two evolution curves. Different might be also initial and terminal values of linear regression model. From character of our data linear fitting was sufficient and only usable. These two types of features were added to $\varDelta^{res}$ to form a set of 585 features, 195 measures in different cortex locations with 3 characteristics for each ($\varDelta^{res}$, beginning, and end).

To mention another alternative, it was possible to join several features from a single curve together, e.g. starting point and slope of linear regression. Then statistical testing with two-dimensional features would be applied. Due to different confidence intervals some slightly insignificant features could become significant (and vice versa). However disadvantage would appear with no possibility to discern whether differences were caused by slopes or starting points.

Feature selection

Feature selection is used for reducing the dimensionality of the data. It leads to simplification of data evaluation and to reduction of data processing complexity. Special programs for feature selection were implemented in Matlab (release 14, version 7.0.1). Two different methods for discriminant analysis of two relaxation classes were used: Fisher classifier and classifier made of artificial neural networks. Both were taken from Matlab toolboxes.

Fisher discriminant analysis is well-established classification method for multivariate normal distributions of each class (Therrien, 1989). In case of unequal covariance matrices, quadratic variant of Fisher discriminant analysis is preferred. Multivariate normal densities with covariance estimates stratified by group are estimated. Then by using the likelihood ratio any introduced element may be classified into one of the classes. Having the same cardinality of our two classes, we used Fisher classifier for equal prior probabilities for each class. Nonnormality of the data could violate optimal properties of classification rules. However it is known, that they could perform quite well even when normality assumption is not fulfilled.

Artificial neural networks (Kvasnička et al., 1997) are structures inspired by functioning of biological neural networks formed by neurons and synapses. Interconnected groups of artificial neurons use a computational model for information processing based on a connectionist approach to computation. Their global behaviour is determined by the connections between the processing elements and element parameters. During their training weights of connection between individual neuron are flexibly trained.

We used feed-forward back propagation network with three layers. Our optimizations and estimates led us to four neurons in hidden layer. This respects a number of possible regions in feature distributions, where element from one relaxation class may prevail those from the other class. Method of gradient descent was chosen for modification of weights between training epochs moving towards lower classification error.

From classification of a set of elements by any methods one obtain numbers of well and wrong classified elements. From them probability of misclassification - misclassification rates or errors are computed. We have two classes of features R^- and R^+ (less and more successful relaxation). Conditional probability of misclassification for each class was defined. Probability for misclassification of elements belonging to R^- as R^+:

$$P(R^+|R^-) = \frac{\textit{number of misclassified elements from } R^-}{\textit{number of all } R^- \textit{ elements}} \tag{6.2}$$

and misclassification of elements from R^+ as R^-:

$$P(R^-|R^+) = \frac{\textit{number of misclassified elements from } R^+}{\textit{number of all } R^+ \textit{ elements}} \tag{6.3}$$

A total error, as a measure of classification efficiency, is defined as

$$P = \frac{\textit{number of all misclassified elements}}{\textit{number of all elements}} \tag{6.4}$$

Later in text we use labeling E1 and E2 for $P(R^+|R^-)$ and $P(R^-|R^+)$.

Discriminant analysis can be performed in two modes: classification without and with testing. In the former method is trained on all available data and error rates are computed from the same data set. In the latter, before training some portion of available data is let aside and after parameters are fixed by training, elements from this testing set are applied in order to obtain error rates.

Usually it is not possible to test all combinations of features due to computational time demands. One may choose from several selection algorithms. Concerning feature selection methodology, there are three basic ways how to create set of selected features: forward (gradual building set of features) or backward selection (gradual reducing), or hybrid way, so called floating search methods using both building and reducing according to defined rules (Theodoridis and Koutroumbas, 1999). We used building alternative, where features are added to previously selected ones. By this technique we obtain semi optimal set of features, usually with not far from the best possible misclassification rates.

Let us illustrate technique of forward feature selection in case of testing procedure involved. Let portion of training data is 90 % (training set cardinality 0.9), so 10 % of data is taken aside for testing purposes. We have already chosen *N - 1* features before and we are attempting to add feature X to *N - 1* preceding features. In one single cycle 90 % of data is randomly selected. During training, parameters for classification purposes are obtained. Then resting 10 % of data is taken as new data we need to classify. In fact, classes are known, thus we may calculate classification errors. This cycle is repeated according to number of trials in order to objectify results by choosing of different 90 % subsets of original data set. One obtains a set of triplets of errors (total and two partial errors). For each error mean and standard deviation is calculated. Mean of total error is a criterion for feature selection: Feature X would be added to N - *1* preceding features if it has smallest mean error compared to other feature candidates.

Random choice of our data for training was constrained in a way that 90 % from each class was always taken. For Fisher classifier number of trails was set to 100 and for artificial neural networks to 10. Both were restricted by computational time. Feature selection without testing works in a similar way, just it is simpler, with number of trials equals 1 as 100 % of data is taken as training set. Then results are provided without standard deviations of classification errors.

6.2 Characteristics of sensori-motorical rest

Firstly, we focus on characteristics for a group of all artefact-free resting sessions, whether more or less successful according to subjective assessment, in order to discover general features of the resting process. An assumption is that strong nonzero trend reflects certain changes in physiological functioning. During this task we test sensitivity of measures used in these conditions in order to find the most appropriate EEG characteristics for observing such subtle changes.

Trends of 195 different measures at different locations were investigated at two levels: average and individual. In the former for each measure 88 evolution graphs were computed (from 8 persons per 11 artefact-free sessions). These evolutions were averaged. Then moving average was applied. Residual relative change (criterion I) and p-value of nonzero slope in testing linear regression model (crit. II) were computed. In the latter for each single measurement moving average was applied and residual relative change was computed. Mean of these individual Δ^{res} served as criterion III. Another important entry was a percentage of sessions where trends had the same direction (decrease or increase) as average trend (crit. IV). We looked for the most sensitive characteristics according to these four criteria. Naturally, 4 charts looked differently. At average level number of trends were very strong. Thus criterion II was not practical as most of the averaged curves were so distinctly steep, that their p-value was lower than 10^{-10} which resulted in its rounding to 0. In some cases out of these, the number of sessions possessing trend in opposite direction was very high (e.g. 44%). Thus we had to take into account single session level. There we chose a treshold of 70% for criterion IV. From them several weaker results according to criterion I were omitted.

In tab. 6.1 measures with the strongest trends are listed with their values of Δ^{res} from their averaged graphs, means of Δ^{res} obtained from graphs derived from single sessions, percentages of sessions holding the same trend directions as the averaged trends, p-values reflecting their nonzero trends, initial and terminal values, and relative change (terminal value divided by initial value, in percents) of linear regression model of averaged curves during 3-minute evolutions. Measures are listed according to their type and number of appearances in different cortex locations. In Fig. 6.3 samples of averaged behavior of measures in certain cortex locations with strongest trends of time evolution during resting conditions are depicted.

Difference between values of Δ^{res} and means of Δ^{res} is due to the fact that former is obtained from averaged graphs while latter is a mean from single graphs. Understanding follows from a point, that 88 graphs with some residuals around linear trend, when put together, decrease residuals by averaging of these "fluctuations".

According to Tab. 6.1 sensori-motorical rest can be the best characterized by trends of following EEG features: First and foremost by decrease of absolute alpha-1 power across all cortex regions. This was supported not only by decrease of total power in some areas (both frontal, C3P3, and P4O2) but also by decrease of relative alpha-1 power in backward (P3O1, P4O2), F4C4, and C3P3 locations. Also absolute beta-2 power decreased in central regions (C3P3, C4P4). Both relative powers in theta-1 and in gamma bands increased in P3O1 region. Spectral edge 95 and 80 increased in F3C3. From untraditional measures spectral decay decreased in P3O1 and C3P3 and relative length increased in F3C3 area. No interdependency measures were included in significant results. Evolution of these measures is not (to greater extent) sensitive to different quality of psycho-physiological rest, rather they might be considered as general characteristics of such rest. Decrease of total power over the whole cortex implies that overall brain activity gradually diminished during the resting process.

Inter-session differences are presented in column percentage. The best unidirectional trends are starting from level of 84 %, i.e. 16 % of cases having direction of trends in opposite direction. This implies level of credibility for potential use for discrimination purposes.

The largest changes according shifts from initial to terminal values were approximately 50 % reduction in relative change of absolute power of alpha-1 band across all cortex

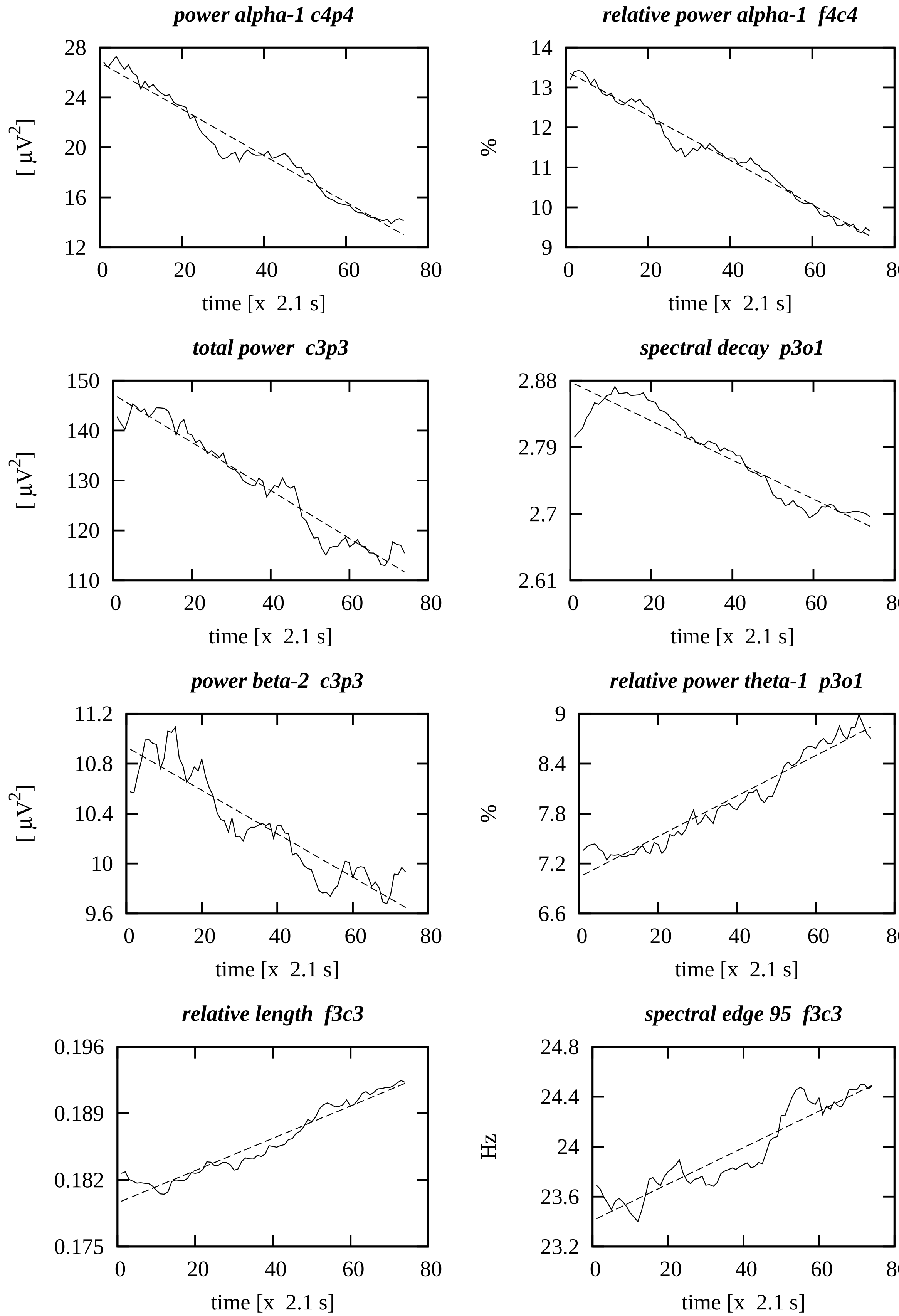

Figure 6.3: Samples of measures at particular cortex locations with the strongest trends during resting conditions.

Table 6.1: Evolution characteristics of resting EEG: Measures in particular locations, with 4 criteria: Δ^{res} (residual relative change) derived from averaged curves, means of Δ^{res} obtained from curves derived from single sessions, percentages of sessions holding the same trend directions as the averaged trends, and p-values reflecting nonzero trends according linear regression F-test. Then initial and terminal values, and relative change (terminal value divided by initial value, in percents) of the linear regression model of averaged curves during 3-minute evolutions follow. Beginning and end values hold different units (μV^2, %, dimensionless, or Hz). Measures are listed according to their type and number of appearances in different cortex locations.

measure	location	r. res. change criterion I	m. r. res. change crit. III	percent. crit. IV	p-val crit. II	begin	end	rel. change
power alpha-1	c4p4	-17.99	-1.35	74	<1.E-10	26.61	13.01	49
power alpha-1	p3o1	-15.89	-1.51	84	<1.E-10	15.15	7.97	53
power alpha-1	p4o2	-15.88	-1.43	76	<1.E-10	16.63	8.44	51
power alpha-1	c3p3	-15.55	-1.67	81	<1.E-10	25.29	11.1	44
power alpha-1	f3c3	-12.68	-1.24	74	<1.E-10	14.16	6.88	49
power alpha-1	f4c4	-10.58	-1.00	70	<1.E-10	16.64	8.27	50
relative p. alpha-1	f4c4	-22.28	-1.07	72	<1.E-10	13.36	9.29	70
relative p. alpha-1	p4o2	-17.47	-1.54	74	<1.E-10	13.73	9.76	71
relative p. alpha-1	p3o1	-17.27	-1.37	78	<1.E-10	12.82	9.43	74
relative p. alpha-1	c3p3	-17.04	-1.32	77	<1.E-10	13.99	9.65	69
total power	c3p3	-13.92	-1.03	73	<1.E-10	146.76	111.67	76
total power	f3c3	-10.2	-1.30	81	<1.E-10	89.72	74.46	83
total power	p4o2	-9.03	-0.72	70	<1.E-10	94.46	79.59	84
total power	f4c4	-8.12	-0.93	72	<1.E-10	90.33	75.27	83
spectral decay	p3o1	-9.37	-1.69	78	<1.E-10	2.88	2.68	93
spectral decay	c3p3	-8.06	-1.23	70	<1.E-10	2.96	2.8	95
power beta-2	c3p3	-7.79	-0.87	72	<1.E-10	10.92	9.65	88
power beta-2	c4p4	-5.41	-0.85	74	<1.E-10	9.55	8.74	92
relative p. theta-1	p3o1	13.32	0.92	70	<1.E-10	7.06	8.84	125
relative length	f3c3	12.96	1.53	72	<1.E-10	0.18	0.19	106
spectral edge 95	f3c3	8.61	1.20	72	<1.E-10	23.42	24.49	105
power alpha-2	f3c3	-7.3	-0.95	73	<1.E-10	22.46	15.5	69
spectral edge 80	f3c3	5.74	0.97	73	<1.E-10	14.01	14.66	105
relative p. gamma	p3o1	5.21	1.35	70	<1.E-10	1.73	2.02	117

regions. These strongest sensitivities displayed by powers in alpha bands may be regarded as one of basic features of sensori-motorical rest and relaxation. However, according to some authors increase of alpha power should be present (Lindsley, 1952; Brown, 1970; Foster, 1990). In spite of the fact that during our resting conditions we detected no increase in appearance of alpha waves during 3 minutes, consistent increase of alpha waves in our data could be found. Focus on shorter time windows shows that relative power in alpha-2 band in average increased during the first 30 seconds in all cortex regions. In the literature commonly accepted fact on alpha wave increase during rest and relaxation (Foster, 1990) should be rather related to eye closing phenomenon, by which resting is usually initiated, and to kind of lighter rest: rest with shorter time span and perhaps with closed eyes only in sitting position.

In the F3C3 location increased spectral edges can be interpreted in a way that relative power from 0.5 Hz up to approx. 14 and 24 Hz significantly decreased mainly due to relative alpha-1 (8-10 Hz) decrease. Relative length reflects the same fact in this channel: increased contribution of higher frequencies which makes trace of EEG signal longer. Two significant decreases of spectral decay also reflect increased appearance of higher bands to expense of lower bands.

6.3 Discrimination of two relaxation categories

The goal of this section is to discover even more subtle changes than in 6.2, namely to find out special EEG features bound to 'successful' relaxation, expressed on the contrast of 'unsuccessful' or 'less successful' relaxation. We referenced objective EEG characteristics to subjective assessment of relaxation. Recordings were divided into two groups according their subjective evaluation of general well-being during the relaxation period. For each subject groups were formed separately; four artefact-free sessions were taken with the lowest scoring and four with the highest one. Categories denoted as R^- and R^+ indicate subjectively less and more successful relaxation. Ideally, choice from 7-point bipolar scale would look for one subject like [-3,-3,-3,-3] for R^- and [3,3,3,3] for R^+ category. However, in real data the lowest and the highest values were not occuring in some subject's ratings. A typical sample looked as [-1,-1,0,0] for R^- and [1,1,1,1] for R^+ category or another sample as [-2,1,2,2] for R^- and [3,3,3,3] for R^+ category. From these samples it can be seen, that the two categories can not be regarded as unsuccessful and successful relaxation, but only less and more successful relaxation as compared one with the other.

First, for each group averaged graphs were counted (out of 32 cases: 8 persons x 4 sessions) and moving average was applied. From obtained curves it seemed apparent that many measures in certain locations reflected distinctive evolution for each relaxation class (curves were not intersecting, evolving apart from each other). Then, in order to find features capable to distinguish two relaxation categories, parametric and nonparametric tests were utilized (section 4.6). The first of them was two-sample heteroscedastic student's t-test. As only some of our data were normally distributed, for the rest of the data we used nonparametric Kruskall-Wallis test.

Out of 585 features used, 11 passed t-test with p-value treshold set to 0.05. All of them passed Shapiro-Wilk test for normality (p-value > 0.05) for both classes, interpreted as not violating normality. In addition 15 more features were obtained from Kruskall-Wallis test (treshold for p-value also 0.05). For these data normality was violated by Shapiro-Wilk test, p-value < 0.05 at least in one of the categories R^- or R^+. In the results all three types of features are represented. On Fig. 6.4 there are presented category-average curves where two relaxation categories differ by either initial values, trends or terminal values.

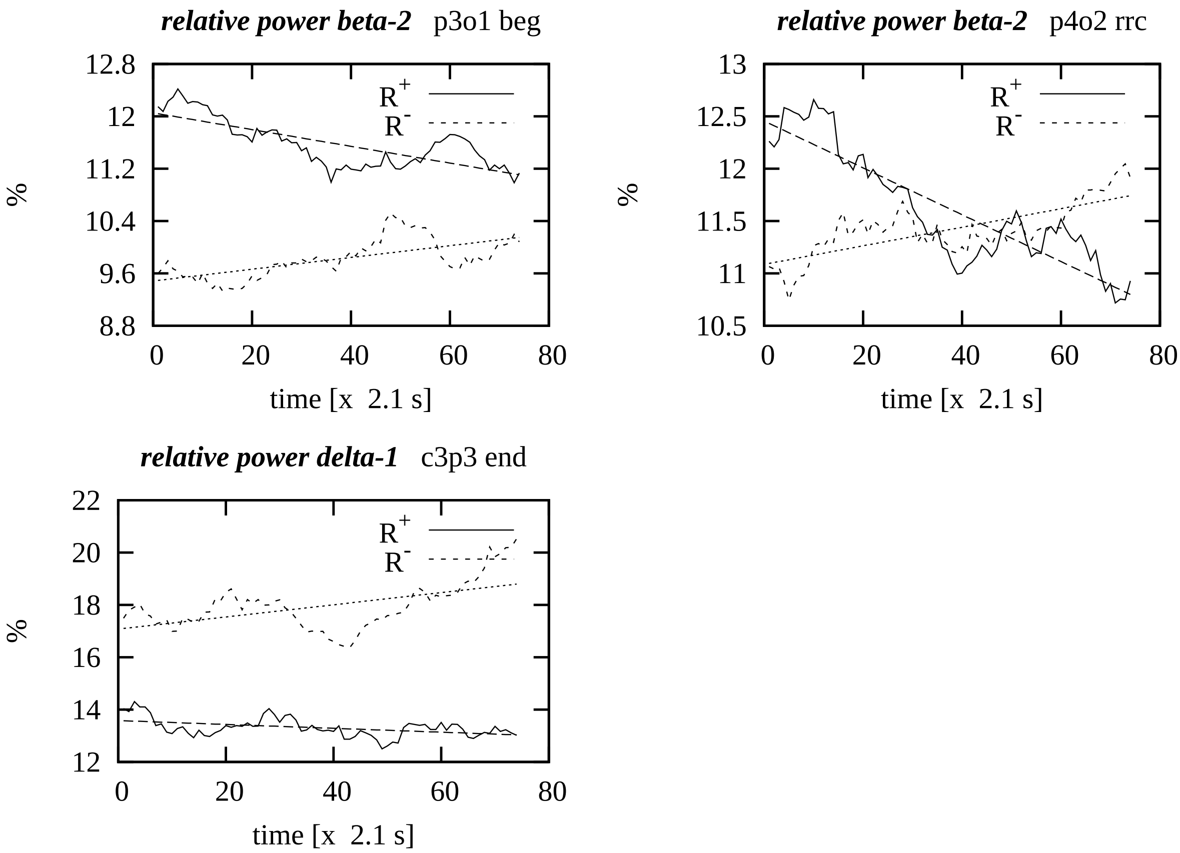

Figure 6.4: Two relaxation categories differ by three types of features related to linear regression: initial values (beg), trends (rrc), and terminal values (end). Classes R^- and R^+ indicate subjectively less and more successful relaxation. Samples of category-average curves are presented.

Out of selected features from both tests, 4 had to be excluded due to nonlinear manner of their averaged curves (coherence gamma PO Δ^{res} and end feature, and coherence delta-2 PO Δ^{res} and end feature as well). As it may be seen from Fig. 8.13 in appendix C, they violate linear model more expressively and would rather demand quadratic regression model. For other selected features linear regression model showed to be acceptable for application in this part of the thesis.

9 features resulting from t-test are listed in the fist table of Tab. 6.2 and 13 features obtained from Kruskall-Wallis test are displayed in the second table of Tab. 6.2. Averaged curves for these selected features are displayed in appendix C, 8.10 - 8.12.

From the last column of Tab. 6.2 it can be seen that data behavior is not quite uniform at personal level: A number of persons (out of 8) are displayed, for which shift from personal average within 1 class to personal average within the second class holds the same direction as shift of interpersonal averages. At the level of single sessions values from both categories were much more mixed, there were only a few cases of intra-subject features (within single person) where classes were separated, i.e. 4 values of one category apart from 4 values of another category. Overlapping of the categories is to be seen from polygons (appendix C, 8.14-8.17). Polygons are kept separately for both tests, i.e. the first 9 pictures displays features where both categories did not violate normality and at the rest of the pictures at least in one class normality was violated.

In the discriminative set of features appeared features based on absolute and relative delta-1 powers the most frequently (8 out of 22 cases)(Tab. 6.2). Features from the left hemisphere were presented in the results more frequently, especially left back region P3O1. It appears that during more agreeable relaxation states the slowest waves of delta-1 range are less contributed in some cortex areas. Namely in F4C4 and P3O1 regions where means of inicial and terminal values were separated for both absolute and relative delta-1 powers. Presenting results from higher frequency ranges, delta-2 power started from higher values and it was increasing (F4C4), and theta-1 power (P3O1) increased as well. Higher terminal relative alpha-1 power (F3C3) and higher initial beta-2 relative power (P3O1) occured. Also decrease of beta-2 relative power(P4O2) happened, together with higher initial spectral edge 80 and 95 (P3O1), and slight decrease of contribution of higher frequency bands (C4P4, relative length). Histogram-based entropy indicated slight decrease of complexity in F4C4. Moreover increase in hemisphere cooperation was detected in certain cases. Higher terminal coherence in delta-1 range(FC) and higher initial gamma coherence (FC) indicated higher synchronization of neuronal sources oscillating in these ranges. Increase in mutual information (CP) signalised improvement of overall cooperation of hemispheres in central area.

From some graphs in Fifs. 8.10 - 8.12 it may seem, that for Δ^{res} features it is characteristical that for one group it rises while for another it has opposite trends for the most of the single session (unaveraged) evolutions. In fact, such generalization is not possible and it is to be seen also from polygons (appendix C, Figs. 8.14 - 8.17). To show some quantification, for the best oppositely running trends (according to p-val, t-test), power

Table 6.2: Features with the largest differences between 2 relaxation categories: Upper table: List of EEG features obtained from parametric t-test that were able to discern means of two categories. Lower table: Features obtained from Kruskall-Wallis test for non-normal data distributions. Features consist of measure, cortex location, and one of the following characteristics: beginning, end, or relative residual change (rrc). After feature identification means for classes R^- and R^+ (less and more successful relaxation) are presented, and p-value of particular test. In the last column number of subjects (out of 8) are presented, for which shift from personal average from one class to personal average from another class holds the same direction as shift from interpersonal averages.

T-test:

	feature			mean R-	mean R+	p-val	# pers.
1	coherence gamma	fc	beg	0.14	0.19	0.009	8
2	power delta-2	f4c4	rrc	-0.61	0.56	0.024	7
3	mutual information	cp	rrc	-0.99	0.14	0.033	7
4	power delta-1	c4p4	rrc	-0.69	0.35	0.033	6
5	relative p. beta-2	p3o1	beg	9.49	12.04	0.036	6
6	relative p. delta-1	f4c4	beg	22.65	18	0.036	6
7	relative length	c4p4	rrc	1.4	-0.14	0.043	8
8	hist. based entropy	f4c4	rrc	0.83	-0.19	0.046	7
9	power theta-1	p3o1	rrc	-0.39	0.69	0.048	6

Kruskal-Wallis test:

	feature			mean R-	mean R+	p-val	# pers.
1	relative p. delta-1	p3o1	end	22.39	17.15	0.006	7
2	power delta-1	f4c4	beg	22.22	19.92	0.013	6
3	spectral edge 80	p3o1	beg	11.76	13.28	0.013	7
4	power delta-1	p3o1	beg	26.61	17.58	0.015	6
5	power delta-1	p3o1	end	19.05	16.93	0.016	5
6	relative p. delta-1	f4c4	end	21.73	17.53	0.019	7
7	relative p. delta-1	c3p3	end	18.79	13.04	0.022	6
8	relative p. beta-2	p4o2	rrc	0.15	-0.54	0.034	7
9	power delta-2	f4c4	beg	13.04	9.14	0.041	8
10	spectral edge 95	p3o1	beg	19.53	21.47	0.049	7
11	coherence delta-1	fc	end	0.28	0.33	0.049	7
12	spectral edge 95	p4o2	rrc	0.82	-0.18	0.050	6
13	relative p. alpha-1	f3c3	end	7.66	9.49	0.050	5

delta-2 F4C4 Δ^{res}, feature holds for less successful relaxation 59% of single cases in decreasing direction, and 69% of cases in increasing direction for more successful relaxation; power delta-1 C4P4 Δ^{res} feature 69% for class R^- and 63% for R^+.

6.4 Classification of relaxation level

Almost real-time acquisition of information about relaxation level based on selected EEG measures would require set of characteristics capturing distinctive and more or less uniform behaviour in majority of measurements from different subjects and different measurement sessions. In this section preliminary results obtained by procedure of feature selection indicate candidates for practical discrimination of EEG relaxation level. For researching this problem, we used 2 kinds of classifiers. We took all 585 features and worked with data matrix of dimension 64 x 585.

Fisher classifier

As the first classification method we used Fisher quadratic classifier for single and multi-dimensional approach. Multi-dimensional approach was realized for feature selection, with cases without and with separate testing data. Normality assumption was fulfilled only in part of feature distributions (in the most significant cases approximately in 2/3). However this type of classifier is able to perform quite well even when some data are not normally distributed.

Classification in one dimension was applied only in mode without testing. Chart of the most suitable candidates is displayed in 6.3. Overall error starts at the level of 31% for frontal alpha-2 coherence Δ^{res} feature. E1 and E2 are conditional misclassification rates related to $P(R^{+}|R^{-})$ and $P(R^{-}|R^{+})$. Such a high total error rate implies that no single measure is useful for appropriate discrimination.

In multidimensional classification we were able to reduce error expressively by proper feature selection. Results for feature selection without testing are displayed in Tab. 6.4. In each dimension a feature was added to previous features in order to obtain the lowest possible error. Two cases are presented which differ on direction of searching process. When one is searching for feature that has to be added to N - 1 preceding features to form N dimensional feature vector, there might be candidates with the same total classification error. Algorithm is supposed to choose one with the smallest one, if there are more candidates with the smallest error, it depends on particular program, which one is selected. Thus outcome may differ with different order of candidate features' testing. Null error reached in 9-10 dimensions is obtained due to classificator overtraining, as in 10 dimensions space is filled very sparsely. Under such conditions and when method is applied in mode without testing, linear separability is fully achieved.

Table 6.3: Chart of the features with the most distinctive classes according to Fisher classifier. Feature is marked by measure, location, and one of the following characteristics: beginning (beg), end, or relative residual change (rrc). In the last 3 columns total classification error and two partial errors are stated.

Fisher classifier
1 dimension

	feature			**E**	**E1**	**E2**
1	coherence alpha-2	fc	rrc	0.31	0.47	0.16
2	relative p. theta-1	c3p3	rrc	0.34	0.25	0.44
3	relative p. beta-2	p3o1	beg	0.34	0.16	0.53
4	coherence delta-1	f3c3	end	0.34	0.44	0.25
5	relative p. beta-2	c4p4	rrc	0.36	0.50	0.22
6	power delta-1	c4p4	rrc	0.36	0.19	0.53
7	power delta-2	f4c4	rrc	0.36	0.44	0.28
8	spectral edge 80	f3c3	rrc	0.36	0.25	0.47
9	spectral entropy	p4o2	rrc	0.36	0.16	0.56
10	hist. based entropy	c4p4	rrc	0.36	0.38	0.34
11	coherence gamma	fc	rrc	0.36	0.44	0.28
12	relative p. delta-1	p3o1	end	0.36	0.34	0.38
13	relative p. alpha-1	p3o1	end	0.36	0.16	0.56
14	relative p. delta-2	p4o2	rrc	0.38	0.22	0.53
15	relative p. theta-1	f3c3	rrc	0.38	0.44	0.31
16	spectral edge 80	p4o2	rrc	0.38	0.41	0.34
17	spectral edge 90	p4o2	rrc	0.38	0.25	0.50
18	spectral decay	p3o1	rrc	0.38	0.16	0.59
19	relative length	f4c4	rrc	0.38	0.25	0.50
20	relative p. beta-2	p4o2	beg	0.38	0.41	0.34
21	power beta-2	f4c4	beg	0.38	0.12	0.62
22	spectral entropy	f4c4	beg	0.38	0.41	0.34
23	spectral entropy	p3o1	beg	0.38	0.41	0.34
24	relative length	p4o2	beg	0.38	0.50	0.25
25	coherence delta-1	po	beg	0.38	0.62	0.12
26	coherence beta-2	cp	beg	0.38	0.22	0.53
27	coherence gamma	fc	beg	0.38	0.41	0.34
28	relative p. theta-2	f4c4	end	0.38	0.50	0.25
29	spectral edge 50	f4c4	end	0.38	0.53	0.22
30	coherence alpha-1	po	end	0.38	0.44	0.31

Table 6.4: Feature selection according to Fisher classifier. Two cases are presented which differ due to different order of candidate features' testing. Feature is marked by measure, location, and one of the following characteristics: beginning (beg), end, or relative residual change (rrc). In the last 3 columns total classification error and two partial errors are stated.

Feature selection
Fisher classifier
only training

case 1	**feature**			**E**	**E1**	**E2**
1	coherence alpha-2	fc	rrc	0.31	0.47	0.16
2	relative p. theta-1	c4p4	rrc	0.22	0.31	0.12
3	coherence beta-1	po	beg	0.17	0.22	0.12
4	relative p. delta-2	c4p4	rrc	0.11	0.09	0.12
5	relative p. delta-2	p4o2	rrc	0.08	0.09	0.06
6	coherence alpha-1	cp	rrc	0.05	0.06	0.03
7	coherence delta-2	fc	rrc	0.05	0.03	0.06
8	power beta-2	c3p3	rrc	0.03	0.03	0.03
9	relative p. theta-1	f3c3	rrc	0.02	0.03	0.00
10	relative p. gamma	c4p4	rrc	0.00	0.00	0.00

case 2	**feature**			**E**	**E1**	**E2**
1	coherence alpha-2	fc	rrc	0.31	0.47	0.16
2	spectral edge 95	p4o2	rrc	0.22	0.34	0.09
3	relative p. beta-1	f3c3	rrc	0.17	0.25	0.09
4	relative p. theta-2	f4c4	end	0.16	0.19	0.12
5	relative p. delta-2	f4c4	rrc	0.12	0.16	0.09
6	coherence gamma	cp	end	0.11	0.12	0.09
7	coherence theta-1	cp	beg	0.06	0.06	0.06
8	coherence alpha-2	cp	end	0.03	0.03	0.03
9	total power	f3c3	end	0.00	0.00	0.00

Two trials were executed for feature selection with 10% of data used for testing. The outcome yielded 12% error for dimension 10, further diminishing to 3-4% reached for dimension of 17-25 (Tabs. 6.5 - 6.6). If number of trials be expressively higher than used (100), results of the both trials might be identical. In our case features differ expressively, so one can not prefer or select a single set for practical purposes. When a portion of data excluded for testing purposes was increased to 40%, error in one case reached 16% for dimension (Tab. 6.7).

While in Tab. 6.4 the first feature naturally has to be the same as the leader of Tab. 6.3, in Tabs. 6.5 - 6.7 the first member is different. While in both cases with 10% of testing data this feature (coherence alpha-2 FC Δ^{res}) was chosen in front places, unlike in case with 40% of testing data (6.7).

Neural network classifier

As the second method for discrimination purposes, artificial neural network classifier was applied. Again with single and multi-dimensional approach, in modes with and without testing procedure.

Classification in one dimension yielded smaller errors than counterpart - Fisher method. The most suitable candidates start with overall error of 20% by relative power in beta-2 range in C4P4 with beginning feature (Tab. 6.8).

For feature selection in mode without testing null error was reached already within 4 dimensions (Tab. 6.9) in both performed runs. In this case overtraining of the system was present, as neural networks are known to be universal approxiamtors. Superior performance over Fisher discrimination should be understood also due to its to focus on more polygon regions, while Fisher only to one - around mean of fitted normal distributions. However these 'islands' in polygons might disappear if size of the class sets was increased.

Feature selection with 10% of testing data reached total error of 32% for dimension 10, and further 10% error for D = 21 (Tab. 6.10). In this case Fisher approach performed in a superior way.

Distributions of feature values are documented by polygons in appendix C, Fig. 8.18-8.22. Differences in most of the individual features from 1 dimensional classification by both methods are visible also from behavior of respective averaged curves (appendix C, Fig. 8.23). In Tab. 6.11 sumarization of the classification results is provided.

In various classification tasks we obtained number of different EEG features. We did not focus to interpretation of obtained sets of features, as it is not a goal of this section. Within sets of selected features it is not relevant to interpret features individually. For such a purpose the section 6.3 has served. Here we demonstrate the ability of discrimination methods to separate EEG relaxation data and express approximate number of dimension needed.

Table 6.5: Feature selection according to Fisher classifier. 10% of data assigned for testing. Trial 1. Feature is marked by measure, location, and one of the following characteristics: beginning (beg), end, or relative residual change (rrc). In the last 6 columns total and two partial classification errors with their standard deviations are stated.

Feature selection
Fisher classifier
with testing

trial1	feature			E	std(E)	E1	std(E1)	E2	std(E2)
1	coherence delta-1	fc	end	0.31	0.15	0.34	0.25	0.29	0.24
2	relative p. beta-1	f3c3	end	0.27	0.19	0.25	0.25	0.28	0.24
3	power delta-1	f3c3	end	0.23	0.17	0.32	0.28	0.15	0.21
4	relative p. delta-2	c3p3	end	0.19	0.13	0.25	0.24	0.12	0.2
5	power delta-2	f3c3	end	0.14	0.14	0.17	0.22	0.12	0.19
6	coherence alpha-2	fc	rrc	0.14	0.14	0.13	0.18	0.16	0.21
7	total power	f3c3	end	0.13	0.13	0.1	0.16	0.17	0.22
8	spectral edge 50	f4c4	end	0.14	0.14	0.14	0.19	0.15	0.22
9	power beta-2	p4o2	end	0.12	0.13	0.08	0.16	0.16	0.21
10	coherence beta-1	po	beg	0.12	0.13	0.08	0.16	0.16	0.22
11	relative p. theta-2	f4c4	beg	0.11	0.12	0.1	0.17	0.12	0.18
12	relative p. beta-2	c3p3	rrc	0.1	0.14	0.06	0.16	0.14	0.21
13	coherence theta-2	cp	end	0.11	0.13	0.07	0.15	0.15	0.2
14	relative p. beta-1	p3o1	beg	0.08	0.12	0.06	0.14	0.1	0.16
15	relative p. theta-2	c4p4	beg	0.06	0.11	0.04	0.12	0.08	0.14
16	power beta-1	f4c4	beg	0.06	0.1	0.05	0.12	0.07	0.14
17	relative p. alpha-1	f3c3	beg	0.04	0.1	0.05	0.12	0.04	0.12
18	relative p. alpha-1	c4p4	end	0.06	0.11	0.07	0.15	0.04	0.11
19	coherence theta-1	po	beg	0.05	0.11	0.06	0.17	0.04	0.12
20	hist. based entropy	c3p3	end	0.06	0.1	0.08	0.16	0.04	0.12
21	spectral edge 80	c3p3	rrc	0.08	0.11	0.07	0.14	0.08	0.17
22	power beta-2	p3o1	end	0.07	0.11	0.06	0.13	0.09	0.19
23	hist. based entropy	f3c3	rrc	0.08	0.11	0.06	0.15	0.1	0.18
24	spectral entropy	c4p4	rrc	0.06	0.1	0.05	0.15	0.07	0.17
25	power delta-2	p4o2	rrc	0.05	0.09	0.06	0.15	0.04	0.12
26	power delta-1	p4o2	rrc	0.07	0.11	0.03	0.11	0.1	0.2
27	power alpha-2	p3o1	beg	0.04	0.1	0.03	0.12	0.06	0.15
28	relative p. theta-2	p4o2	end	0.08	0.14	0.05	0.16	0.12	0.26

Table 6.6: Feature selection according to Fisher classifier. 10% of data assigned for testing. Trial 2. Feature is marked by measure, location, and one of the following characteristics: beginning (beg), end, or relative residual change (rrc). In the last 6 columns total and two partial classification errors with their standard deviations are stated.

Feature selection
Fisher classifier
with testing

trial 2	**feature**			**E**	**std(E)**	**E1**	**std(E1)**	**E2**	**std(E2)**
1	coherence delta-1	fc	end	0.33	0.14	0.4	0.25	0.26	0.24
2	relative p. beta-1	f3c3	end	0.27	0.19	0.25	0.23	0.3	0.28
3	relative p. beta-2	p4o2	end	0.24	0.2	0.28	0.28	0.19	0.26
4	coherence alpha-2	fc	rrc	0.24	0.16	0.28	0.26	0.21	0.24
5	relative p. theta-1	f3c3	rrc	0.19	0.16	0.18	0.25	0.21	0.2
6	power alpha-1	f4c4	beg	0.17	0.16	0.17	0.21	0.18	0.24
7	relative p. alpha-2	f4c4	end	0.16	0.17	0.17	0.22	0.16	0.24
8	spectral edge 95	c3p3	end	0.17	0.15	0.13	0.21	0.21	0.2
9	relative p. theta-1	p3o1	end	0.14	0.13	0.12	0.17	0.17	0.22
10	relative p. alpha-1	f3c3	end	0.13	0.13	0.09	0.16	0.17	0.23
11	coherence gamma	po	rrc	0.15	0.13	0.12	0.2	0.18	0.22
12	relative p. alpha-2	p4o2	beg	0.13	0.13	0.08	0.17	0.17	0.2
13	coherence delta-2	po	rrc	0.13	0.14	0.12	0.19	0.13	0.21
14	relative p. beta-1	c3p3	beg	0.1	0.13	0.12	0.2	0.09	0.15
15	power alpha-1	f3c3	rrc	0.1	0.11	0.11	0.18	0.08	0.15
16	coherence theta-1	fc	end	0.09	0.13	0.12	0.2	0.06	0.14
17	relative p. delta-1	p4o2	end	0.1	0.11	0.08	0.14	0.11	0.18
18	coherence beta-2	cp	rrc	0.09	0.13	0.1	0.17	0.08	0.17
19	power alpha-2	c4p4	beg	0.09	0.11	0.11	0.17	0.07	0.15
20	coherence delta-2	cp	beg	0.08	0.11	0.1	0.19	0.06	0.13
21	power delta-2	f4c4	rrc	0.06	0.1	0.04	0.11	0.07	0.16
22	spectral entropy	c3p3	end	0.04	0.09	0.06	0.15	0.03	0.09
23	relative p. delta-2	p3o1	beg	0.04	0.08	0.06	0.15	0.03	0.11
24	spectral entropy	c3p3	beg	0.04	0.09	0.06	0.15	0.03	0.11
25	relative p. delta-2	f4c4	rrc	0.03	0.08	0.05	0.13	0.02	0.09
26	coherence gamma	cp	rrc	0.05	0.09	0.03	0.11	0.06	0.15
27	relative p. gamma	f4c4	rrc	0.03	0.08	0.04	0.14	0.02	0.07
28	power theta-2	c4p4	beg	0.07	0.12	0.04	0.13	0.09	0.21

Table 6.7: Feature selection according to Fisher classifier. 40% of data assigned for testing. Feature is marked by measure, location, and one of the following characteristics: beginning (beg), end, or relative residual change (rrc). In the last 6 columns total and two partial classification errors with their standard deviations are stated.

Feature selection
Fisher classifier
with testing

	feature			E	std(E)	E1	std(E1)	E2	std(E2)
1	coherence gamma	fc	beg	0.36	0.06	0.37	0.13	0.35	0.13
2	relative p. delta-1	c3p3	end	0.28	0.07	0.32	0.11	0.24	0.11
3	power beta-2	p4o2	end	0.24	0.08	0.24	0.13	0.24	0.13
4	coherence beta-2	cp	rrc	0.21	0.06	0.18	0.11	0.24	0.12
5	spectral decay	p4o2	rrc	0.2	0.06	0.17	0.11	0.22	0.12
6	mutual information	cp	rrc	0.17	0.06	0.15	0.1	0.2	0.13
7	relative p. delta-1	c4p4	rrc	0.17	0.05	0.15	0.1	0.19	0.12
8	relative p. gamma	f4c4	rrc	0.16	0.06	0.15	0.12	0.17	0.12
9	spectral decay	p4o2	end	0.16	0.06	0.13	0.1	0.18	0.14
10	coherence delta-2	c3p3	end	0.17	0.07	0.17	0.12	0.18	0.13
11	relative p. theta-2	p3o1	rrc	0.18	0.07	0.15	0.12	0.22	0.14
12	relative p. theta-2	c4p4	rrc	0.19	0.08	0.17	0.15	0.21	0.14
13	power gamma	c4p4	beg	0.21	0.08	0.19	0.15	0.23	0.17
14	relative p. delta-1	p4o2	beg	0.21	0.09	0.17	0.15	0.25	0.19
15	power theta-2	p4o2	end	0.22	0.08	0.16	0.14	0.28	0.21
16	power delta-1	f4c4	rrc	0.25	0.1	0.21	0.18	0.28	0.21
17	shannon entropy	c3p3	beg	0.27	0.09	0.28	0.22	0.25	0.2
18	relative p. beta-2	p3o1	end	0.33	0.13	0.27	0.28	0.39	0.33

One-dimensional classification approach is not useful for practical purposes, as errors are too high. When we focus our view to Fisher type of discriminant analysis, and restrict ourselves up to 10 dimensions, from 3 cases of feature selection with testing, promising results yielded error 12 - 16 %. With permission up to 25 dimensions, error of 3 - 4 % was achieved (for training set cardinality equaled to 0.9). Obtained feature vectors should be considered as preliminary, although these particular vectors might be tested on any other EEG relaxation data. There might exist a number of feature vectors of acceptable (not too high) dimension N with similar and relatively sufficiently low classification errors.

Table 6.8: Chart of the features with the most distinctive classes according to classification by neural networks. Feature is marked by measure, location, and one of the following characteristics: beginning (beg), end, or relative residual change (rrc). In the last 3 columns total classification error and two partial errors are stated.

Neural networks
1 dimension

	feature			**E**	**E1**	**E2**
1	relative p. beta-2	c4p4	beg	0.20	0.06	0.34
2	power theta-2	f4c4	rrc	0.23	0.28	0.19
3	power delta-1	f3c3	beg	0.23	0.16	0.31
4	coherence delta-1	f3c3	end	0.23	0.25	0.22
5	relative p. theta-1	c3p3	rrc	0.25	0.25	0.25
6	relative p. gamma	p3o1	rrc	0.25	0.28	0.22
7	relative p. delta-1	c4p4	rrc	0.27	0.09	0.44
8	relative p. theta-2	c3p3	rrc	0.27	0.34	0.19
9	power delta-1	p3o1	rrc	0.27	0.34	0.19
10	hist. based entropy	f4c4	rrc	0.27	0.34	0.19
11	coherence delta-2	f3c3	rrc	0.27	0.19	0.34
12	coherence alpha-2	f3c3	rrc	0.27	0.41	0.13
13	spectral edge 50	f3c3	beg	0.27	0.38	0.16
14	spectral entropy	p4o2	beg	0.27	0.25	0.28
15	power alpha-1	p4o2	end	0.27	0.28	0.25
16	spectral decay	c3p3	end	0.27	0.28	0.25
17	mutual information	fc	end	0.27	0.38	0.16
18	relative p. delta-1	f4c4	rrc	0.28	0.16	0.41
19	power delta-1	p4o2	rrc	0.28	0.03	0.53
20	power delta-2	p3o1	rrc	0.28	0.34	0.22
21	power beta-2	p4o2	rrc	0.28	0.06	0.50
22	hist. based entropy	c4p4	rrc	0.28	0.19	0.38
23	relative length	c4p4	rrc	0.28	0.19	0.38
24	coherence delta-2	cp	rrc	0.28	0.28	0.28
25	coherence alpha-1	fc	rrc	0.28	0.34	0.22
26	coherence beta-2	po	rrc	0.28	0.53	0.03
27	relative p. alpha-1	f3c3	beg	0.28	0.28	0.28
28	relative p. beta-1	c3p3	beg	0.28	0.25	0.31
29	relative p. beta-2	p4o2	beg	0.28	0.19	0.38
30	power beta-2	f4c4	beg	0.28	0.41	0.16
31	coherence theta-1	cp	beg	0.28	0.22	0.34
32	relative p. delta-1	p3o1	end	0.28	0.38	0.19
33	relative p. gamma	c3p3	end	0.28	0.09	0.47
34	coherence alpha-1	po	end	0.28	0.41	0.16

Table 6.9: Feature selection according to classification by neural networks. Two cases are presented which differ due to neural network's inherent variations in learning process. Feature is marked by measure, location, and one of the following characteristics: beginning (beg), end, or relative residual change (rrc). In the last 3 columns total classification error and two partial errors are stated.

Feature selection
Neural networks
only training

trial 1	**feature**			**E**	**E1**	**E2**
1	coherence delta-1	po	beg	0.17	0.19	0.16
2	spectral decay	c3p3	rrc	0.03	0	0.06
3	relative p. gamma	c4p4	rrc	0.02	0.03	0
4	power theta-2	c3p3	rrc	0	0	0

trial 2	**feature**			**E**	**E1**	**E2**
1	coherence delta-1	fc	end	0.22	0.19	0.25
2	relative p. theta-2	f3c3	rrc	0.06	0.06	0.06
3	relative p. delta-1	c4p4	rrc	0.02	0	0.03
4	relative p. theta-2	p3o1	beg	0	0	0

From sections 6.3 and 6.4 we obtained quite a lot of different features. On the contrary to what one could expect, results from t-test (section 6.3) and one-dimensional Fisher classifier were not alike. In spite of the fact that both of them use estimates of normal distributions, quantification methods are different with ability to prefer different qualities of their distributions. At first, we used for classification only the strongest results from the section 6.3. But later we realized that t-test and Fisher classifier might not prefer the same shapes in polygons. Probably with increasing number of data in classes, feature distributions would become smoother and the outcomes would not differ so extensively. Many features yielded similar significance in t-test and in total error in classification, thus changing of their order is plausible. However we may also emphasize features that performed well in both tasks (discernment of population mean from the section 6.3 and classification task from the section 6.4). From t-test and one dimensional Fisher classification these were delta-2 power F4C4 Δ^{res}, delta-1 power C4P4 Δ^{res}, and relative beta-2 power P3O1 beginning. From Kruskall-Wallis test and one dimensional Fisher classification these were

Table 6.10: Feature selection according to classification by neural networks. 10% of data assigned for testing. Feature is marked by measure, location, and one of the following characteristics: beginning (beg), end, or relative residual change (rrc). In the last 6 columns total and two partial classification errors with their standard deviations are stated.

Feature selection
Neural networks
with testing

	feature			**E**	**std(E)**	**E1**	**std(E1)**	**E2**	**std(E2)**
1	power alpha-2	f4c4	beg	0.22	0.19	0.33	0.27	0.1	0.16
2	relative p. gamma	c3p3	beg	0.22	0.14	0.17	0.18	0.27	0.31
3	spectral edge 95	c4p4	rrc	0.2	0.19	0.3	0.29	0.1	0.16
4	relative p. gamma	f3c3	end	0.27	0.2	0.2	0.28	0.33	0.22
5	spectral entropy	f4c4	rrc	0.28	0.26	0.27	0.26	0.3	0.33
6	power gamma	p3o1	rrc	0.27	0.14	0.27	0.21	0.27	0.21
7	relative p. theta-2	p4o2	beg	0.25	0.12	0.23	0.16	0.27	0.21
8	spectral entropy	f4c4	end	0.27	0.18	0.27	0.31	0.27	0.21
9	relative p. gamma	c4p4	beg	0.3	0.17	0.27	0.26	0.33	0.27
10	relative p. theta-1	p3o1	beg	0.32	0.18	0.2	0.23	0.43	0.22
11	power theta-1	p4o2	beg	0.27	0.22	0.2	0.23	0.33	0.35
12	relative p. alpha-1	f3c3	rrc	0.18	0.17	0.13	0.17	0.23	0.27
13	lin. correlation	cp	beg	0.18	0.15	0.1	0.16	0.27	0.26
14	coherence beta-1	po	rrc	0.2	0.11	0.2	0.17	0.2	0.17
15	relative p. beta-1	f3c3	end	0.18	0.15	0.2	0.23	0.17	0.28
16	coherecne delta-1	po	end	0.18	0.12	0.17	0.18	0.2	0.17
17	power theta-1	f3c3	beg	0.18	0.12	0.2	0.17	0.17	0.24
18	power beta-1	p3o1	end	0.18	0.18	0.23	0.22	0.13	0.17
19	spectral edge 50	p4o2	beg	0.13	0.13	0.17	0.18	0.1	0.16
20	power gamma	c3p3	rrc	0.13	0.11	0.17	0.24	0.1	0.16
21	coherecne delta-2	po	beg	0.1	0.12	0.1	0.16	0.1	0.16

relative delta-1 P3O1 end and coherence delta-1 FC end feature.

Table 6.11: Sumarization of the classification results. Total errors for different classification tasks in particular dimensions. 1D: single feature, FS: feature selection, training cardinality: training data set cardinality.

Dimension	Fisher classifier				Neural networks	
	1D	FS			1D	FS
		training cardinality:				train.card.:
		0.9		0.6		0.9
		trail 1	trial 2			
1	0.31				0.2	
3						0.2
8				0.16		
10		0.12	0.13			
17		0.04				
21						0.1
25			0.03			

6.5 Discussion on relaxation

Compared to other imaging methods like fMRI, PET, it is difficult to formulate any physiological interpretation of captured processes. On the other hand fNMR or PET techniques, which are able to localize certain physiological activity are much more expensive methods. In case we used more dense montage, amount of data would increase, however question would be, weather it would have brought more useful information. Still we obtained a large number of different resulting measures at different cortex locations. From them simple interpretation and generalization would be desirable. Unfortunately in area of psychophysiology there is often no straightforward way to interpret obtained results in the frame of elementary physiological processes, like e.g. decrease in total power interpreted as attenuation of cortex activity. Already shift to lower frequency bands or decrease in signal complexity may be interpreted in different ways, both deactivation or activation of cortex activity, depending on the circumstances. There also rises another question, whether there should be highlighted measures with topologically broader distinctive performance, or one should prefer selecting only those measures performing the best at single cortex locations. Concerning physiological correlates, generally one could look for certain locations that show distinct behavior reflected in evolution of measures and try to locate relevant cortex functioning centers according to their anatomical displacement. An opposite strategy would be to look for topologically widest changes that can be detected more easily.

Concerning practical application of knowledge regarding detection of resting states, physiological mechanisms of arousal and attention are currently studied for scientific, clinical and technical purposes. Our study may belong to broader topics from which one of the most actual areas is for example reliable interactions between human subject and artificial system (e.g. of transportation nature) and in other situations where human factor is directly involved, and undesirable change of operator's state may have severe consequences. Topic of sensori-motorical rest may be regarded from above-mentioned frame, as it is supposed that under resting conditions change of arousal and decrease of attention and reactivity may occur.

During our resting conditions (3-minute session in darkened room in lying position with eyes closed) we assume that subjects started from unrelaxed or less relaxed state and had an opportunity to achieve kind of release of greater extent than at the beginning of 3- minute session. Neurophysiological indicators for a state of sensori-motorical and mental rest are usually considered to be the increase of alpha and theta frequencies (Lindsley, 1952; Brown, 1970; Foster, 1990) and inter-hemispheric synchronization, especially frontal alpha coherence (Travis, 2001). However, in our study we detected significant decrease of alpha-1 powers (8- 10 Hz). Both absolute and relative alpha-2 power decreased according to averaged curves, but not significantly according to our criteria set in the section 6.3. One could expect, that at least neighbouring lower intervals might increase. Actually we recognized one significant relative theta-1 power increase (backward left location) while other relative powers in delta-2, theta-1, and theta-2 ranges (2-8 Hz) increased in average (insignificantly) in all cortex regions. Further average increases in overall hemisphere synchronization (both linear correlation and mutual information) were obtained only in backward location.

In both sections 6.3 and 6.4 three types of features (Δ^{res}, beginning, end) were analyzed according to subjective answer to the task "Assess a level of your relief accomplished during relaxation period." One may differ between subjective feelings at the end of 3-minute relaxation period and subjective feeling during the whole 3 min period, where also initial subjective state could be accounted. For example more successful relaxation was taken also when it already started from subjectively better starting position. As participants were not suggested to distinguish between these two types of assessment, probably some merged these two questions together. Suggestion for modification would be to repeat task in the sections 6.3 and 6.4 with new classes organized according to subtraction of subjective feeling after relaxation (in our forms achieved during relaxation) and before relaxation 8.2. With classes formed in this way we would exclude class elements reflecting situation "positive start - positive end" from our interest. Rather we would be focus on R^+ class build from elements reflecting "poor beginning - positive end". Such recognition task would be directed towards physiological correlates of processes worth to train. Worth for building or increasing voluntary ability to evoke such beneficial changes. However, with such a regrouping, we headed a problem of having not enough variety of these subtracted values necessary for forming two distinct and numerous groups, as pairs of subjective feeling were often similar. By this regrouping of the classes we would eliminate one "deviation" in subjective assessment, illustrated in the following example. Let us have 2 different relaxation sessions. Case 1: assessment of subjective feeling before: 2, feeling after (in this meaning not applied in our protocol): 2. Case 2: assessment of subjective feeling before: - 2, feeling after: 2. Now, subjective effectiveness in the second case was superior, thus enthusiastic subject in the second case could evaluate state accomplished during relaxation by value 3, while in the first case the same state by 1.

In task from the section 6.3 three groups of features are presented: Beginnings can discriminate state of the subject without waiting to measures' development. Direction of trend represented by Δ^{res} reflects evolution. End features are less meaningful compared to beginnings as they reflect no distinct end point for resting, just end of the recording period.

In the section 6.4 we have shown that in principle discrimination of two relaxation states from EEG signal is possible. However, results should be considered with caution as preliminary mainly from two following reasons. Small amount of data (32 in each group) and referencing only to subjective assessments of participants. In principle, the latter cannot be in area of psychophysiology fully replaced. It can be improved by more sophisticated efforts, for example by referencing to more physiological outcomes (like data from cardio-vascular, respiratory, and muscular systems, brain imagines, components secreted to blood). Unfortunately literature on these topics is more or less missing, or related references are focused to in some way similar phenomena (e.g. meditation). Herein solved discrimination and classification tasks could contribute to increased differentiation by combination with other physiological indicators mentioned above. Such combination could result in more expressive results; increased significance of difference for classes and in diminished classification error.

Our results give appropriate starting point for potential practical applications. Naturally, such step should be preceded by larger data acquisition with consecutive discrimination. For more realistic classification approach, first of all, expressively higher number of input data should be used, and then number of trials in feature selection with testing should be massively increased to obtain more representative samples of features. Then also tasks with lower training set cardinality would be reasonable to use (e.g. 0.6).

Finally, one of the main questions of this part of the thesis could be laid and answered. The question is of a high psycho-physiological value: What is relaxation? Here we are able to answer it in the frame of EEG characteristics. Relaxation is sensori-motorical rest characterized by EEG trends obtained in the section 6.2 that differs from not so successful relaxation by features captured in the section 6.3. And practically, but not with naked eye or hand, it can be discriminated from not so successful relaxation by classification methods from the section 6.4.

In the section 6.3, majority of out-coming measures' evolutions from t-test display an interesting behavior: Convergence of both curves into common level, like if some correction of both states was performed to achieve certain equilibrium for optimal performance. In such case sessions from both categories should end up with indiscernable subjective results. This may point to the problem already mentioned above in this discussion, namely whether subjects were able to discern between terminal and initial subjective states while processing task formulated as "Assess a level of your relief accomplished during 3-minute relaxation period". This task was meant to evaluate ending state without interference of preceding evolving subjective states.

From additionally modified and developed measures both relative length and spectral decay showed to be useful in characterizing of resting process, as they appeared among the most sensitive trends 6.1. The rise of relative length correlates with fall of spectral decay. Both changes might be interpreted in a way, that higher frequencies increased their appearance in overall EEG activity. For discrimination of relaxation states relative length occurred in one cortex location for discerning opposite (averaged) trends.

General question is whether to prefer absolute or relative power bands. From the point of view of stronger significance we may always choose from these pairs those ones holding more significant properties. The choice may be connected to behavior of total power. Illustrating for trends, when total power decreases, decrease of alpha power would be stronger than decrease, if any, of relative alpha powers. But, for example, relative theta powers may display stronger rising trends, because absolute theta powers are components of decreasing total power. From physiological point of view remaining question is whether changes in absolute or in relative powers reflect better physiological character of local cortex activity.

Established Δ^{res} showed to be more practical measure for rating sensitivity than p-values of linear regression F-test. Another final remark, while attempting for relaxation, subjects may suffer a bit by unpleasant electrode cap montage.

7

Summarization of results and contribution to praxis

7.1 Summarizing results

In this section we briefly summarize the novel results of the study to make the contribution of the thesis more evident. In this theses contributions to two exploratory research areas reflecting brain functioning were addressed:

- Impact of repetitive audio-visual stimulation (AVS) on human cortex activity

- Exploration of EEG characteristics during psychosomatic relaxation

In the context of the two tasks performance and sensitivity of untraditional EEG measures during subtle physiological changes was compared to traditional ones.

Main items of the contribution of this thesis are listed bellow.

- Revelation of unique EEG characteristics during brain AVS training.

In the first part of the presented work we have demonstrated that repetitive use of AVS affects not only direct and transient features of EEG, but alters EEG characteristics also on long-term time scale. In order to identify direct, transient, as well as long-term changes in human cortex under repetitive impact of AVS various linear and nonlinear measures were estimated.

- Impact of AVS directly during the stimulation in different frequency bands, and long-term evolution of this impact (section 5.2).

Entrainment of brain waves was evaluated as ratio of relative powers in narrow frequency bands comprising stimulation frequencies (17, 4, 2, and 10 Hz in separate time windows) to respective relative powers obtained from prestimulation sessions. Such direct reaction to AVS was well developed in majority of stimulation sessions. Entrainment reaction spread from occipital areas to other cortex regions. In frontal region average reaction was attenuated from 4 to 7-times. The highest increase of average relative band power, 30 times, occured in the right occipital location during 17 Hz stimulation. Single session maximum occured in left backward region during 17 Hz stimulation as well, reaching 217-times higher relative power compared to prestimulation period. The number of sessions with at least 1.5-time increase of respective relative power was registered from almost full number of cases (95-100%) in occipital regions to 46-85% in frontal regions. Total power during stimulation increased in majority of cases, with the highest increases of 1.6-times during 2 and 4 Hz stimulation in frontal and backward cortex locations. Certain trends in entrainment during the whole experiment period were observed, mainly increases for 4 and 2 Hz stimulation in central locations.

- Transient effects of AVS (a few minutes after AVS influence) and their time progress (section 5.3).

Transient effects were understood as differences in individual measures during 3-minute post stimulation period in respect to 3-minute prestimulation period. Wilcoxon matched-paired test was chosen to quantify differences between data recorded after and before stimulation.

The strongest changes in spectral domain occured in higher frequency bands 12 - 45 Hz across all cortex regions. Absolute power from this interval decreased after stimulation in comparison with period prior to stimulation (for collection of these results see appendix B, Fig. 8.4 and 8.5).

From EEG complexity measures spectral entropy decreased in P3O1, Shannon entropy displayed decrease in C3P3, and correlation dimension increase in C4P4 location.

Positive shifts were obtained for interdependencies evaluated synchronization between left and right hemisphere in both lower and higher frequency ranges. Overall interhemispheric cooperation slightly improved in wider frequency spectrum, inspite of the fact that both linear correlation and mutual information did not shift significantly.

Power attenuation in beta range may be understood through the fact that during post AVS resting session subjects were already lying for 25 minutes in darkened room with eyes closed. Their resting state differed from their normal conscious brain state more than that during resting session prior to AVS. Thus their conscious was altered from wake one connected with activity in beta domain.

Trends in transient effects:

From values of each individual measure obtained after AVS values obtained prior to stimulation were subtracted. Trends during the whole training process were tested by significance of nonzero slope in linear regression model.

Higher number of significant trends was found within relative band powers: Increases in theta-1 and theta-2 bands, and increases in beta-1 and beta-2 in frontal channels (for collection of these results see appendix B, Fig. 8.6 and 8.7).

Spectral entropy increased on the right side of the cortex and spectral decay increased in frontal right area. From other complexity characteristics we found that Shannon entropy significantly decreased in F4C4 region, which was opposed by increase of correlation dimension in the same area.

Connectivity between hemispheres in parieto-occipital region strengthen gradually, as both interdependency measures linear correlation coefficient and mutual information increased significantly. Increases were obtained for coherence in alpha-1 band in central regions, and beta-1 coherence in central and parieto-occipital areas.

In summary, mainly positive development of relative powers in 4-8 Hz and 12-30 Hz range, and in various coherences were found. These results may indicate that subjects, as the training progressed, were able to utilize the sessions more effectively in some respect.

- Long-term effects of AVS from the perspective of the whole AVS training (section 5.4).

From long-term perspective evolution of examined measures during the whole experiment period was analyzed from EEG data with respect to the significance of their linear regression. Increased power in lower frequency bands (4-10Hz) in frontal and central cortex locations was observed (for collection of these results see appendix B, Fig. 8.8 and 8.9). Total power (0.5-45 Hz) increased in the right central region. Moreover, its dynamics during the whole course of the experiment displayed a shift from the left to the right hemisphere. Other spectral trends were: left central decrease of delta-1 power, left frontal and central increase of alpha-2, and central increase of beta-2 power. Spectral edge 95 decreased in occipital locations.

Spectral entropy as a linear complexity measure significantly increased in central left area. Spectral decay increased in all monitored cortex areas. Relative length showed to be sensitive in some locations, as it increased in C3P3 and decreased in P3O1 area. Increase in both histogram-based entropy estimators was obtained in F3C3 location. Decreasing trends occured in correlation dimension for frontal and central locations.

Both linear correlation coefficient and mutual information significantly decreased in parieto-occipital parts. Inter-hemispheric coherence in alpha-1 band displayed increase between frontal parts, while theta-1 and theta-2 coherences displayed opposite trends in this region.

Our results show that regular training with AVS does induce changes in the cortex functioning, such as those commonly reported to be features specific to relaxation or altered states of consciousness. It seems that AVS training could be more effective in inducing long-continuint changes of EEG than regular 20 minute listening to relaxation music.

- Investigation of efficiency of linear and nonlinear measures for EEG analysis in the context of long-term AVS (section 5.4).

As a contribution to linear characteristics, we found significant trends in the behaviour of some non-linear measures. Changes in mutual information exactly follow changes in linear correlation. Actually, mutual information appeared to be more sensitive than linear correlation.

However, trends of spectral entropy do not match changes in nonlinear complexity measures. This may be example of a case when nonlinear complexity measures might represent new possible indicators of dynamical changes of resting EEG, or these changes might be indexed better by a combination of linear and non-linear EEG variables.

Another relationship between non-linear and linear measures may be given by possible connection between the spectral features of data and dimensional estimates. It is possible that the decreasing trends of CD and increasing trend of theta and alpha band powers are reflections of the same spectral changes of EEG signals.

- Design of modified and new EEG measures.

Spectral decay showed to be one of the most sensitive measures able to detect changes at all monitored cortex regions during long-term AVS. Relative length, newly proposed measure of complexity of EEG signal, belonged also to sensitive measures in some cortex locations (sections 4.4 and 5.4).

- Testing the effects of popular AVS device on the subjective states of participants.

Direct effect (section 5.2): Quite often participants reported different pleasant and colorful visions during certain stages of the stimulation session. Sometimes personal reminiscences surfaced. In one subject unbearable body feeling arose, so that he considered to withdraw from the experiment.

Transient effect (section 5.3): Subjective measure evaluating general release accomplished during the second relaxation period indicated subjectively better relaxation performance compared to the first resting interval. After half of an hour of resting participants felt significantly better, which was reflected in a rise of subjective evaluation of general release during the second relaxation period compared to the first relaxation period.

Long-term effect (section 5.4): General well-being before each day relaxation period (answering question "How do you currently feel?") displayed no significant trend. However, subjective measure which evaluated general release accomplished during the relaxation interval ("Assess a level of your relief accomplished during the prestimulation period.") showed significantly increasing trend towards better performance. Both subjective measures were rated on 7-point bipolar scale. In spite of the fact that from subjective results certain progress of relaxing effects is apparent, spontaneous relaxation abilities evaluated at the end of the whole experiment were perceived as unchanged.

- Description of EEG characteristics during human psychosomatic relaxation.

In the second part of the thesis firstly EEG characteristics of rest were revealed in a form of regression trends. Then more successful relaxation was discerned from less successful relaxation by set of EEG features.

  - Regression trends of EEG measures during sensori- motorical rest (section 6.2).

On the contrary to general expectations, during resting conditions - 3-minute session in darkened room in lying position with eyes closed - both alpha-1 and relative alpha-1 powers were decreasing. Decrease of total power over the whole cortex implied gradual diminishing of overall brain activity during the resting process. EEG complexity expressed by spectral decay decreased in central and occipital region of the left hemisphere.

  - EEG based discrimination of two relaxation categories (section 6.3).

Categories were formed according to subjective assessments of participants. Set of EEG features was selected according their capability to recognize more from less successful relaxation. Quite a few features pointed to lower contribution of the slowest waves (delta-1 range) in some cortex areas as a distinctive characteristic of more successful relaxation.

  - Classification of the relaxation level (section 6.4).

Feature selection technique was applied for reduction of a set of EEG features in order to propose practical tool for discrimination of two relaxation classes. Within this technique methods of discriminant analysis were employed in a form of Fisher classifier and artificial neural networks. Under restriction to ten dimension, results of feature selection yielded total classification error 12 - 16 %. With permission up to 25 dimension, error of 3 - 4 % was achieved for training set cardinality 0.9. The promising results of this exploratory study might progress into EEG descriptors of human relaxation abilities with possible application in clinical, pharmacological and self-regulative areas.

- Development of complex Octave/Matlab software implementation for EEG processing and analysis.

Complex programs include flexible manipulation with EEG data, digital filtering, routines for calculation of spectral, complexity, and interdependency measures, evolutions of these measures in subsequent time windows and feature selection algorithms with Fisher and artificial neural network classification. Produced software should be freely available on our web site.

- For EEG analysis we combined a wider range of different measures, traditional spectral and contemporary nonlinear ones. In some cases nonlinear characteristics were sensitive to subtle physiological changes and might be added to descriptors of addressed processes. From additionally modified and developed measures both relative length and spectral decay showed to be useful for characterizing process of long-term AVS, sensorimotorical rest, and for discernment of successful relaxation.

Author of this thesis contributed substantially to the following parts of this research project:

- Design of experimental setup for laboratory brain training AVS experiment.
- Design of methodology on EEG data processing, analyzing, displaying and evaluating.
- Laboratory management and operation.
- Data analyzes and programming of complex Octave/Matlab codes.

7.2 Contribution to praxis

- We conducted basic research in the field of AVS. We showed that brain wave entrainment is well developed in distant cortex regions and that AVS training leads to transient and long-term effects. To our knowledge, this is the first study dealing with EEG characteristics under repetitive AVS stimulation during a longer time period. Contribution of this thesis is in better understanding and enhancement of AVS phenomena. This ought to help in designing further clinical studies possibly resulting in establishment of new diagnostic and treatment tools for variety of psychological and neurological disorders. Recommendation for AVS training is, that long-term AVS training may increase brain wave entrainment and enhance relaxation abilities.

- New method for investigating rest and relaxation status from EEG was developed and tested. We have built a set of different criteria for assessment of trends in EEG measures, have chosen appropriate types of EEG features, and appropriate length of data recordings.

- We determined new EEG characteristics of general rest. Moreover we provide EEG features of more successful relaxation. Finally, our promising classification results might be developed into EEG descriptors for recognition of human relaxation status. Potential benefit of obtained EEG characteristics is in variety of areas, e.g. sleep medicine, pharmacy, human artificial system interaction, neurofeedback training and self-regulation.

- We documented that both linear (spectral) and nonlinear approaches for EEG analysis are useful for utilization at cortex processes under studied conditions. In some cases nonlinear characteristics were sensitive to subtle physiological changes and were suitable for addition to descriptors of addressed processes. From modified and newly developed measures both measure of relative length and spectral decay showed to be useful for characterizing processes of long-term AVS, sensorimotorical rest, and for discernment of successful relaxation. Therefore we recommend application of these nontraditional measures in EEG analysis.

- Freely available software was coded in Matlab environment. Complex programs include flexible manipulation with EEG data, digital filtering, routines for calculation of spectral, complexity, and interdependency measures; computation of measures' evolutions in subsequent time windows; and feature selection algorithms with Fisher and artificial neural network classification.

Bibliography

Abarbanel, H. D. I. et al., 1996. Analysis of Observed Chaotic Data. p. 554.

Accardo, A. et al., 1997. Use of the fractal dimension for the analysis of electroencephalographic time series. Biological Cybernetics 77, 339–350.

Adrian, E. and Matthews, B., 1934. The Berger rhythm: Potential changes from the occipital lobes in man. Brain 57, 355–385.

Aftanas, L. and Golocheikine, S., 2001. Human anterior and frontal midline theta and lower alpha reflect emotionally positive state and internalized attention: high-resolution EEG investigation of meditation. Neuroscience Letters 310, 57–60.

Aftanas, L. and Golocheikine, S., 2002. Non-linear dynamic complexity of the human EEG during meditation. Neuroscience Letters 330, 143–146.

Anderson, D., 1989. The treatment of migraine with variable frequency photostimulation. Headache 29, 154–155.

Anderson, D. et al., 1997. Preliminary trial of photic stimulation for premenstrual syndrome. Obstetrics and Gynaecology 17, 76–79.

Anděl, J., 1985. Matematická štatistika. SNTL. p. 346.

Atwood, H. L. and MacKay, W. A., 1989a. Essentials of neurophysiology. p. 105.

Atwood, H. and MacKay, W., 1989b. Essentials of neurophysiology. B.C. Decker Inc, Toronto.

Banquet, J., 1973. Spectral analysis of the EEG in meditation. Electroenceph. Clin. Neurophysiol. 35, 143–151.

Basar, E. et al., 2001. The selectively distributed theta system: functions. Int. J. Psychophysiol. 39, 197–212.

Bickford, R. D., 1987. Electroencephalography. *in* Adelman, G. (ed.), Encyclopedia of Neuroscience. Birkhauser, Cambridge (USA). pp. 371–373.

Birbaumer, N. and Schmidt, R., 1999. Biologische psychologie. Springer, Berlin.

Brauchli, P. et al., 1995. Electrocortical, autonomic, and subjective responses to rhythmic audio-visual stimulation. Int. J. Psychophysiol. 19, 53–66.

Breakspear, M. and Terry, J., 2002. Topographical organization of nonlinear interdependance in multichannel human EEG. Neuroimage 16, 822–835.

Bronzino, J. D., 1995. Principles of Electroencephalography. In: J.D. Bronzino ed. The Biomedical Engeneering Handbook. CRC Press, Florida. p. 201–212.

Brown, B., 1970. Recognition of aspects of consciousness through association with EEG Alpha activity represented by a light signal. Psychophysiology 6, 442–452.

Brunet, D., Young, G. et al., 2000. Electroencephalography, Guidelines for Clinical Practice and Facility Standards. College of Physicians and Surgeons of Ontario, Canada.

Callaway, E. and Harris, P. R., 1974. Coupling between cortical potentials from different areas. Science 183, 873–875.

Cantero, J. et al., 1999. Alpha EEG coherence in different brain states: an electrophysiological index of the arousal level in human subjects. Neuroscience Letters 271, 167–170.

Carter, J. and Russell, H., 1993. A Pilot Investigation of Auditory and Visual Entrainment of Brainwave Activity in Learning-Disabled Boys. Texas Researcher, J. of the Texas Center for Educational Research 4, 65–73.

Collura, T., 1998. A Guide to Electrode Selection, Location, and Application for EEG Biofeedback. Ohio.

Critchley, H. et al., 2001. Brain activity during biofeedback relaxation: a functional neuroimaging investigation. Brain 124, 1003–12.

da Silva, F., 1987. EEG analysis: theory and practice. *in* E. Niedermeyer and F. da Silva (eds), Electroencephalography, Basic principles, Clinical Applications and related fields. Urban and Schwarzenberg, baltimore, MD.

Dieter, J. and Weinstein, J., 1995. The effects of variable frequency photo-stimulation goggles on EEG and subjective conscious state. J. Ment. Imag. 19, 77–90.

Effects of Electrode Placement, 2004. California.
*http://www.focused-technology.com/electrod.htm

Elbert, T. et al., 1994. Chaos and physiology: deterministic chaos in excitable cell assemblies. Physiol. Rev. 74, 1–47.

Facts on ERP, 1995. The Research Imaging Center, University of Texas.
*http://ric.uthscsa.edu/facts/erp.html

Foster, D., 1990. EEG and subjective correlates of alpha-frequency binaural-beat stimulation combined with alpha biofeedback. Memphis State University.

Fundamentals of Biomedical Engineering. Electroencephalogram, 2002. The university of Sydney.
*http://www.eelab.usyd.edu.au/ELEC3801/notes/Electroencephalogram.htm

Gel'Fand, I. and Yaglom, A., 1959. Calculation of the amount of information about a random function contained in another such function. Amer. Math. Soc. Transl. 12, 199–246.

Gevins, A. S. and Rmond, A. (eds), 1987. Handbook of electroencephalography and clinical neurophysiology, Methods of analysis of brain electrical and magnetic signals. p. 683.

Graham, R., 1977. Perceptual processes and hypnosis: support for a cognitive-state theory based on laterality. Ann.N.Y.Acad.Sci. 296, 274–283.

Grassberger, P. and Procaccia, I., 1983. Measuring the strangeness of strange attractors. Physica 9D, 189–208.

Gray, C. M. et al., 1989. Oscillatory responses in cat visual cortex exhibit intercolumnar synchronization which reflects global stimulus properties. Nature 338, 334–337.

Jasper, H. H., 1958. The ten-twenty electrode system of the International Federation. Electroenceph. Clin. Neurophysiol. pp. 371–375.

Jeong, J., 2004. EEG dynamics in patients with Alzheimer's disease.. Clin. Neurophysiol. 115, 1490–1505.

Jin, S. H. et al., 2002. Nonlinear dynamics of the EEG separated by independent component analysis after sound and light stimulation. Biol. Cybernetics 86, 395–401.

Kaiser, D. A., 1994. Interest in Films as Measured by Subjective & Behavioral Ratings and Topographic EEG, Methodological Issues. Los Angeles.
*http://www.skiltopo.com/papers/applied/articles/dakdiss2.htm

Kobayashi, T. et al., 2000. Correlation Dimension of human sleep electroencephalogram. Psychiatry and Clinical Neurosciences 54.

Kondraske, G. V., 1986. Neurophysiological measurements. *in* J. Bronzino (ed.), Biomedical Engineering and Instrumentation. PWS Publishing, Boston. pp. 138–179.

Krakovska, A., 1995. Correlation dimension underestimation. Acta Physica Slovaca 45, 567–574.

Kvasnička, V. et al., 1997. Úvod do teórie neurónových sieti. p. 285.

Lazarev, V. et al., 2001. Photic driving in the electroencephalogram in children and adolescents: harmonic structure and relation to the resting state. Brazilian Journal of Medical and Biological Res. 34, 1573–1584.

Lindsley, D., 1952. Psychological phenomena and the electroencephalogram. Electroenceph. Clin. Neurophysiol. 4, 443.

Lubar, J. F., 1989. Electroencephalographic biofeedback and neurological applications. *in* J. Basmajian (ed.), Biofeedback: Principles and Practice (3rd ed.). Baltimore, MD: Williams and Wilkins Publishers. pp. 67–90.

Malmivuo, J. and Plonsey, R., 1995. Bioelectromagnetism. Oxford University Press.

Miller, N., 1971. Learning of visceral and glandular responses. *in* T. Barber (ed.), Biofeedback and selfcontrol. Chicago-New York. pp. –.

Moddemeijer, R., 1989. On estimation of entropy and mutual information of continuous distributions. Signal Processing 16, 233–248.

Montgomery, D. et al., 1994. Clinical outcome of a single case study of EEG entrainment for closed head injury. Proc. Assoc. Appl. Psychophysiol., Biofeedback 25, 82–83.

Morse, D., 1993. Brain Wave Synchronizers: A Review of Their Stress Reduction Effects and Clinical Studies Assessed by Questionnaire, Galvanic Skin Resistance, Pulse Rate, Saliva, and Electroencephalograph. Stress Medicine 9, 111–126.

Nagel, H. N., 1995. Biopotential Amplifiers. In: J.D. Bronzino ed. The Biomedical Engeneering Handbook. CRC Press, Florida. p. 1185–1195.

Niedermeyer, E. and da Silva, F., 1993. Electroencephalography: Basic principles, clinical applications and related fields, 3rd edition. Lippincott, Williams & Wilkins, Philadelphia.

Nunez, P. L., 1995. Neocortical Dynamics and Human EEG Rhythms. Oxford University Press, New York.

Ogilvie et al., 1991. Behavioral, event-related potential, and EEG/FFT changes at sleep onset. Int. J. Psychophysiol. 28, 54–64.

Ossebaard, H., 2000. Stress reduction by technology? An experimental study into the effects of brainmachines on burnout and state anxiety. Applied psychophysiology and biofeedback 25, 93–101.

Paluš, M., 1996. Nonlinearity in Normal Human EEG: Cycles, Temporal Asymmetry, Nonstationarity and Randomness, Not Chaos. Biological Cybernetics 75, 389–396.

Paluš, M. et al., 1999. Is Nonlinearity Relevant for Detecting Changes in EEG?. Theory of Biosciences 118, 179–188.

Pereda, E. et al., 1999. Interhemispheric differences in wake and sleep human electroencephalograms: a comparison between non-linear and spectral measures. Neuroscience Letters 263, 37–40.

Pereda, E. et al., 2001. Acessment of changing interdependencies between human electroencephalograms using nonlinear methods. Physica D: Nonlinear phenomena 148, 147–158.

Picton, T. W. et al., 2000. Guidelines for using event-related potentials to study cognition: Recording standards and publication criteria. Int. J. Psychophysiol. 37, 127–152.

Pigeau, R. and Frame, A., 1992. Steady state visual evoked responses in high and low alpha subjects. Electroenceph. Clin. Neurophysiol. 84, 101–109.

Press, W. H. et al., 1988. Numerical Recipes in C. p. 735.

Quiroga, R. Q. et al., 2000. Learning Driver-Response Relationships from Synchronization Patterns. Phys. Rev. E 61, 5142.

Quiroga, R. Q. et al., 2002. Performance of different synchronization measures in real data: A case study on electroencephalographic signals. Phys Rev E 65, 041903.

Rappelsberger, P., 2000. EEG coherence analysis: a method to visualise functional connections. *in* B. Saletu et al. (eds), Electrophysiological Brain Research in Preclinical and clinical Pharmacology and Related Fields. Facultas Universittsverlag Wien. pp. 33–44.

Regan, D., 1989. Human brain electrophysiology: Evoked potentials and evoked magnetic fields in science and medicine. Elsevier, New York.

Reiterer, S., 2002. EEG-Coherence Analysis and Foreign Language Processing. Differences between Language Students (English) and Students of other Disciplines during the Processing of Natural Language Stimuli in British English, American English and German. PhD thesis. University of Vienna, Faculty of Human and Social Sciences. Biological Psychology.

Rezek, I. and Roberts, S., 1998. Stochastic complexity measures for physiological signal analysis. IEEE Trans. on Biomedical Engineering 44(9)(9).

Rosenfeld, J. et al., 1997. The effects of alpha (10 Hz) and Beta (22 Hz) "entrainment" stimulation on the alpha and beta EEG bands. Applied Psychophysiol. & Biofeedback 1, 3–20.

Rosipal, R., 2001. Kernel-Based Regression and Objective Nonlinear Measures to Assess Brain Functioning. PhD thesis. University of Paisley, Scotland.

Russell, H., 1997. Intellectual, auditory and photic stimulation changes in functioning in children and adults. Biofeedback 25, 16–17.

Sakamoto, H. et al., 1993. Preservation of alpha rhythm shortly after photic driving. International Journal of Neuroscience 73, 227–233.

Salansky, N. et al., 1998. Response of the Nervous System to Low Frequency Stimulation and EEG Rhythms: Clinical implications. Neuroscience and Biobehavioral Reviews 22, 395–409.

Schurmann, M. and Basar, E., 2001. Functional aspects of alpha oscillations in the EEG. Int. J. Psychophysiol. 39, 151–158.

Shannon, C. E. and Weaver, W., 1949. The mathematical theory of communication. University of Illinois Press, Urbana, IL.

Sigeti, D., 1995. Survival of deterministic dynamics in the presence of noise and the exponential decay of power spectra at high frequency. Physical Review E 52, 2443–2457.

Solomon, G., 1985. Slow wave photic stimulation in the treatment of headache - a preliminary study. Headache 25, 444–44.

Sterman, M. B., 1996. Physiological origins and functional correlates of EEG rhythmic activities: implications for self-regulation. Biofeedback & Self-Regulation 21, 3–33.

Takens, F., 1981. Detecting strange attractors in fluid turbulence. *in* D. Rand and L. Young (eds), Dynamical systems and turbulence. Springer, Berlin. pp. 366–381.

Tansey, M., 1985. Brainwave signatures an index reflective of the brain's functional neuroanatomy: further findings on the effect of EEG sensorimotor rhythm biofeedback training on the neurologic precursors of learining disabilities. Int. J. Psychophysiol. 3, 85–99.

Theiler, J., 1986. Spurious dimension from correlation algorithms applied to limited time-series data. Phys. Rev. A 34, 2427–2432.

Theodoridis, S. and Koutroumbas, K., 1999. Pattern recognition. Academic Press.

Therrien, C., 1989. Decision, Estimation and Classification: an Introduction to Pattern Recognition and Related Topics. John Wiley and Sons, New York.

Timmermann, D. et al., 1999. Effects of 20-minute audio-visual stimulation (AVS) at dominant alpha frequency and twice dominant alpha frequency on the cortical EEG. Int. J. Psychophysiol. 32, 55–61.

Townsend, R. E. et al., 1975. Stabilzation of alpha freqency by sinusoidally modulated light. Electroenceph. Clin. Neurophysiol. 39, 515–518.

Travis, F., 2001. Autonomic and EEG patterns distinguish transcending from other experiences during Transcendental meditation. Int. J. Psychophysiol. 42, 1–9.

Tyner, F. S. and Knott, J. R., 1989. Fundamentals of EEG technology, Volume 1: Basic concepts and methods. Raven Press, New York.

Vavrinský, E., 2005. Tenkovrstvové mikroelektródy pre elektrochemické vodivostné senzory aplikované v biomedicínskom monitorovaní stresu. PhD thesis. Slovak Technical University in Bratislava, Faculty of Electrical Engineering and Informatics, Department of microelectronics.

Walter, V. and Walter, W. G., 1949. The central effects of rhythmic sensory stimulation. Electroenceph. Clin. Neurophysiol. 1, 57–86.

Weiss, S., 1994. EEG als Korrelat mentaler Prozesse. Spektralanalyse des Spontan-EEG in Ruhe und whrend sprachlicher Aufgaben. PhD thesis. University of Vienna.

Zahradníková, J.: 2004. Testing of the Brain machine efficiency. Master's thesis. Czech Technical University in Praque, Faculty of Electrical Engineering, Department of Cybernetics.

Author's references

Foreign reviewed journals (CC):

TEPLAN, M. - KRAKOVSKÁ, A. - ŠTOLC, S.: EEG responses to long-term audio-visual stimulation. International Journal of Psychophysiology, 2006, Vol. 59/2, 81-90.

Inland reviewed journals:

TEPLAN, M.: Fundamentals of EEG measurement. In: Measurement Science Review, 2, 2002. http://www.measurement.sk

ŠTOLC, S. - KRAKOVSKÁ, A. - TEPLAN, M.: Audiovisual stimulation of human brain : linear and nonlinear measures. Measurement Science Review, 3, 2003, 95-98. http://www.measurement.sk/

TEPLAN, M. - KRAKOVSKÁ, A. - ŠTOLC, S.: EEG in the context of audiovisual stimulation. Measurement Science Review, 3, 2003, 17-20. http://www.measurement.sk/

Foreign reviewed conference proceedings:

TEPLAN, M. - KRAKOVSKÁ, A. - ŠTOLC, S.: Linear and nonlinear EEG measures in the context of brain training. In: EMBEC'02. 2. European Medical and Biological Engineering Conference. IFMBE Proceedings. Ed.: Hutten, H., Krsl, P. Graz, Austria, Verlag der Technischen Universitt Graz, 2002, 606-607.

Inland reviewed conference proceedings:

ŠTOLC, S. - KRAKOVSKÁ, A. - TEPLAN, M.: Audiovisual stimulation of human brain: linear and nonlinear measures. In: MEASUREMENT 2003. 4th International Conference on Measurement. Bratislava, Slovak Republic, Institute of Measurement Science, SAS, 2003, 204-207.

TEPLAN, M. - KRAKOVSKÁ, A. - ŠTOLC, S.: EEG in the context of audiovisual stimulation. In: MEASUREMENT 2003. 4th International Conference on Measurement. Bratislava, Slovak Republic, Institute of Measurement Science, SAS, 2003, 136-139.

TEPLAN, M. - KRAKOVSKÁ, A. - ŠTOLC, S.: Measures of EEG in the context of long-term audio-visual stimulation. In: MEASUREMENT 2005. 5th International Conference on Measurement. Bratislava, Slovak Republic, Institute of Measurement Science, SAS, 2005, 225-228.

Foreign reviewed conference abstracts:

KRAKOVSKÁ, A. - TEPLAN, M. - ŠTOLC, S.: Nonlinear filtering of EEG and its effect on complex measures estimation. In: 22nd European Dynamics Days. International Conference. Book of Abstract. Heidelberg, Germany, 15-19 July, 2002, 66.

TEPLAN, M. - KRAKOVSKÁ, A. - ŠTOLC, S.: Dynamics of EEG during brain training. In: 22nd European Dynamics Days. International Conference. Book of Abstract. Heidelberg, Germany, 15-19 July, 2002, 66.

TEPLAN, M. - KRAKOVSKÁ, A. - ŠTOLC, S.: Audiovisual stimulation of human brain and EEG measures. In: 23nd European Dynamics Days 2003. Book of Abstracts. Palma de Mallorca, Spain, September 24-27, 2003, 80.

TEPLAN, M. - KRAKOVSKÁ, A. - ŠTOLC, S.: Long-term effects of audio-visual stimulation on human EEG. In: Coherence and Electromagnetic fields in Biological Systems. Abstract book. Praha, July 1-4, 2005, 60-62.

8

Appendixes

8.1 Appendix A: Forms for audio-visual stimulation

Entrance form

Name:
Date of birth:

Experiences with Brain maschine, relaxation, meditation, joga, or other similar training:

Motivation and expectation before experiment:

	yes	no	neutral
Passive attendance			
Active ambition to learn relaxation			
Curiosity and interest on Brain machine technology			
I assume no effects			
I hope to improve my relaxation skills			
I am affraid of possible negative effects			

Health problems in connection with potentially increased risk due to attendance in the experiment (neurological affections, mental problems, drugs, etc.):

Other comments:

I have been acquainted with the experiment, its conditions and possible risks.

Signiture confirming your voluntary attendance:

Figure 8.1: Form designed for filling at the beginning of the whole experiment (section 4.5).

Form

Name: Date: Session no.:

Time: Min. and max. impedance:

Evaluation before stimulation

How do you currently feel: very badly

-3	-2	-1	0	1	2	3

very well

	no	neutral	yes	comment
momentary mind to follow the session				
physical fatique				
sleepy				
emotional comfort				
recet intake of drugs, alcohol, etc.		--------		

Evaluation after stimulation

Assess a level of your relief accomplished during the prestimulation period (ring a proper value):

tension

-3	-2	-1	0	1	2	3

relax

Assess a level of your relief accomplished during the poststimulation period:

tension

-3	-2	-1	0	1	2	3

relax

How do you currently feel: very badly

-3	-2	-1	0	1	2	3

very well

	no	neutral	yes
emotional comfort after session			

Drowsiness and sleep:

	certainly no	may be	certainly yes
prestimulation period			
during stimulation			
poststimulation period			

Have you accomplished any mental freeing of the background and of your problems:

	certainly no	may be	certainly yes
prestimulation period			
during stimulation			
poststimulation period			

Special experiences

Different visions:

Other mental experiences and states:

Figure 8.2: Form designed for filling before and after each day measurement (section 4.5).

Output form

Name:

Evaluate your overall attendance and experiences:

	yes	no	neutral	comment
Passive attendance				
Could you relax actively?				
Do you suppose any effects of this method?				
Would you expect any negative effects?				

Overall evaluation of drowsiness and sleep:

	exceptionally	occasionally	often
pre and post stimulation periods			
stimulation periods			

Overall evaluation of mental freeing of the background and of your problems:

	exceptionally	occasionally	often
pre and post stimulation periods			
stimulation periods			

Can you compare your release during non-stimulation and stimulation periods?

Do you think, have you improved your relaxation skills?

Your overall evaluation of the experiment:

Do you think, is there anything to learn while using Brain machines?

How did you feel during the rest of your session days?

Were your expectations from before the experiment fulfilled?

Evolution of visions (increased or decreased intensity, positive or negative emotional charge):

Overall evaluation of visions:

Overall evaluation of other mental experiences and states:

Comment to experiment setup, etc.:

Other comment:

Figure 8.3: Form designed for filling after completion of the whole experiment (section 4.5).

8.2 Appendix B: Collection of results for audio-visual stimulation

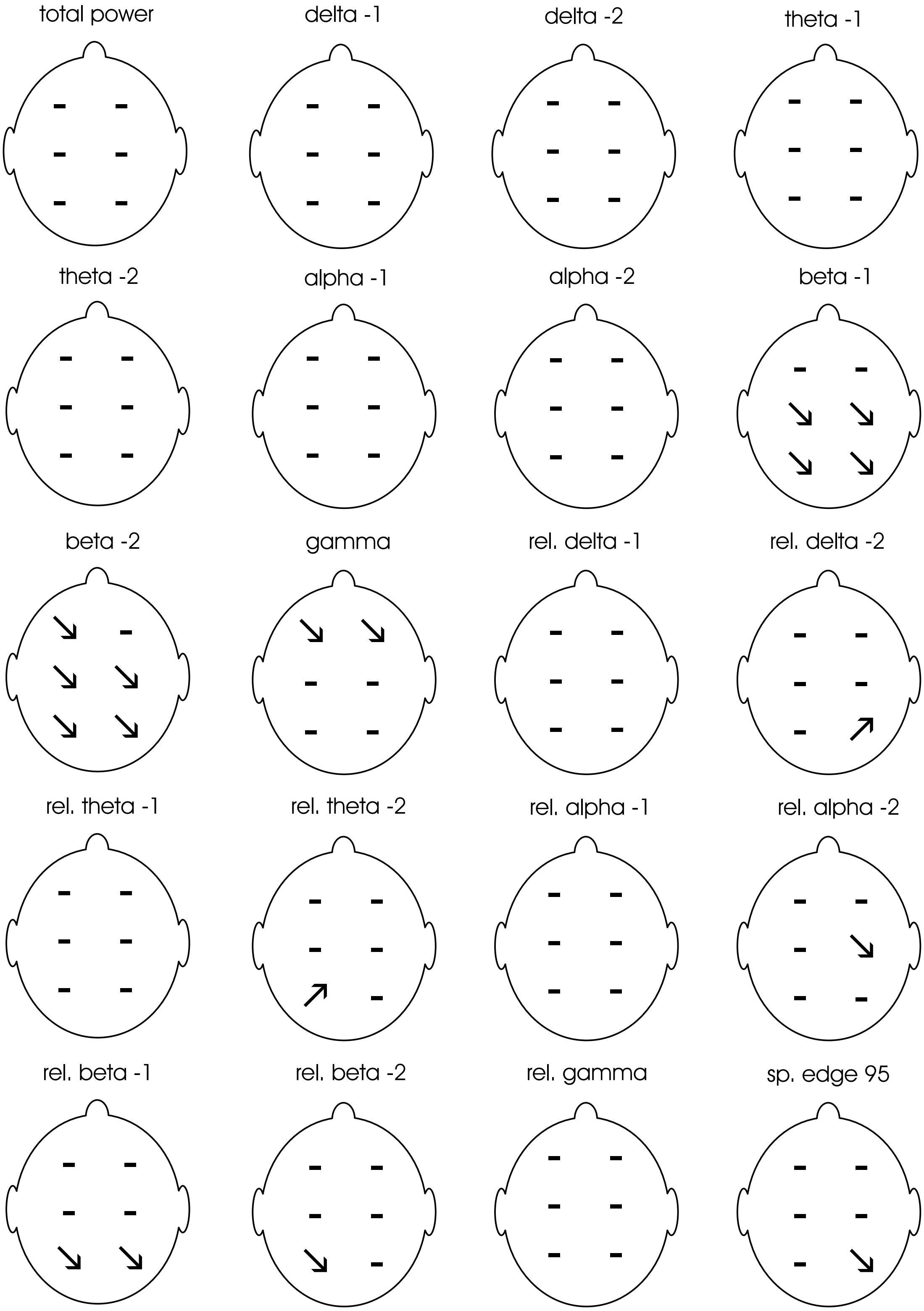

Figure 8.4: Transient AVS effects: changes from prestimulation to poststimulation period. Schematic depicting of significant increase (↗) and decrease (↘) (section 5.3).

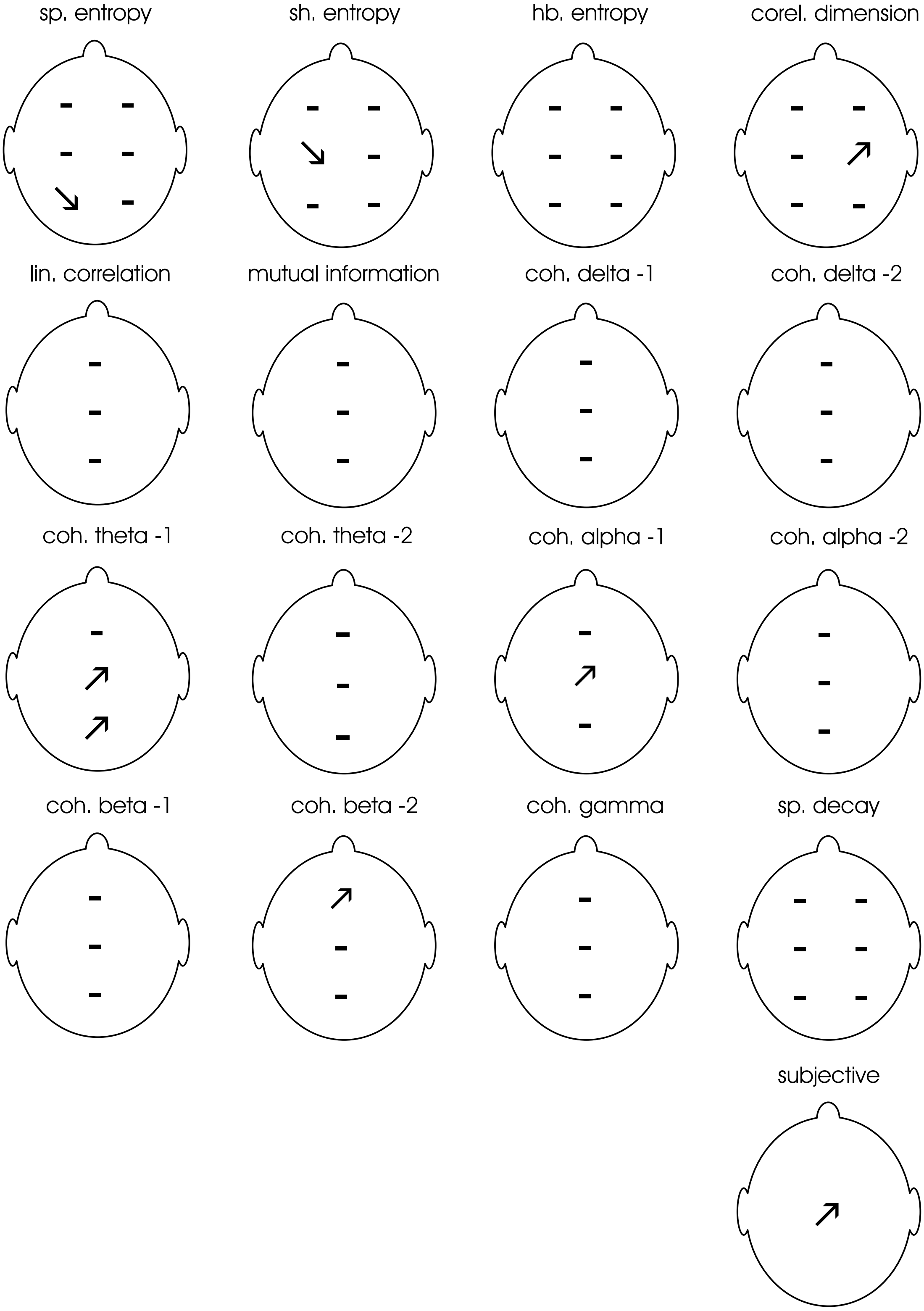

Figure 8.5: Continuation of Fig. 8.4.

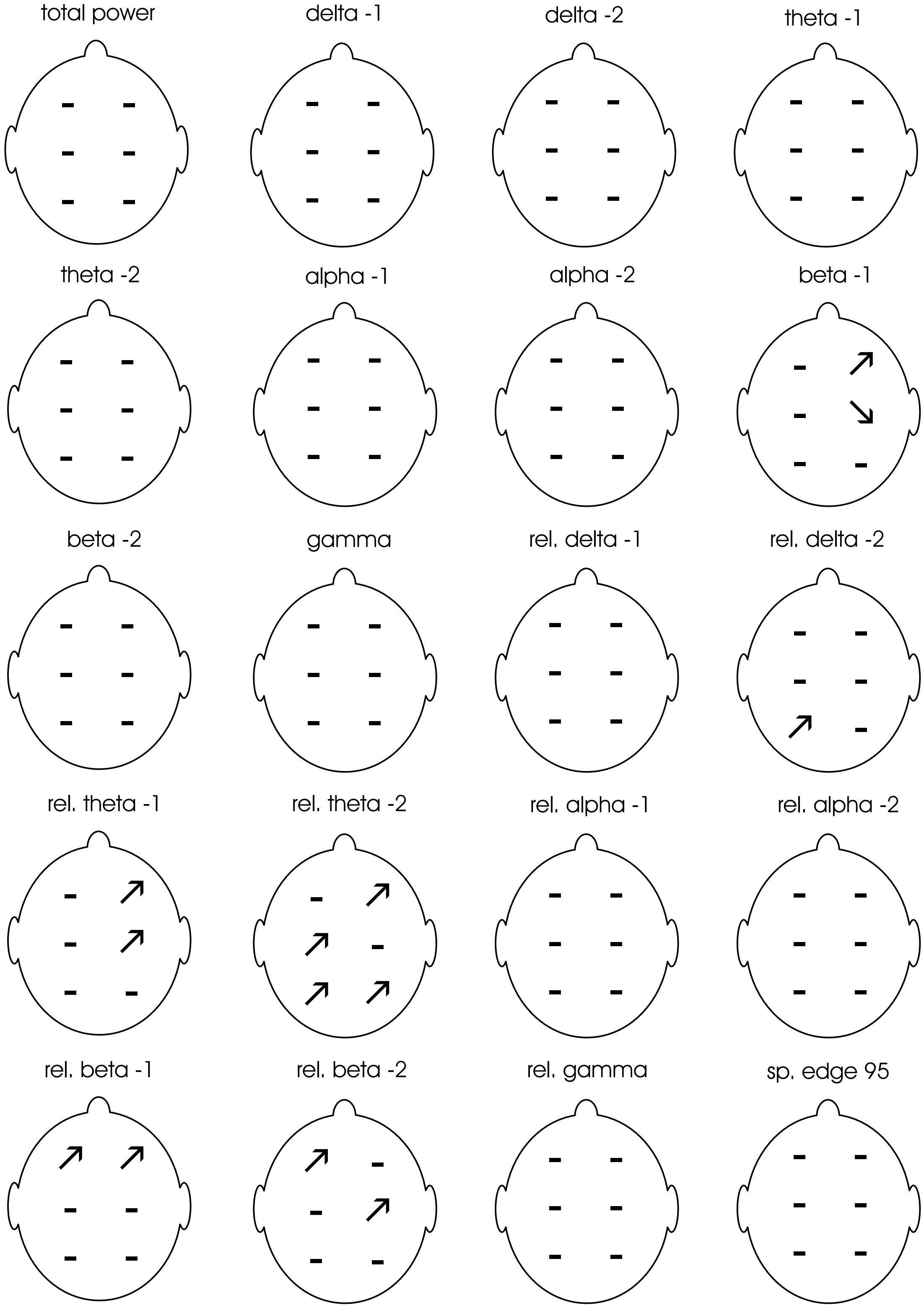

Figure 8.6: Trends in transient AVS effects. Schematic depicting of significant increase ($\nearrow$) and decrease ($\searrow$) (section 5.3).

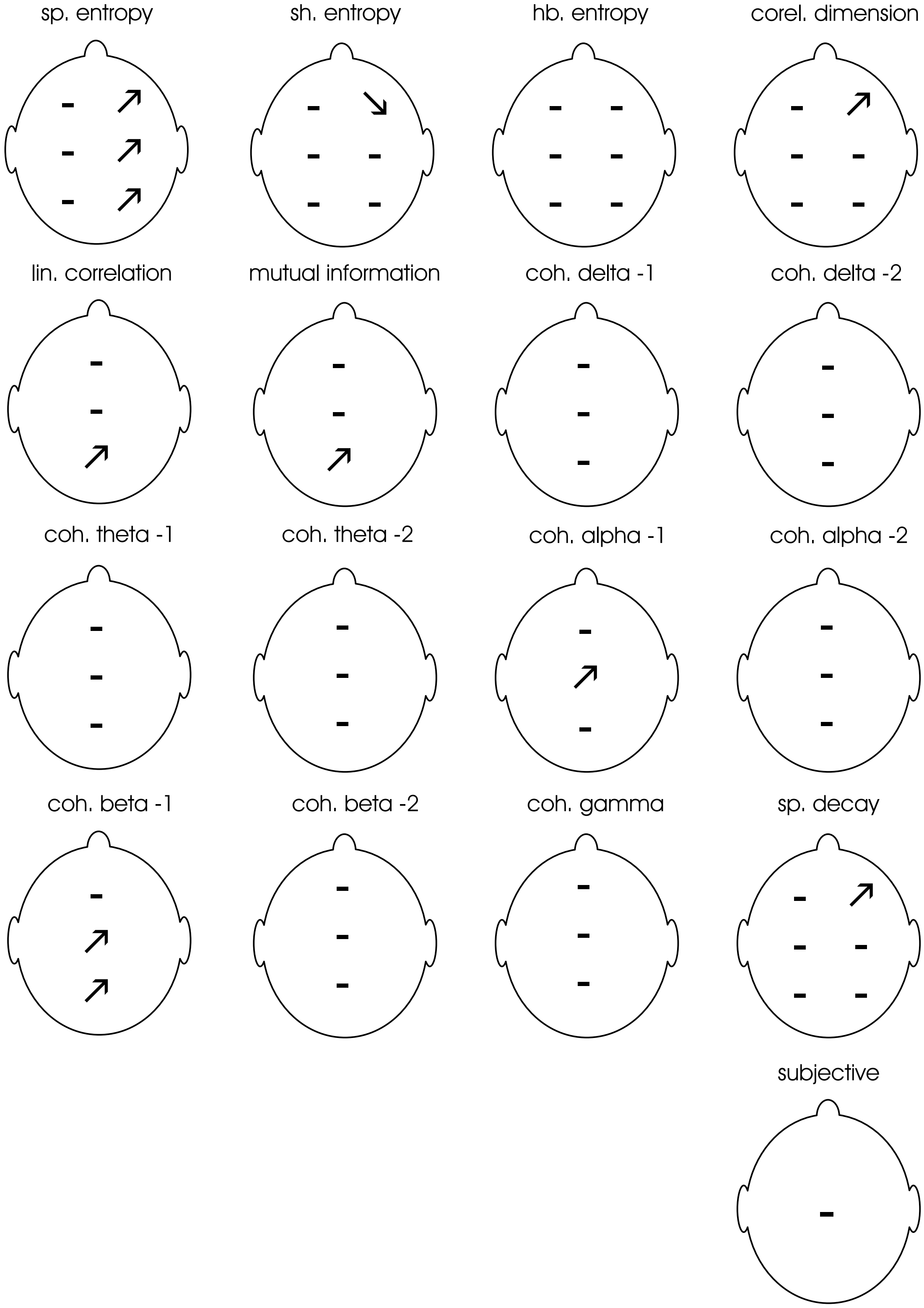

Figure 8.7: Continuation of Fig. 8.6.

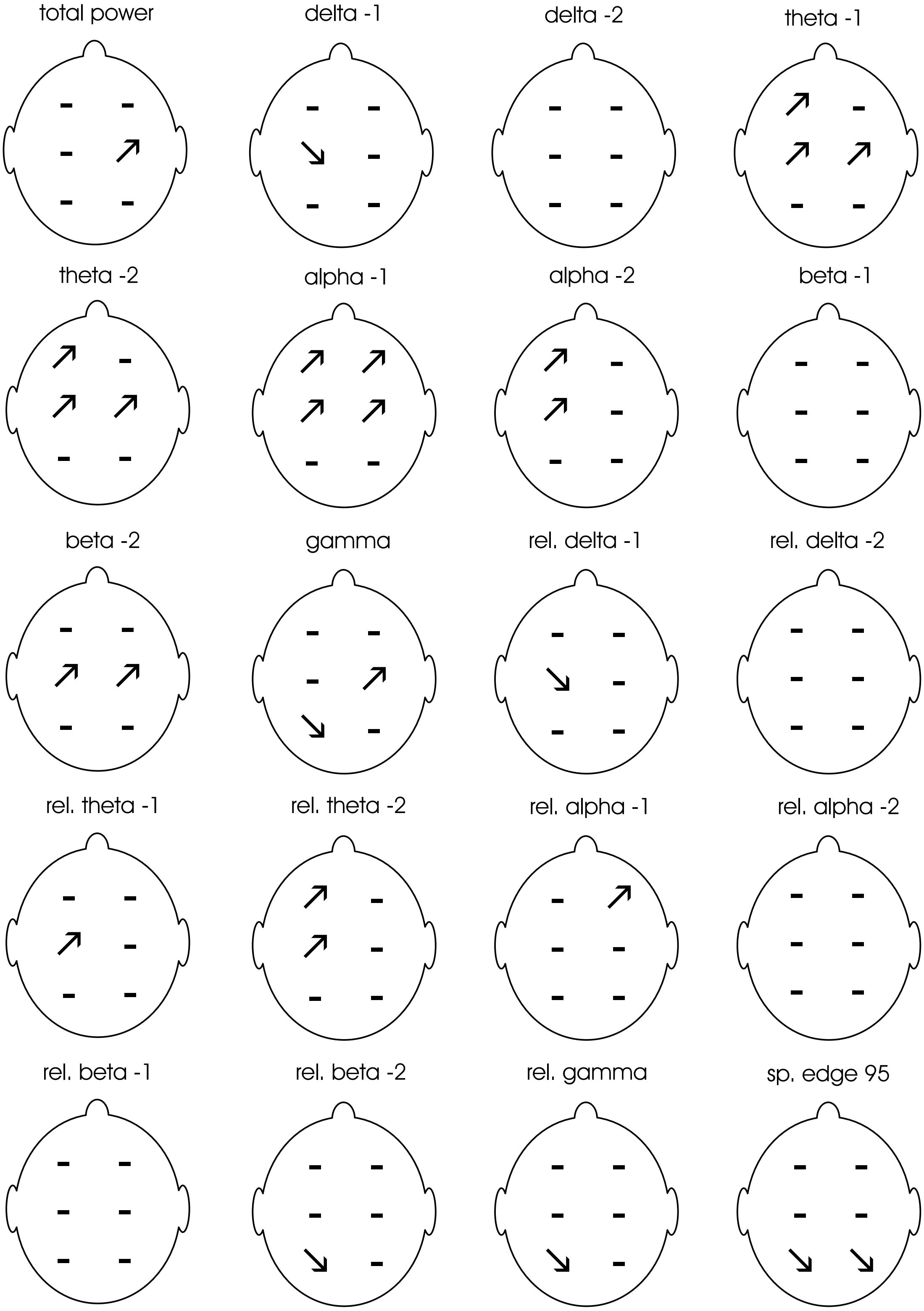

Figure 8.8: Long-term AVS effects: changes during the whole training period. Schematic depicting of significant increase (↗) and decrease (↘) (section 5.4).

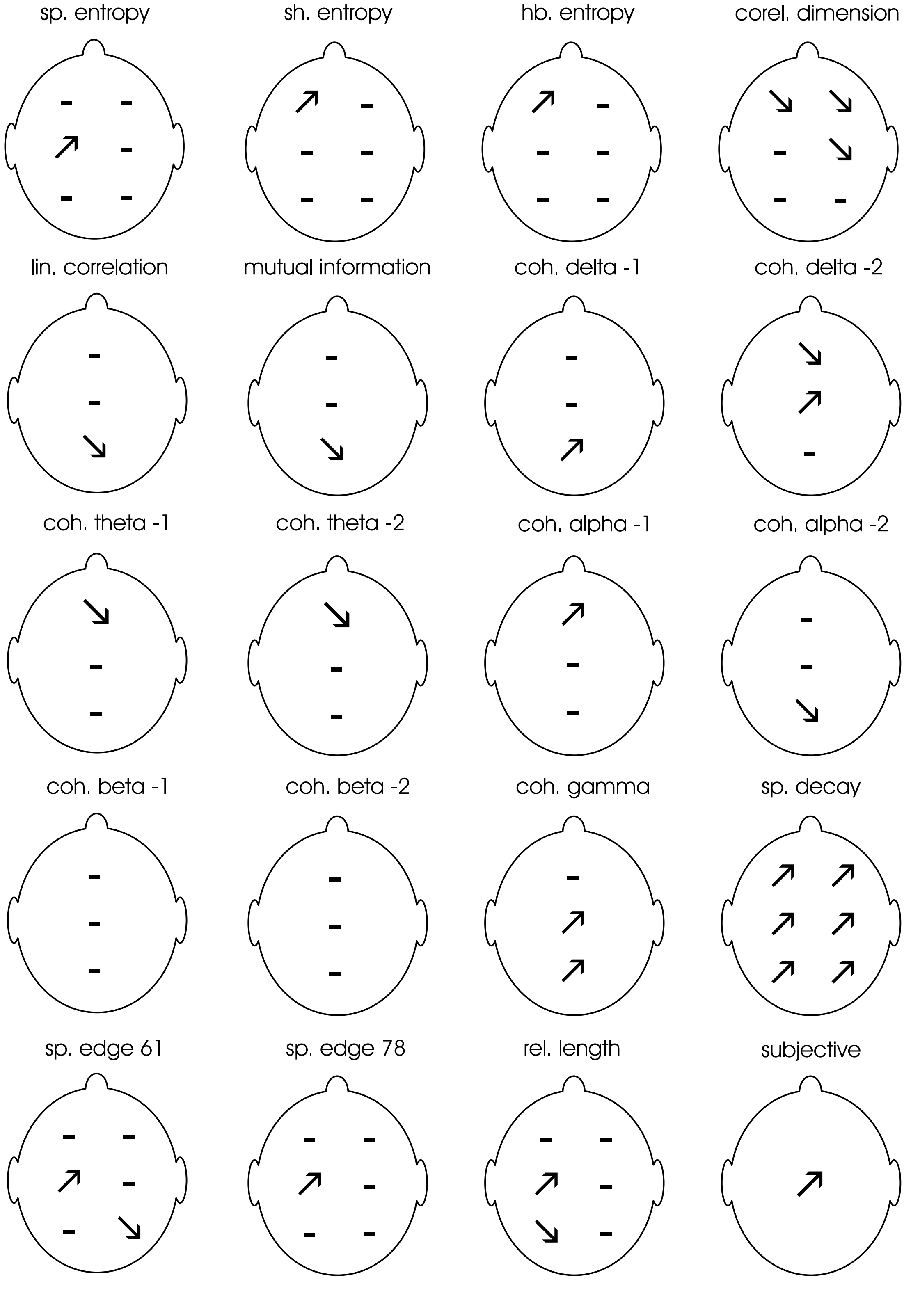

Figure 8.9: Continuation of Fig. 8.8.

8.3 Appendix C: Additional material for characteristics of relaxation

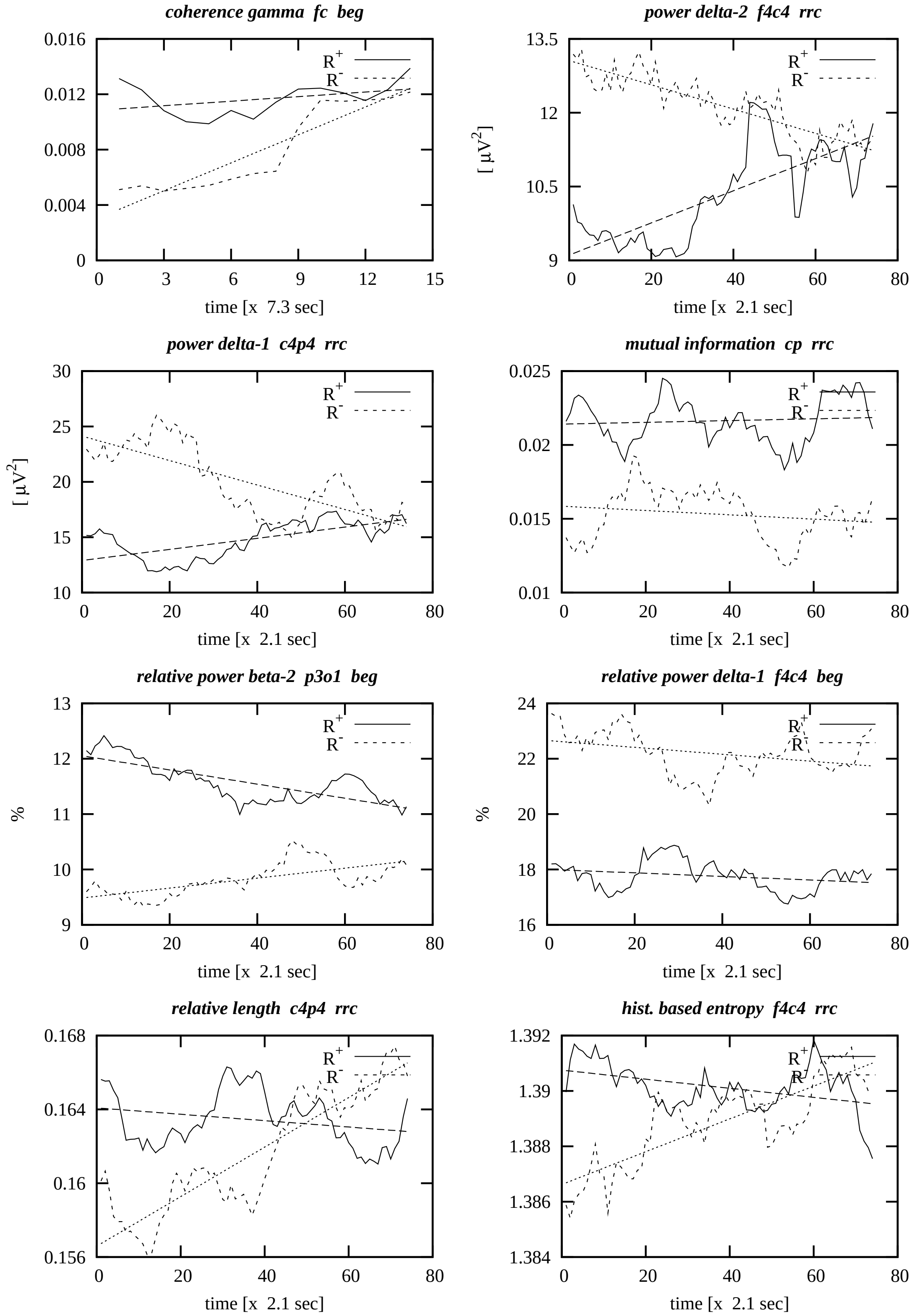

Figure 8.10: Averaged curves for the most distinctive features (measure + location + one of the following characteristics: beginning, end, or relative residual change (rrc)) for normally distributed samples (t-test). Classes R^{-} and R^{+} indicate subjectively less and more successful relaxation (section 6.3).

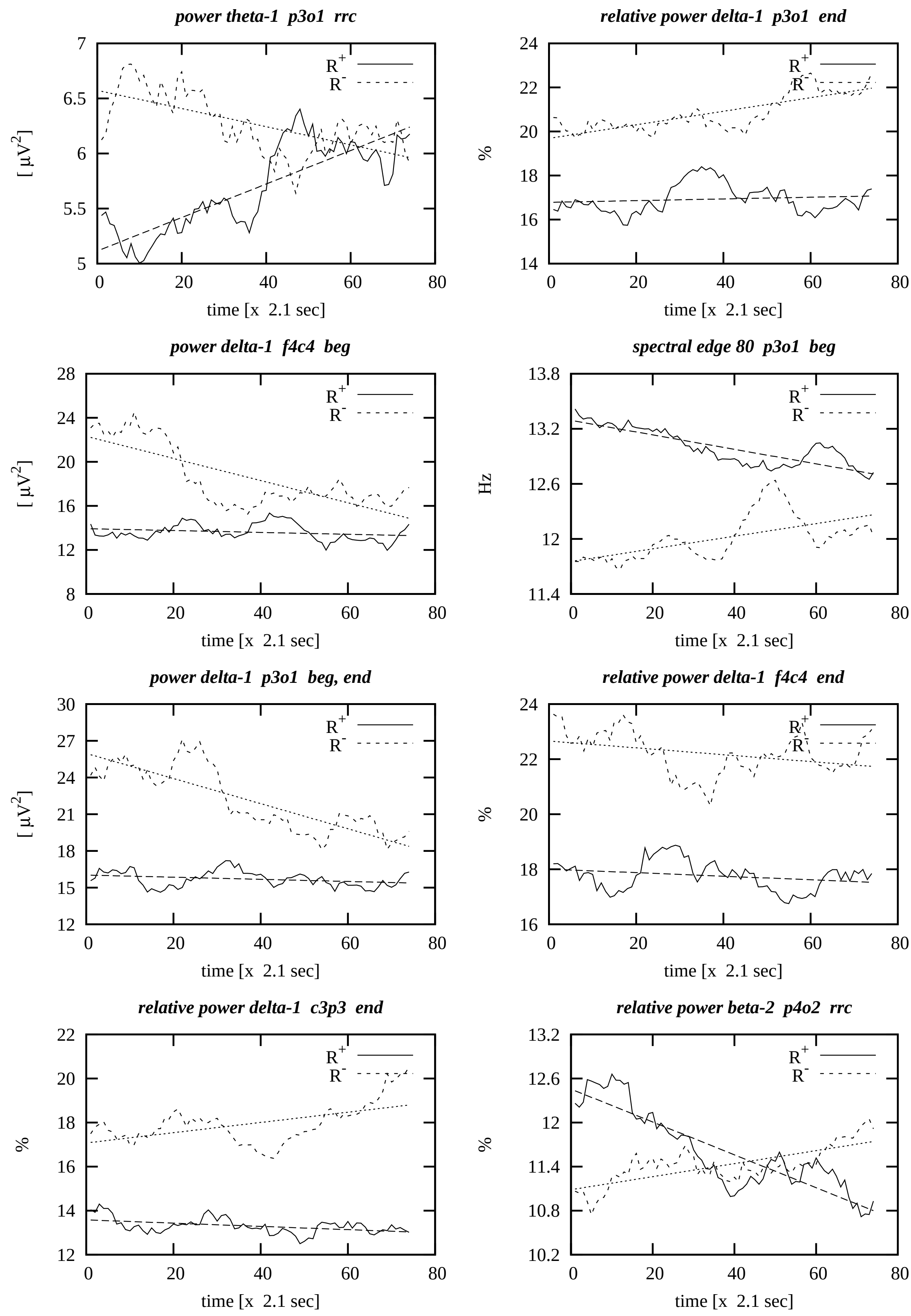

Figure 8.11: Averaged curves for the most distinctive features (measure + location + one of following characteristics: beginning, end, or relative residual change (rrc)) obtained from t-test (the first picture) and from Kruskall-Wallis test (all others). Classes R^- and R^+ indicate subjectively less and more successful relaxation (section 6.3).

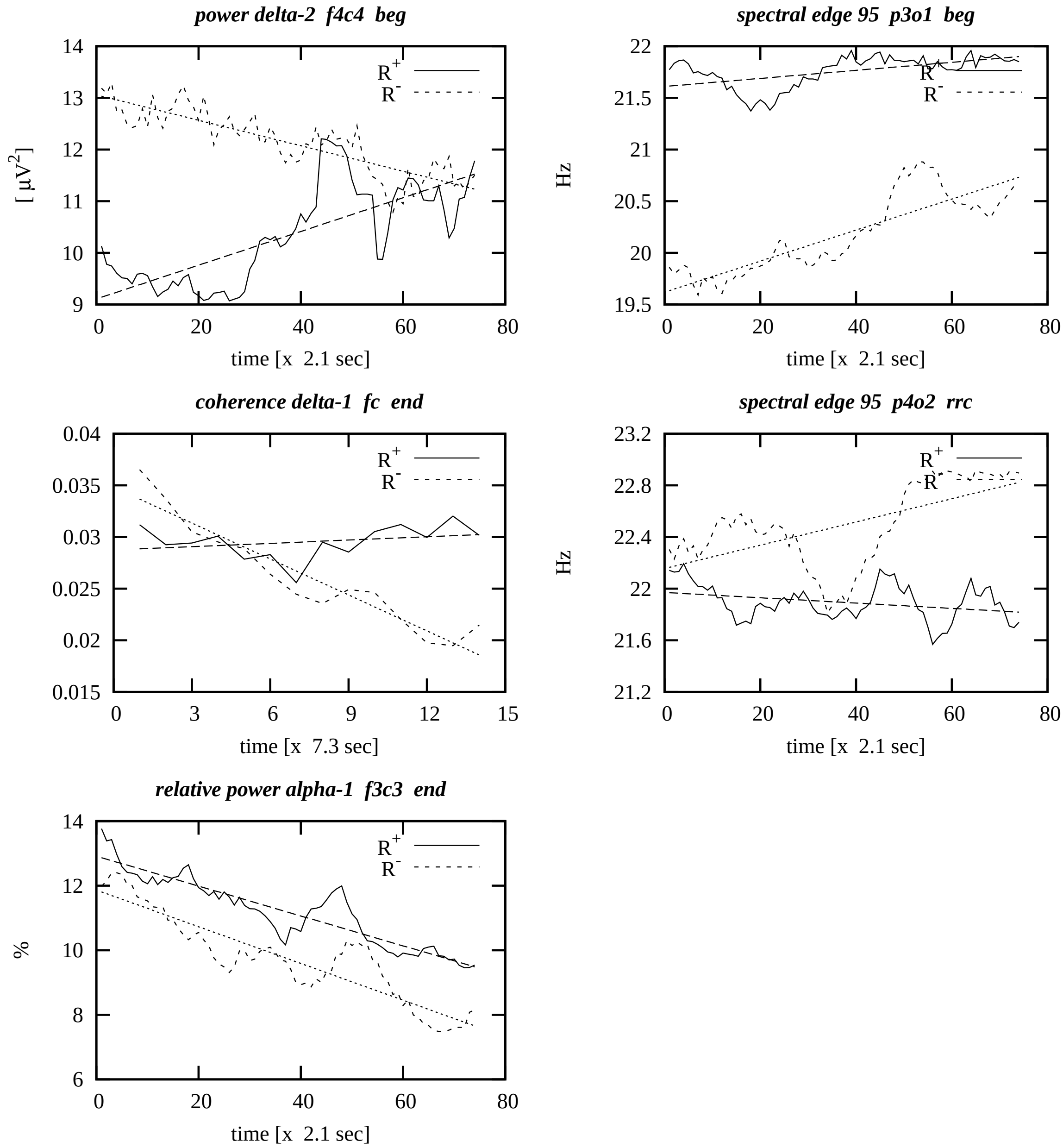

Figure 8.12: Continuation of Fig. 8.11.

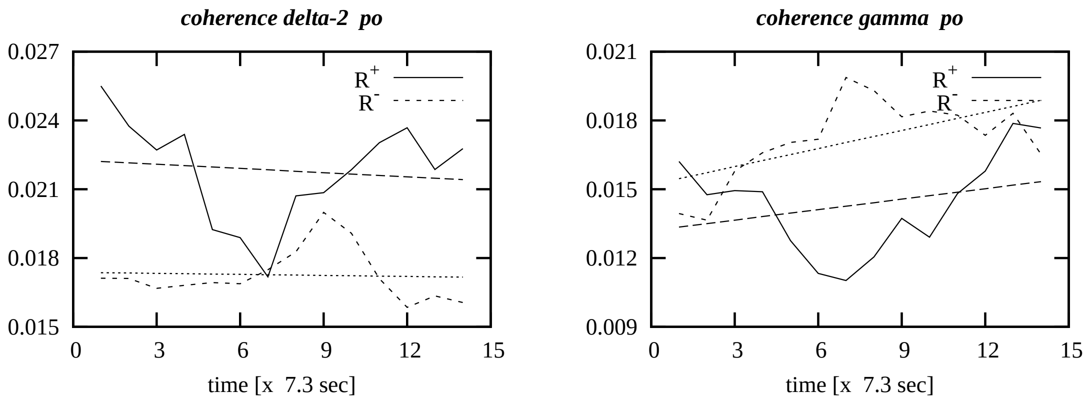

Figure 8.13: Demonstration of measures where linear regression model was not appropriate. Abbreviation "po" designates posterio-occipital region, classes R^- and R^+ indicate subjectively less and more successful relaxation (section 6.3).

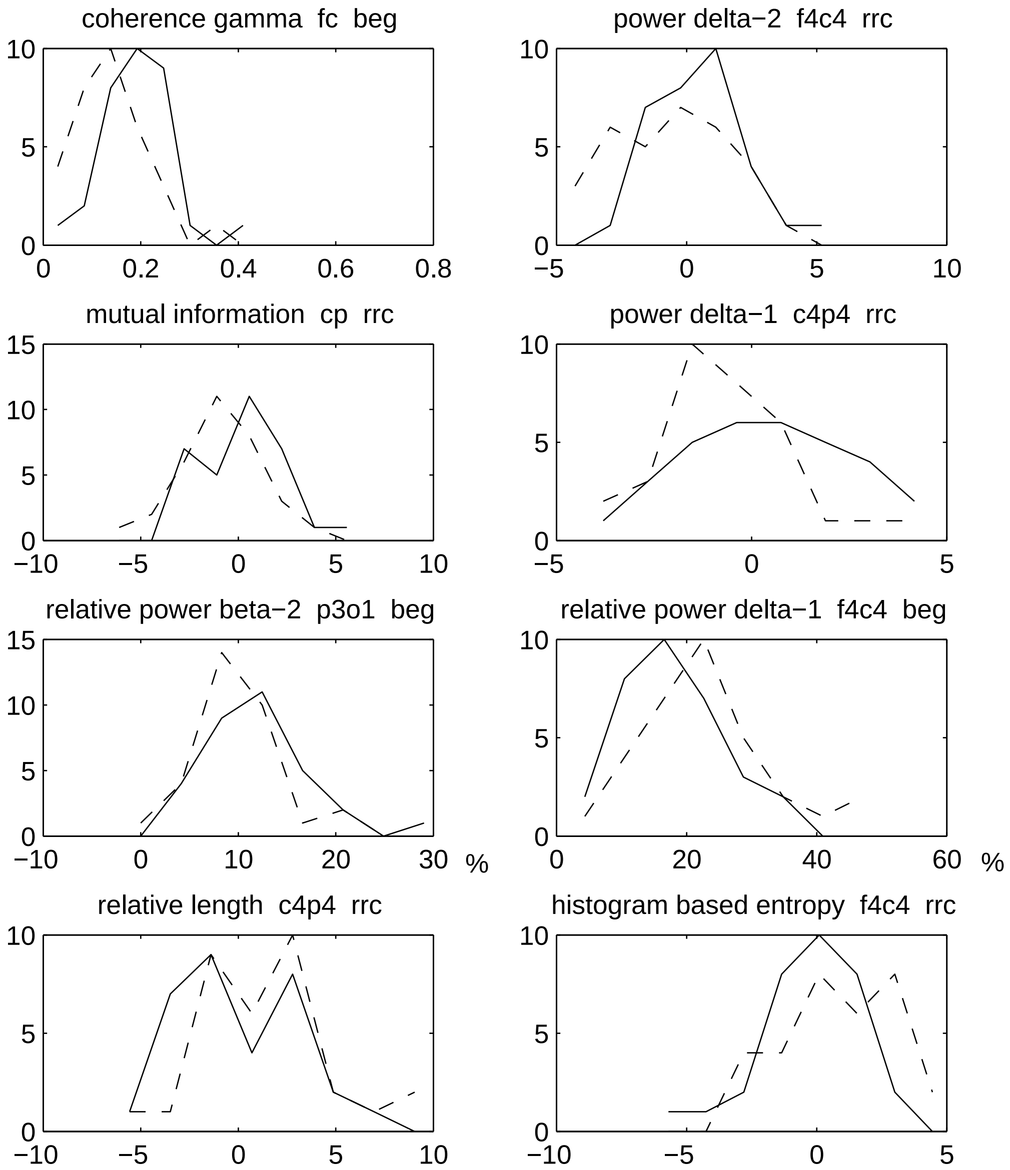

Figure 8.14: Polygons of features with the most distinctive mean according to t-test. Feature is marked by measure, location, and one of the following characteristics: beginning, end, or relative residual change (rrc). Polygons are displayed in order from the most distinctive features (from left to right). Solid and dashed lines indicate classes of subjectively more and less successful relaxation (section 6.3).

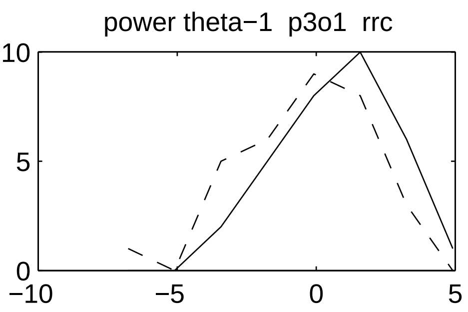

Figure 8.15: Continuation of Fig. 8.14.

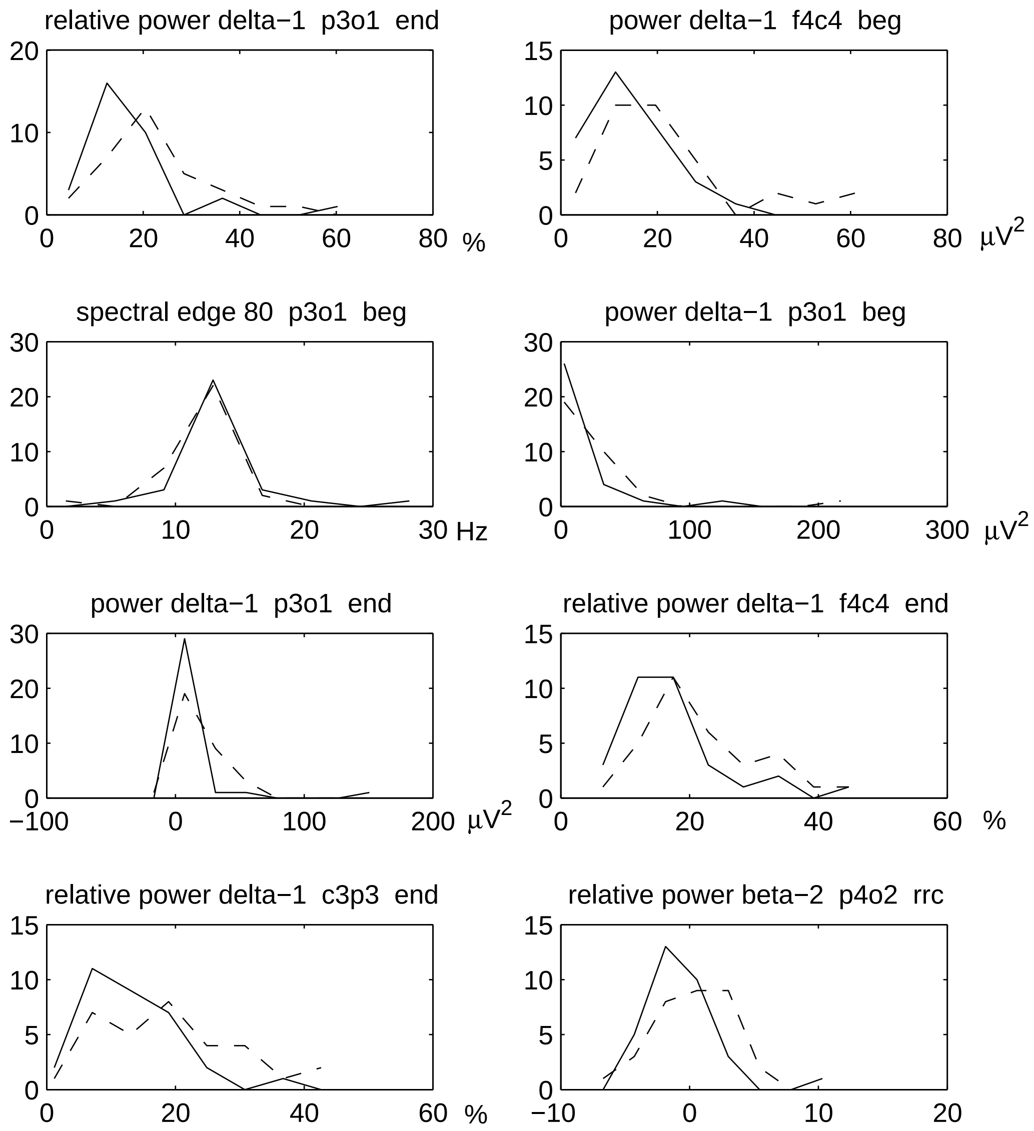

Figure 8.16: Polygons of features with the most distinctive mean according to Kruskall-Wallis test. Displayed in the order from the most distinctive features (from left to right). Feature is marked by measure, location, and one of the following characteristics: beginning, end, or relative residual change (rrc). Solid and dashed lines indicate classes of subjectively more and less successful relaxation (section 6.3).

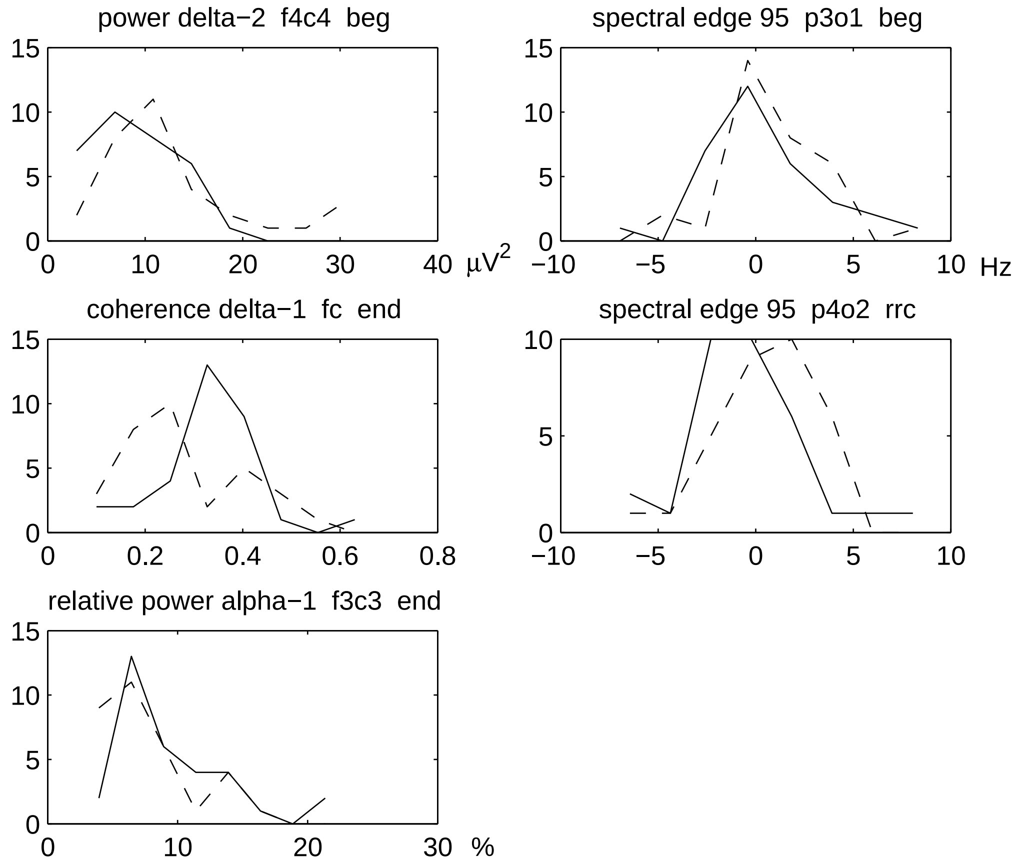

Figure 8.17: Continuation of Fig. 8.16.

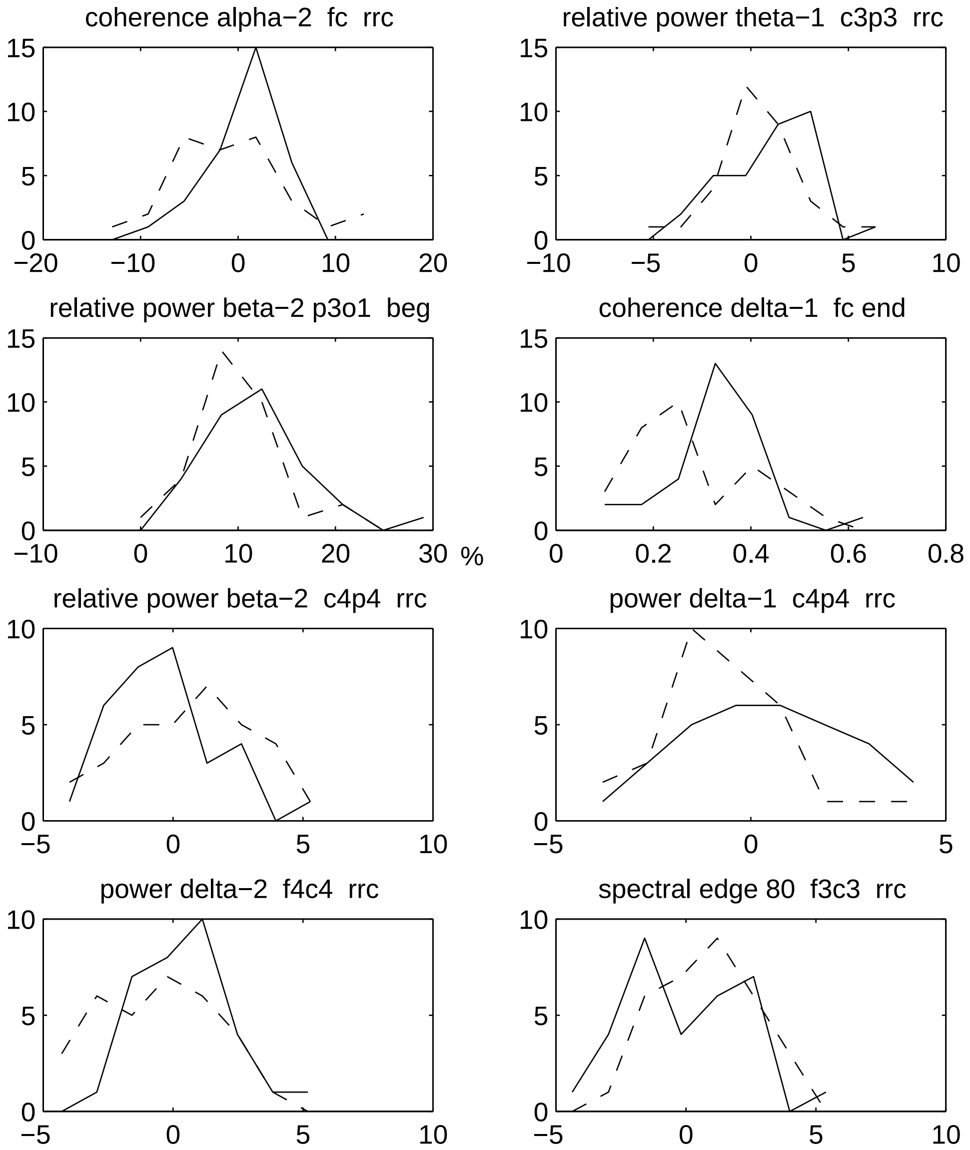

Figure 8.18: Polygons of features with the lowest error in Fisher quadratic classification for single features. Displayed in the order from the most distinctive features (from left to right). Feature is marked by measure, location, and one of the following characteristics: beginning, end, or relative residual change (rrc). Solid and dashed lines indicate classes of subjectively more and less successful relaxation (section 6.4).

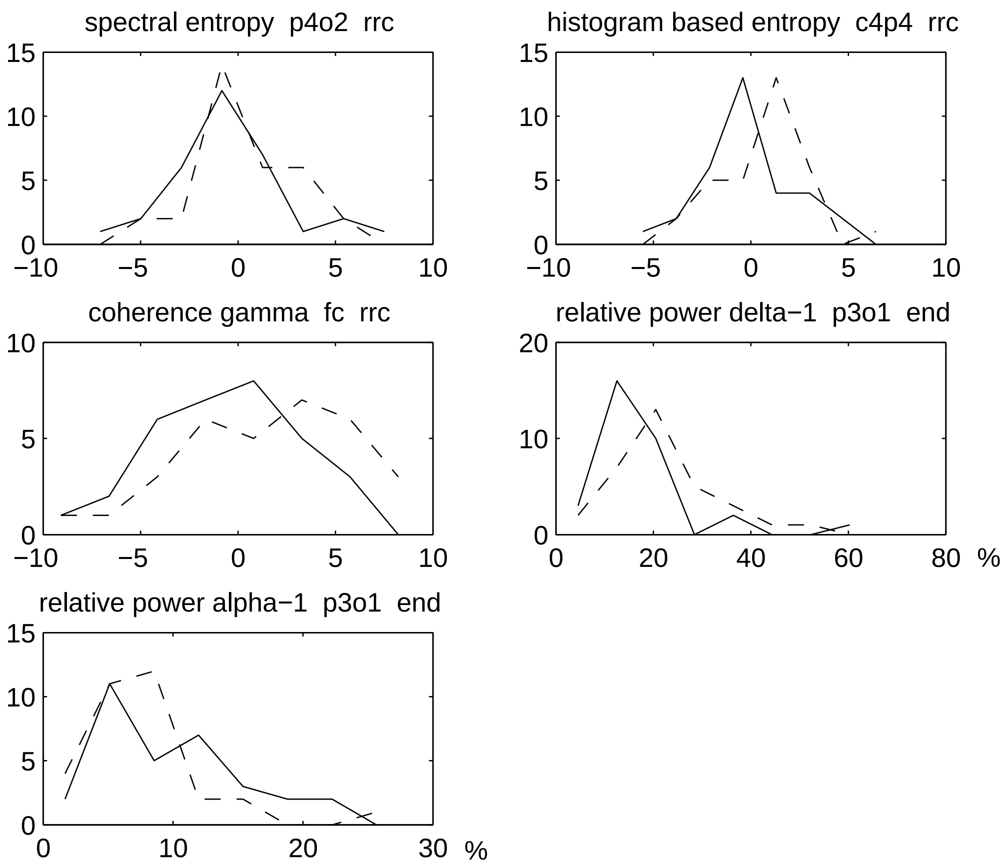

Figure 8.19: Continuation of Fig. 8.18.

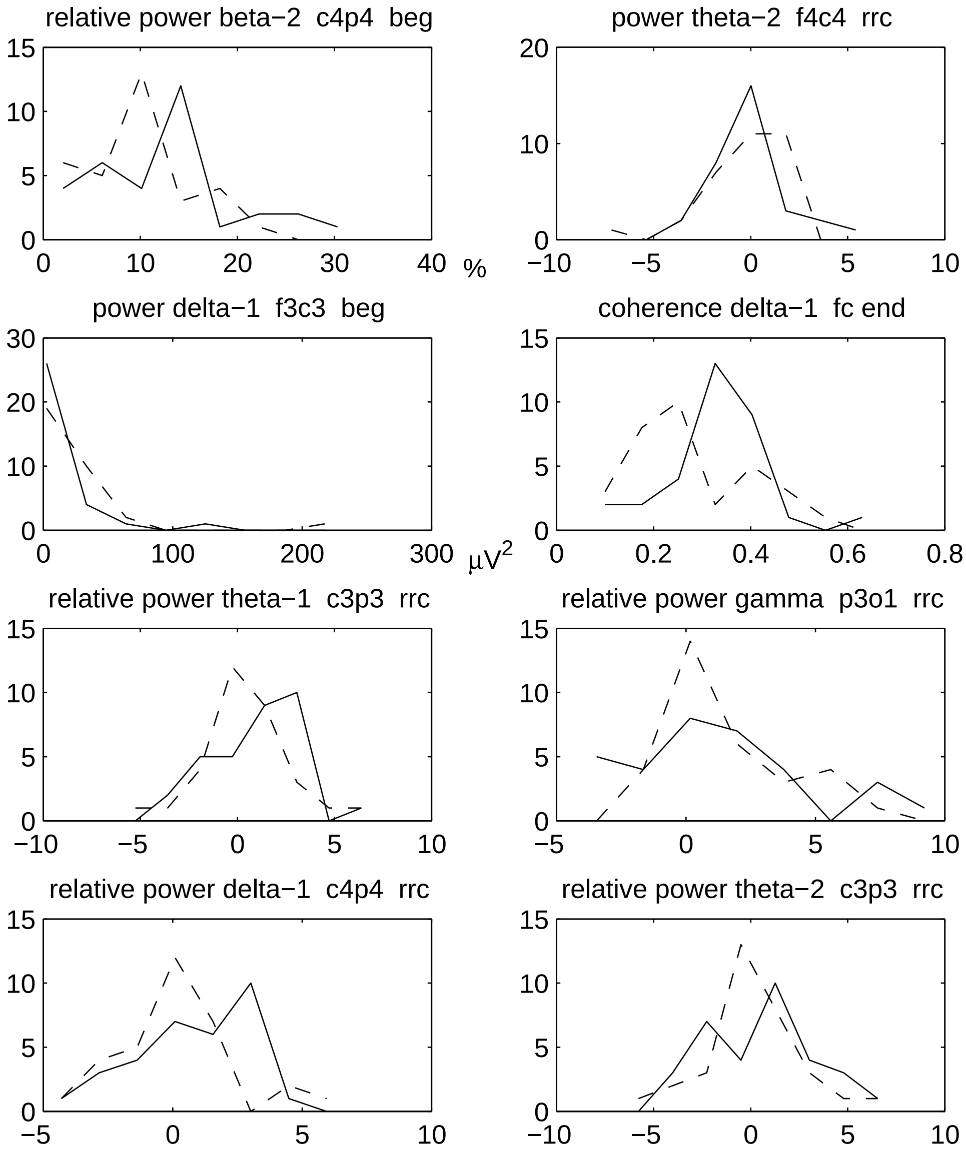

Figure 8.20: Polygons of features with the lowest error from Neural network classifier. Displayed in the order from the most distinctive features (from left to right). Feature is marked by measure, location, and one of the following characteristics: beginning, end, or relative residual change (rrc). Solid and dashed lines indicate classes of subjectively more and less successful relaxation (section 6.4).

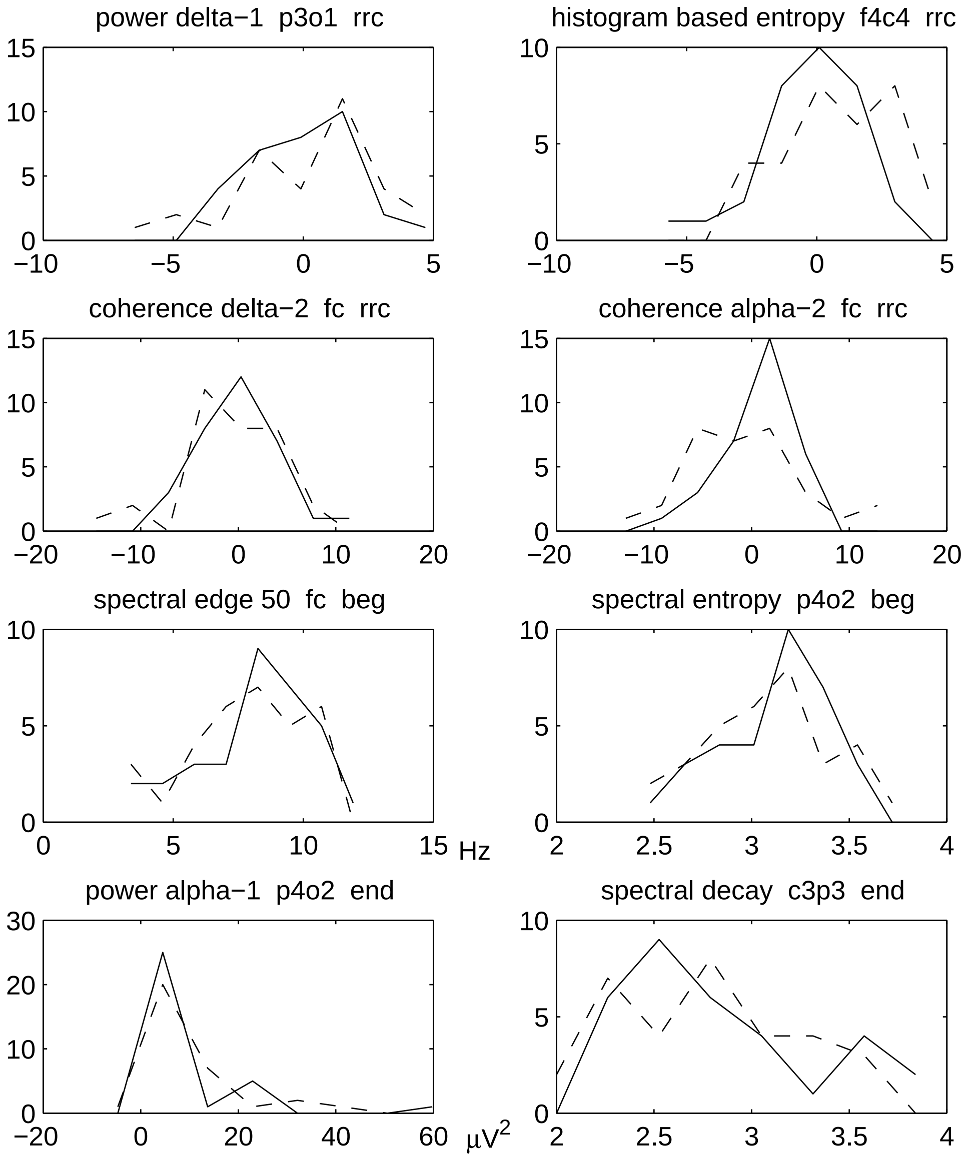

Figure 8.21: Continuation of Fig. 8.20.

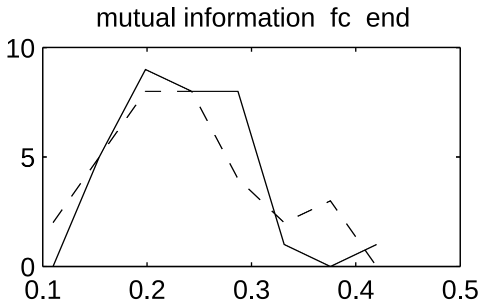

Figure 8.22: Continuation of Fig. 8.20.

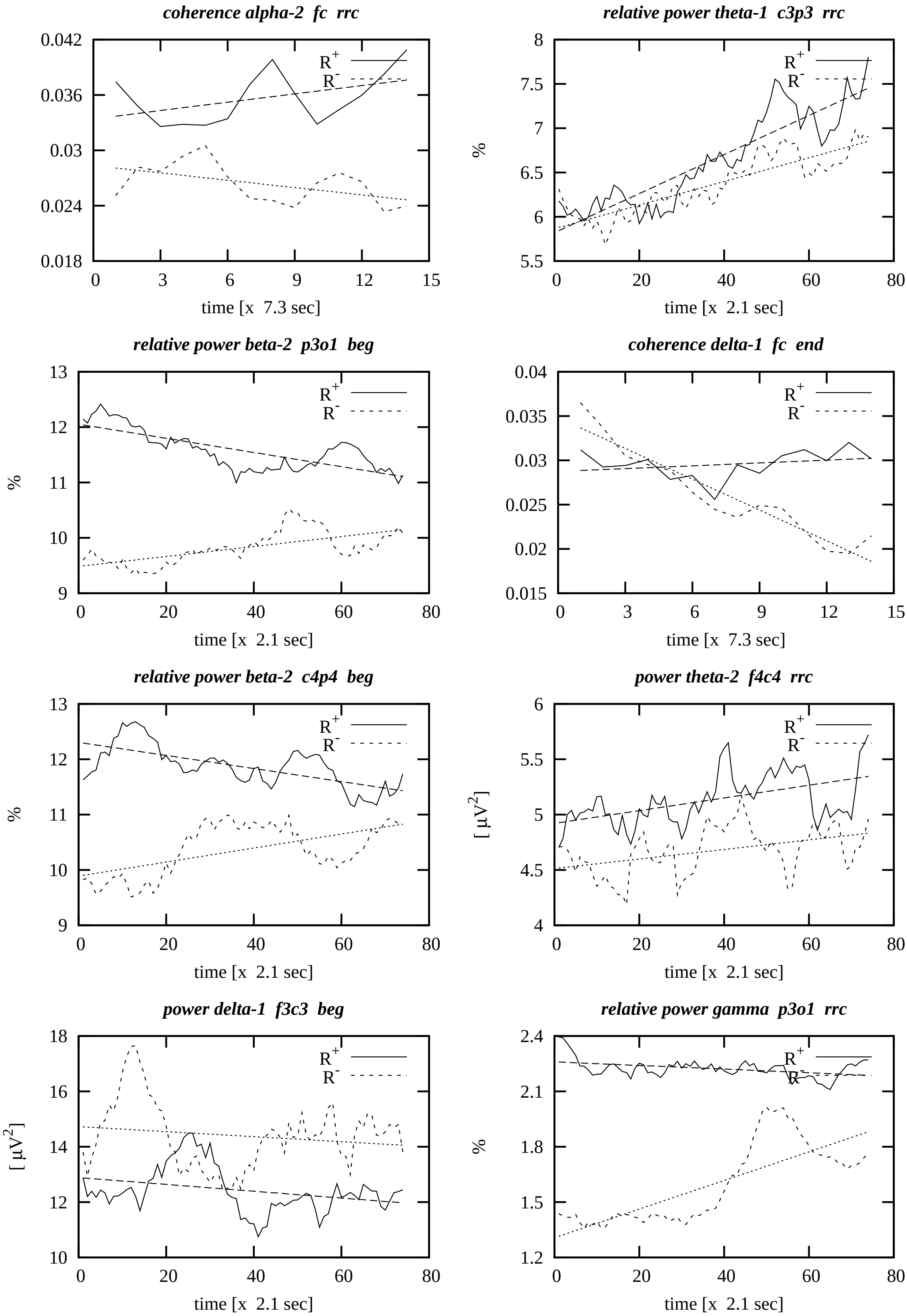

Figure 8.23: Averaged curves for the most distinctive features from Fisher and Neural network classifier in one dimension. Feature is marked by measure, location, and one of the following characteristics: beginning, end, or relative residual change (rrc). Classes R^- and R^+ indicate subjectively less and more successful relaxation (section 6.4).